Agilent
Trusted Answers

Applications of ICP-MS

ICP-QQQ Applications in Geochemistry, Mineral Analysis, and Nuclear Science

Application Compendium

Agilent ICP-QQQ
10 Years
of enabling
industry advances

Explore New Opportunities in Geochemistry, Mineral Analysis, and Nuclear Science With the Agilent 8900 ICP-QQQ

The Agilent ICP-QQQ bibliography provides access to a comprehensive listing of peer-reviewed publications showing how innovative Agilent ICP-QQQ systems have helped hundreds of labs to expand their research into areas never before possible.

This compendium includes articles extracted from the Handbook of ICP-QQQ Applications using the Agilent 8800 and 8900

Agilent atomic spectroscopy instruments are known for their robustness, excellent control of interferences, high speed, low running costs, and high accuracy. Since the launch of the Agilent 8800 in 2012, leading research institutes and commercial organizations have benefited from the high performance of triple quadrupole ICP-MS (ICP-QQQ).

The 8800 and its successor, the Agilent 8900 ICP-QQQ, provide tandem mass spectrometry (MS/MS) operation. MS/MS enables the use of controlled reaction chemistry in the collision/reaction cell (CRC), providing the highest analytical performance in novel and demanding applications.

Of the applications that can now be addressed using the 8900 ICP-QQQ, trace element and isotope ratio analysis of geological samples, minerals, and nuclear materials are among the most challenging. ICP-MS/MS enables analysts to resolve difficult spectral overlaps, enabling accurate low-level analysis of key analytes such as rare-earth elements (REE) and platinum group elements (PGE).

ICP-MS/MS can also resolve overlaps – such as isobaric and doubly charged interferences – that cannot be addressed using conventional ICP-MS modes. Direct isobaric overlaps of interest in geochemistry and geochronology that can be addressed using ICP-MS/MS include ^{204}Hg on ^{204}Pb, ^{87}Rb on ^{87}Sr, and ^{176}Yb and ^{176}Lu on ^{176}Hf. Resolving isobaric overlaps is also beneficial in nuclear science, where the radiogenic isotopes of interest are often at the same mass as a natural isotope of another element. While radiometric (decay activity counting) detection methods are superior for very active and therefore short half-life radioisotopes, ICP-MS detection is superior for less active, longer half-life isotopes. Examples where ICP-MS/MS methods have been applied for radioisotope detection include analysis of radiogenic ^{90}Sr, which is overlapped by natural ^{90}Zr, ^{93}Zr (^{93}Nb), ^{135}Cs (^{135}Ba), ^{129}I (^{129}Xe), and ^{151}Sm (^{151}Eu).

MS/MS also supports reaction cell methods to resolve doubly charged ion overlaps including ^{206}Pb^{++} on ^{103}Rh^{+}, and ^{150}Nd^{++} and ^{150}Sm^{++} on ^{75}As^{+}. In addition, MS/MS provides a dramatic improvement in the control of peak tail overlaps, where an intense peak contributes to the signal measured at the neighboring masses. ICP-MS/MS provides two mass filtering steps, each with a mass rejection efficiency of 10^{-7} (meaning only 1 count is registered for every 10 million counts at an adjacent mass). The overall mass rejection of MS/MS is able to separate extremely low-level trace analytes next to high intensity matrix elements, such as ^{237}Np next to ^{238}U.

The range of new applications being addressed using ICP-MS/MS is continuing to expand, and geochemists, material scientists, and nuclear researchers are leading the development of new and exciting methods.

> Return to table of contents
> Search entire document

Table of contents

Some of the applications reported were run on the Agilent 8800 ICP-QQQ, but the current 8900 ICP-QQQ model provides comparable or superior performance.

Direct Measurement of Trace Rare Earth Elements in High Purity REE Oxides

Author

Kazumi Nakano
Agilent Technologies, Japan

Keywords

Rare Earth Elements, REE, rare earth oxide, REO, samarium oxide, gadolinium oxide, oxygen mass-shift, ammonia on-mass

Introduction

The rare earth elements (REEs) are widely used in advanced technologies including high-power permanent magnets, lasers, phosphors used in fluorescent lamps, radar screens and plasma displays. REEs are also used in petroleum refining, automobile catalytic converters and batteries, and in high-technology glasses. It is clear from these examples that REEs play a key role in many types of materials used in high-technology industries. However, the presence of other REEs as contaminants in a purified single-element REE material often impacts the functionality of the final product, so impurities in the REE oxide raw material must be carefully controlled.

ICP-MS is the most commonly used atomic spectrometry technique for the measurement of trace REEs due to its simple REE spectra — particularly when compared to emission techniques. The measurement of mid- and high-mass REEs in a low-mass REE matrix is, however, very challenging for ICP-MS because REEs have among the highest metal-oxide (M-O) bond strengths of any element, and the oxide ions of the low mass REE overlap the preferred isotopes of the mid-mass and high-mass REEs. Table 1 shows the interferences observed in the analysis of trace REEs in high-purity samarium (Sm) oxide and gadolinium (Gd) oxide.

Separation of the trace REE analytes from the REE matrix can be performed utilizing a chelating resin, but this technique is time-consuming and customization is needed according to the analyte and matrix element. The direct analysis of trace REEs in a variety of high-purity REE matrices is therefore desired. In this work, an Agilent 8800 Triple Quadrupole ICP-MS was used for the direct analysis of trace REE in two high-purity REE materials: Sm_2O_3 and Gd_2O_3. Operating the ICP-QQQ in MS/MS mode effectively removes the challenging interferences, enabling the determination of REE impurities at trace levels in these two materials.

Table 1. Preferred isotope for ICP-MS analysis of each REE, and the potential interferences caused by Sm_2O_3 and Gd_2O_3 matrices.

Element	**La**	**Ce**	**Pr**	**Nd**	**Sm**	**Eu**	**Gd**	**Tb**	**Dy**	**Ho**	**Er**	**Tm**	**Yb**	**Lu**
Mass	**139**	**140**	**141**	**146**	**147**	**153**	**157**	**159**	**163**	**165**	**166**	**169**	**172**	**175**
Gd_2O_3							N/A	GdH^+					GdO^+	$GdOH^+$
Sm_2O_3					N/A	SmH^+			SmO^+	SmO^+	SmO^+	$SmOH^+$		

Experimental

Instrumentation: Agilent 8800 #100.

Plasma conditions: Preset plasma/General purpose.

Ion lens tune: Soft extraction tune: Extract 1 = 0 V, Extract 2 = -180 V.

Acquisition parameters: Three cell modes were used with MS/MS acquisition: No gas, O_2 mass-shift, and NH_3 on-mass mode. In MS/MS O_2 mass-shift mode, the REEs were determined as their oxide ions. REE ions react efficiently with the O_2 cell gas and are converted to the oxide ion REE-O^+. For example, in the measurement of $^{153}Eu^+$, Q1 is set to *m/z* 153 ($^{153}Eu^+$) and Q2 is set to *m/z* 169 ($^{153}Eu^{16}O^+$). Cell tuning parameters are summarized in Table 2.

Table 2. CRC tuning parameters.

Cell mode	Unit	No gas	O_2	*NH_3
Scan mode	MS/MS			
Cell gas		N/A	O_2	NH_3
Cell gas flow rate	mL/min	N/A	0.35	9.0
Octopole bias	V	-8	-5	-18
KED	V	5	-8	-8
Cell exit	V	-80	-90	-110
Deflect lens	V	20	10	-3
Plate	V	-80	-90	-110

*10% NH_3 balanced in Ar

Results and discussion

Two high purity REE oxide materials Gd_2O_3 (5N) and Sm_2O_3 (4N8) were gently dissolved in semiconductor grade HNO_3 and diluted to a concentration of 1 ppm (as the REE). The other (trace) REEs were measured in each matrix solution using the three cell modes. The results are given in Figure 1 and Figure 2. As expected, analysis of the 1 ppm Gd solution in no gas mode gave positive errors on some elements due to interferences from Gd polyatomic ions: GdH^+ interferes with $^{159}Tb^+$, GdO^+ interferes with $^{172}Yb^+$ and $GdOH^+$ interferes with $^{175}Lu^+$.

Preliminary studies showed that NH_3 cell gas reacts with many of the polyatomic ions that interfere with the REE. However, NH_3 also reacts quickly with some of the REE ions, leading to reduced sensitivity of < 1 cps/ppt [1], so this mode is only suitable for the measurement of the less reactive analytes: Pr, Eu, Dy, Ho, Er, Tm and Yb. For these elements, NH_3 on-mass mode gave excellent results, including for Yb in the Gd matrix, where the measured Yb background concentration was reduced by four orders of magnitude (Figure 1) indicating effective removal of the GdO^+ overlap. Background signals for Dy, Ho, Er and Tm in the Sm matrix were also dramatically improved (Figure 2).

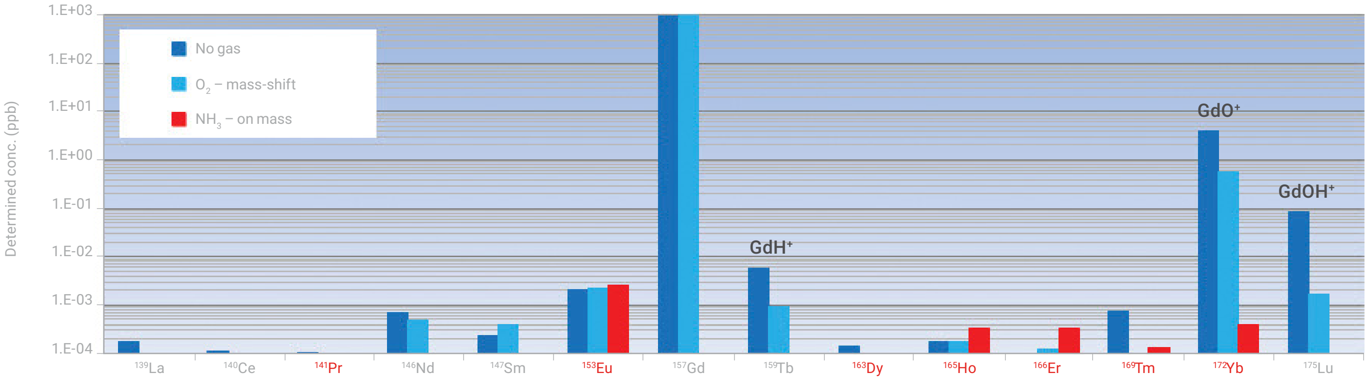

Figure 1. Measured concentration of REE impurities in 1 ppm Gd solution. Gd based interferences are observed on Tb, Yb and Lu. Only the elements in red were measured in NH_3 on-mass mode.

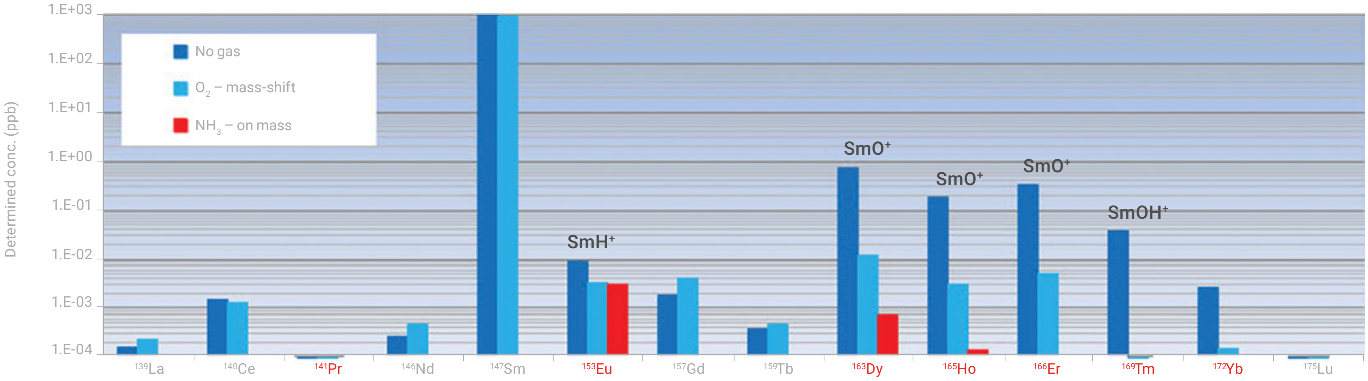

Figure 2. Measured concentration of REE impurities in 1 ppm Sm solution. Sm based interferences are observed on Eu, Dy, Ho, Er, Tm and Yb. Only the elements in red were measured in NH_3 on-mass mode.

For the REEs that react with NH_3 (La, Ce, Nd, Sm, Gd, Tb and Lu), O_2 mass-shift mode and measurement of the target analyte as its REE-O^+ ion is the preferred approach. Most REEs are effectively converted to the oxide ion via reaction with O_2 cell gas [*1*], and this mode was applied to the measurement of Lu in the Gd matrix, avoiding the $GdOH^+$ interference on the Lu^+ isotope and giving a good improvement in the background signal. Compared to no gas mode, O_2 mass-shift mode also gave a good improvement in the background signals for Dy, Ho, Er, Tm and Yb in the Sm matrix, but for all these analytes the backgrounds in NH_3 mode were lower still.

Reference

1. Direct measurement of trace rare earth elements (REEs) in high-purity REE oxide using the Agilent 8800 Triple Quadrupole ICP-MS with MS/MS mode, Agilent application note, 5991-0892EN.

> Return to table of contents
> Search entire document

Removal of MH^+ Interferences in Refined REE Material Analysis

Author

Naoki Sugiyama
Agilent Technologies, Japan

Keywords

Rare Earth Elements, REE, geochemistry, mining, material science, lanthanum, barium, cerium, method of standard additions, MSA, oxygen mass-shift

Introduction

The measurement of Rare Earth Elements (REEs) is of great importance in geochemistry, mining and material science. Manufacturers of high purity REE materials need to quantify metal impurities, including trace levels of the other REEs, in the refined, single element REE matrix. ICP-MS is the technique of choice for the measurement of REEs, but most of the REE isotopes suffer from interference by polyatomic species (predominantly hydride ions, MH^+ and oxide ions, MO^+) derived from other, lower-mass REE elements. While MH^+ interferences are lower in intensity than MO^+ interferences, they present a more challenging problem for REEs that have no isotope free from interference. For example, $^{139}La^+$ is interfered by $^{138}BaH^+$ and $^{140}Ce^+$ by $^{139}LaH^+$. These interferences are too close in mass to be resolved by high-resolution (HR-)ICP-MS [*1*]. In this paper, we describe the removal of the MH^+ interferences using an Agilent 8800 ICP-QQQ in MS/MS mass-shift mode, with oxygen as the reaction gas.

Experimental

Instrumentation: Agilent 8800 #100. The standard glass nebulizer was replaced with a C-flow nebulizer (G3285-80000) for optimal washout between the high matrix samples.

Plasma conditions: Preset plasma/General purpose.

Ion lens tune: Soft extraction tune: Extract 1 = 0 V, Extract 2 = -180 V.

CRC conditions: O_2 gas at 0.3 mL/min, Octopole bias = -5 V, KED = -5 V.

Acquisition parameters: MS/MS mode with O_2 mass-shift method.

Figure 1 illustrates the mechanism of MS/MS O_2 mass-shift mode used for measuring Ce in a La matrix sample. The major isotope of Ce at *m/z* 140 suffers an interference from $^{139}LaH^+$. Q1 is set to *m/z* 140, allowing only the analyte ion $^{140}Ce^+$ and any other ions at *m/z* 140 to pass through to the cell. All other ions not at *m/z* 140 are rejected. In the cell, Ce reacts with oxygen to form CeO^+ at *m/z* 156. Q2 is set to *m/z* 156, allowing CeO^+ to pass to the detector. Since $^{139}LaH^+$ does not react with O_2 to form $^{139}LaOH^+$, it remains as LaH^+ at *m/z* 140 and is rejected by Q2. The same principle is used for the separation of $^{139}La^+$ from $^{138}BaH^+$ in a Ba matrix.

Results and discussion

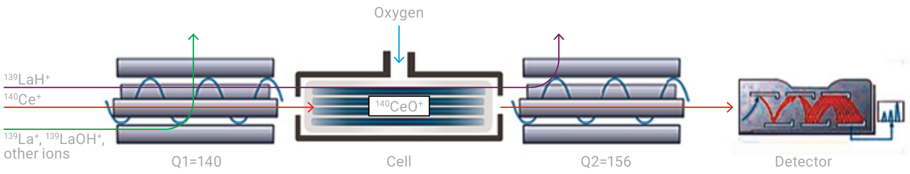

Figure 1. MS/MS mass-shift method with O_2 reaction gas; used for the measurement of Ce, as CeO at *m/z* 156, in a La matrix.

Using the Method of Standard Addition (MSA), the BECs and DLs of La in a matrix of 50 ppm Ba, and Ce in a matrix of 50 ppm La were determined. Data was acquired using MS/MS mode with O_2 mass-shift, and also using Single Quad (SQ) mode with O_2 reaction gas to emulate conventional quadrupole ICP-MS (ICP-QMS) for comparison.

As shown in Figures 2A and 2B, SQ mode with O_2 reaction gas suffers from interferences that prevent the measurement of La in the Ba matrix and Ce in the La matrix, respectively. In contrast, the calibration plots shown in Figures 2C and 2D demonstrate that MS/MS mode with O_2 mass-shift can successfully remove the matrix overlaps to permit the trace quantitation of La in a Ba matrix and Ce in a La matrix. The BECs and DLs achieved were 8.5 ppt and 2.5 ppt respectively for La in a 50 ppm Ba solution, and 10.6 ppt and 0.8 ppt respectively for Ce in a 50 ppm La solution.

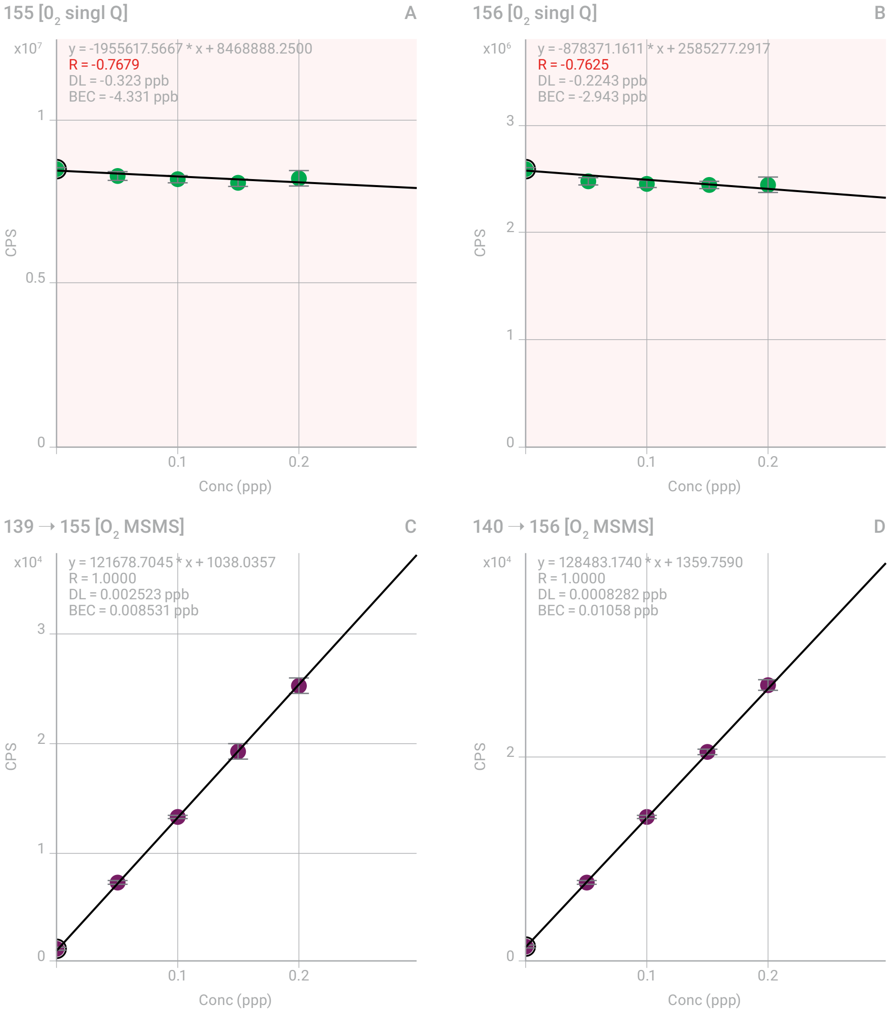

Figure 2. Top: Calibration plots up to 0.2 ppb for La in 50 ppm Ba matrix (A) and Ce in 50 ppm La matrix (B), acquired in SQ mode with oxygen reaction gas (emulating conventional quadrupole ICP-MS). Bottom: Calibration plots up to 0.2 ppb for La in 50 ppm Ba matrix (C) and Ce in 50 ppm La matrix (D) acquired in MS/MS mode with oxygen mass-shift.

Investigation of unexpected product ion observed at *m/z* 156 in the 50 ppm La matrix

The background signals that contributed to the poor result obtained for Ce in the La matrix using SQ mode with O_2 reaction gas (Figure 2B) were investigated by carrying out a precursor ion scan for product ion mass 156. The precursor ion scan capability of the 8800 ICP-QQQ provides a uniquely powerful approach to identifying the source of potential polyatomic and reaction product interferences. Oxygen cell gas was introduced into the cell and a precursor ion spectrum was obtained by scanning Q1 from 2 to 260 u (Figure 3) with Q2 fixed at mass 156. From the spectrum, we can identify which precursor ions react with O_2 to produce product ions at mass 156, overlapping $^{140}CeO^+$ in SQ mode.

Figure 3 shows the precursor ion scan spectrum for product ion mass 156 for the 50 ppm La matrix, with intense peaks at *m/z* 139 ($^{139}La^+$) and 156 ($^{139}La^{16}OH^+$). In SQ mode, as with conventional ICP-QMS, these ions all enter the cell, and with Q2 set to 156 u, the $^{139}La^{16}OH^+$ polyatomic ions contribute to the signal measured at *m/z* 156 (^{140}Ce measured as analyte product ion $^{140}CeO^+$). These unwanted precursor ions cannot be rejected by a CRC operating as a bandpass filter in ICP-QMS, as they are too close in mass to the target analyte precursor ion. Only by using MS/MS mode on the 8800 ICP-QQQ, where Q1 operates as a unit mass filter, can non-target masses (like $^{139}La^{16}OH^+$ in this example) be prevented from entering the cell.

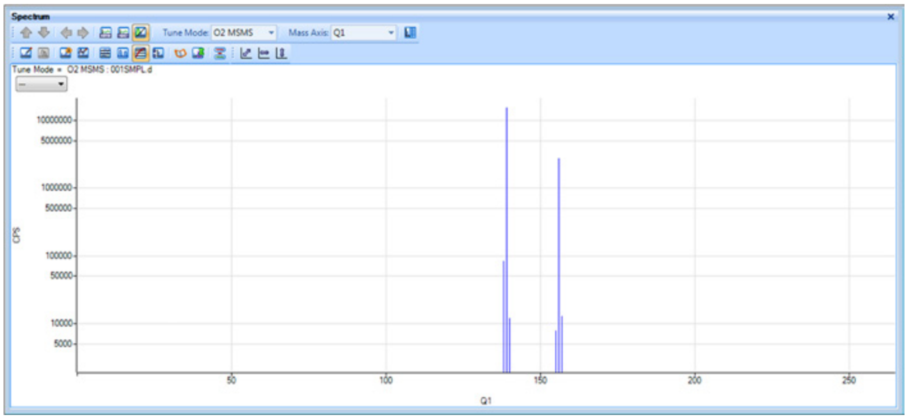
Tune Mode: O2 MSMS

Mass Axis: Q1

Tune Mode = O2 MSMS : 001SMPL.d

Figure 3. Precursor ion scan from 2-260 u for product ion mass 156, in a 50 ppm La matrix. Six peaks are seen at *m/z* = 138, 139, 140, 155, 156 and 157, with the intense peaks at *m/z* 139 and *m/z* 156 being due to $^{139}La^+$ and $^{139}La^{16}O^1H^+$ respectively.

Reference

1. Sabine Becker and Hans Joachim Dietze, J. Anal. At. Spectrom., 1997, vol.12, p881.

More information

Removal of hydride ion interferences (MH+) on Rare Earth Elements using the Agilent 8800 Triple Quadrupole ICP-MS, Agilent publication, 5991-1481EN

Direct Analysis of Trace REEs in High Purity Nd_2O_3

Authors

Juane Song[1], Xiang-Cheng Zeng[1], Dong Yan[1] and Wei-ming Wu[2]

[1]Agilent Technologies, China,
[2]Jiangxi University of Science and Technology, Jiangxi, China

Keywords

Rare earth elements (REE), high purity metals, neodymium, neodymium (III) oxide, oxygen mass-shift, ammonia on-mass, ammonia mass-shift, geochemistry, mining, materials science

Introduction

Advanced technology products containing Rare Earth Elements (REEs) are increasing at a rapid rate. However, the presence of other REEs as contaminants in a purified single-element REE material may affect the functionality of the final product, so impurities in the REE oxide raw material must be carefully controlled.

The measurement of mid- and high-mass REEs in a low-mass REE matrix is challenging for ICP-MS because REEs have high metal-oxide (M-O) bond strengths, and the oxide ions of the low mass REEs overlap the preferred isotopes of the mid-mass and high-mass REEs. For example, in the analysis of trace REEs in high purity Nd_2O_3, $^{145}Nd^{16}OH_2^+$ and $^{146}Nd^{16}OH^+$ overlap the preferred isotope of dysprosium ($^{163}Dy^+$), $^{143}Nd^{16}O^+$ overlaps the only isotope of terbium ($^{159}Tb^+$) and $^{148}Nd^{16}OH^+$ overlaps the sole isotope of holmium ($^{165}Ho^+$). While separation of the trace REEs from the REE matrix can be performed using a chelating resin, this technique is time-consuming and needs to be customized to the particular analyte and matrix under investigation. Clearly there is a requirement for a method capable of the direct analysis of trace REEs in a variety of high purity REE matrices.

Experimental

Instrumentation: Agilent 8800 #100.

Plasma conditions: Preset plasma/HMI-L.

Acquisition parameters:
Five operational modes were evaluated:

- No gas
- Helium mode, 5 mL/min
- O_2 mass-shift, 0.3 mL/min
- NH_3 on-mass, 8 mL/min (NH_3 as 10% NH_3 in He)
- NH_3 mass-shift, 3 mL/min, (NH_3 as 10% NH_3 in He).

Sample and sample prep: High purity Nd_2O_3 (99.999%, purchased from the Baotou Research Institute of Rare Earths, China) was dissolved gently in semiconductor grade HNO_3, and diluted to 500 ppm as Nd_2O_3.

Results and discussion

Thirteen trace REEs were measured in the Nd_2O_3 sample using the five different cell modes, and the results are summarized in Table 1. As expected, the BEC of low- and mid-mass REEs, such as La, Ce, Pr, Sm, Eu and Gd (Pr and Sm were present as impurities) were comparable in all modes, as these elements are free from interferences due to Nd. In contrast, the BECs for high-mass REEs in He mode were lower in He mode than in no gas mode, suggesting that high mass REEs suffered interferences from Nd-derived polyatomic ions.

Table 1. BECs of 13 REEs in 500 ppm Nd_2O_3. All units ug/kg (ppb).

Element	Isotope	No gas	He	O_2 mass-shift	**NH_3 on-mass**	NH_3 mass-shift
La	139	0.143	0.127	0.143	-	-
Ce	140	0.018	0.012	0.011	-	-
Pr	141	1.376	1.202	1.056	-	-
Sm	152	1.061	0.950	0.999	-	-
Eu	153	0.032	0.026	0.028	-	-
Gd	155	0.035	0.046	0.033	-	-
Tb	159	442.6	74.6	1.258	-	0.022
Dy	163	250.3	196	1.161	0.040	-
Ho	165	20.43	16.2	0.101	0.004	-
Er	170	0.065	0.020	0.013	-	-
Tm	169	0.084	0.031	0.003	-	-
Yb	174	0.251	0.120	0.058	-	-
Lu	175	0.014	0.006	0.004	-	-

O_2 mass-shift mode

All 13 REEs react with O_2 efficiently to form REE-oxide ions, as shown below.

$$REE^+ + O_2 \rightarrow REE\text{-}O^+ + O$$

The MS/MS capability of the 8800 ICP-QQQ enables the removal of spectral interferences on each element using "mass-shift". For example in O_2 mass-shift mode, all 13 REEs can be detected as REE-O^+ ions at 16 u higher than the original elemental mass (M+16). From Table 1, it can be seen that O_2 reaction mode with mass-shift further reduced the BEC for Tb, Dy, Ho, Er, Tm, Yb, and Lu, compared to He mode.

While the improvement in O_2 mass-shift mode is significant for Tb, Dy and Ho that suffer intense interference from NdO^+, the BECs of the other high-mass REEs such as Er, Tm, Yb and Lu were also improved in this mode, indicating that these elements also suffer interferences from Nd-based polyatomic ions: $^{150}NdOH_3^+$ interferes with $^{169}Tm^+$, $^{142}NdN_2^+$ (or $^{142}NdCO^+$) and $^{144}NdCN^+$ with $^{170}Er^+$, $^{142}NdO_2^+$ with $^{174}Yb^+$, $^{143}NdO_2^+$ and $^{144}NdONH^+$ (or $^{144}NdC_2H^+$) with $^{175}Lu^+$. The contribution of the above mentioned interferences on Er, Tm, Yb and Lu are not overly significant. However, O_2 mass-shift mode was shown to be an effective approach for the removal of all polyatomic ion interferences, typically leading to a 5-10x lower BEC compared to no gas mode.

NH_3 on-mass mode for Dy and Ho

A previous study showed that NH_3 cell gas reacts with many of the polyatomic ions that interfere with the REEs. However, NH_3 also reacts quickly with some of the REE ions, leading to reduced sensitivity of < 1 cps/ppt for La, Ce, Nd, Sm, Gd, Tb and Lu. NH_3 on-mass mode is valuable for the determination of a limited number of REEs; Pr, Eu, Dy, Ho, Er, Tm and Yb [*1*]. The results in Table 1 show that NH_3 on-mass mode gave excellent results for Dy and Ho in the Nd_2O_3 matrix, with an improvement in BECs of 20x compared to O_2 mass-shift mode.

NH_3 mass-shift mode for Tb

For the REEs that react efficiently with NH_3 (La, Ce, Nd, Sm, Gd, Tb and Lu), NH_3 mass-shift mode can be used. In this study, NH_3 mass-shift mode was investigated for the determination of Tb, and the reaction product ion $TbNH^+$ (*m/z* 174) was found to give the lowest BEC. A BEC of 22 ppt for Tb in a 500 ppm Nd_2O_3 solution was achieved, which is 50x lower than the result achieved in O_2 mass-shift mode, indicating the effective removal of the NdO^+ overlap.

Conclusion

The Agilent 8800 ICP-QQQ with MS/MS capability was used to successfully measure 13 REE impurities in a high-purity Nd_2O_3 sample solution. Tandem MS with MS/MS mode is essential for accurate reaction mode analysis in a complex matrix. On conventional quadrupole ICP-MS, there is no additional quadrupole (Q1) to select which ions can enter the cell. As a result, all ions enter the cell so, when a reactive cell gas is used, a complex and variable population of reaction product ions is created, depending on the sample matrix and other analytes. With ICP-QQQ, the first quadrupole selects only the target mass to pass into the cell, so the reaction chemistry is controlled and consistent. With the combination of HMI and MS/MS reaction cell mode, the 8800 ICP-QQQ provided effective removal of the polyatomic interferences from the Nd matrix.

Reference

1. Naoki Sugiyama and Glenn Woods, Direct measurement of trace rare earth elements (REEs) in high-purity REE oxide using the Agilent 8800 Triple Quadrupole ICP-MS with MS/MS mode, Agilent publication, 2012, 5991-0892EN.

More information

Application note: Routine determination of trace rare earth elements in high purity Nd_2O_3 using the Agilent 8800 ICP-QQQ. Agilent publication 5991-5400EN

> Return to table of contents
> Search entire document

Direct Determination of Challenging Trace Rare Earth Elements in High Purity Lanthanide REE Oxides

Authors

Juan-e Song and Xiang-cheng Zeng
Agilent Technologies, China

Keywords

Rare Earth Elements, REE, rare earth oxides, REO, oxygen mass-shift, ammonia on-mass, ammonia mass-shift

Introduction

ICP-MS is widely used for trace impurity analysis of high purity rare earth element (REE) oxide materials. But the analysis of trace REEs in high purity REE oxide materials remains challenging. Matrix-based polyatomic ions such as $REEO^+$, $REEOH^+$, and $REEH^+$ cause severe spectral interferences on some REE elements. Trace REE analytes can be separated from the REE matrix using a chelating resin, but this technique is time-consuming, and customization is needed per the analyte and matrix element.

In this study, trace REEs in lanthanide oxide materials were determined using an Agilent 8900 ICP-QQQ with O_2 and NH_3 reaction cell gases. Since the analysis of La_2O_3, Tm_2O_3 and Lu_2O_3 is relatively interference free, these matrices weren't included in the study.

Experimental

Instrumentation: An Agilent 8900 Advanced Applications configuration ICP-QQQ was used without any modification. For the analysis of 500 ppm REE matrix samples, 'general-purpose plasma' conditions were selected in the MassHunter software. The preset plasma function automatically sets all plasma-related parameters, simplifying instrument set-up.

Five cell modes were investigated: no gas, helium (He), oxygen (O_2), and ammonia (20% NH_3 in He). Tuning conditions are summarized in Table 1. In NH_3 mass-shift mode, a pre-study was done using 'product ion scan' to identify the most abundant NH_3 cluster ion. The masses of the cluster ions used for the analysis are given in Tables 2 and 3, together with the analytical results.

Table 1. Cell gas mode-related tuning parameters.

Cell gas mode	No gas	He	O_2 mass-shift	NH_3 on-mass	NH_3 mass-shift
Scan Mode	Single Quad		MS/MS		
Octopole bias (V)	-8	-18	-3	-5	-5
Octopole RF (V)	140	180	180	180	180
KED (V)	+5	+4	-7	-7	-7
Axial Acceleration (V)	0	1	1.5	0.5	0.5
He (mL/min)		5		1	1
O_2 (mL/min)			0.45		
NH_3 (mL/min)				4.0 ~ 6.0	1.0 ~ 8.0

Results and discussion

Ten REE oxide materials of the highest-grade purity (5N) including Ce_2O_3, Pr_6O_{11}, Nd_2O_3, Gd_2O_3, Sm_2O_3, Eu_2O_3, Tb_4O_7, Dy_2O_3, Er_2O_3, and Yb_2O_3 were dissolved in semiconductor grade HNO_3 and diluted to 500 ppm (as REE oxide). H_2O_2 was added during the dissolution of Ce_2O_3 and Tb_4O_7. REEs were measured in each matrix solution using the five cell modes specified in Table 1. The results are given in Tables 2 and 3.

As expected, in no gas mode, the BECs for the REEs were relatively high due to spectral interferences. He collision cell mode was able to alleviate some of the interferences, but not all. Previous studies have shown that both O_2 and NH_3 are effective for the removal of polyatomic ions that interfere with the REEs [*1*, *2*]. A drawback of NH_3 mode has been low sensitivity. However, Axial Acceleration of cluster ions in the cell of the 8900 ICP-QQQ increases sensitivity. The results reported in Tables 2 and 3 show that the BECs for all REEs were dramatically improved using a reactive cell gas. The improvement factor data relates to the difference in BEC obtained in reaction mode compared to no gas mode.

Table 2. BECs of REE impurities in 500 ppm Ce, Pr, Nd, and Gd oxide solutions.

Sample			Ce_2O_3			PrO	Nd_2O_3			Gd_2O_3		
Analyte			Pr	Gd	Tb	Tb	Tb	Dy	Ho	Tb	Yb	Lu
Isotope			141	160	159	159	159	163	165	159	172	175
Interference			$^{140}CeH^+$	$^{142}Ce^{18}O^+$	$^{142}Ce^{16}OH^+$	$^{141}Pr^{18}O^+$	$^{142}NdOH^+$, $^{143}NdO^+$	$^{145}Nd^{18}O^+$	$^{148}NdOH^+$	$^{158}GdH^+$	$^{156}GdO^+$	$^{159}GdOH^+$
BEC (ppb)	No gas		6.17	3.36	29.2	10.3	721	163	13.4	2.23	3420	75.0
	He		3.79	11.9	0.725	2.50	234	36.6	3.06	2.16	1200	66.4
	O_2		0.064	0.030	9.76	0.001	1.95	0.804	0.070	0.106	284	0.444
	NH_3	BEC			0.284	0.055	0.039	0.255	0.021		0.030	7.16
		mass pair			(159/174)	(159/244)	(159/174)	(163/163)	(165/165)		(172/172)	(175/260)
Improvement factor			x100	x100	x100	x10,000	x20,000	x1000	x1000	x20	x100,000	x200

Table 3. BECs of REE impurities in 500 ppm Sm, Eu, Tb, Dy, Er, and Yb oxide solutions.

Sample			Sm_2O_3				Eu_2O_3	Tb_4O_7	Dy_2O_3	Er_2O_3	Yb_2O_3
Analyte			Dy	Ho	Er	Tm	Tm	Lu	Ho	Tm	Lu
Isotope			162	165	167	169	169	175	165	169	175
Interference			$^{147}SmO^+$	$^{148}SmOH^+$, $^{149}SmO^+$	$^{150}SmOH^+$	$^{152}SmOH^+$	$^{141}EuO^+$	$^{159}TbO^+$	$^{164}DyH^+$	$^{168}ErH^+$	$^{174}YbH^+$
BEC (ppb)	No gas		0.408	185	44.9	39.0	64.8	3270	2.13	1.26	0.97
	He		0.169	61.9	18.1	13.6	38.20	1670	1.28	1.57	1.38
	O_2		0.083	0.158	0.916	0.240	2.73	26.1	0.057	0.025	0.195
	NH_3	BEC	0.035	0.055	0.092	0.127	0.002	0.244	0.074		
		mass pair	(162/162)	(165/165)	(167/167)	(169/169)	(169/169)	(175/260)	(165/165)		
Improvement factor			x10	x3000	x500	x200	x30,000	x10,000	x50	x50	x5

Conclusion

The Agilent 8900 ICP-QQQ method was used to measure REE impurities in high purity REE oxide materials. REE matrix-based hydride, oxide, and hydroxide polyatomic ion interferences were removed by operating the ICP-QQQ in MS/MS mode with O_2 and NH_3 reaction cell gases. The BECs were improved by one to four orders of magnitude using reactive cell gases compared to no gas mode. The method is suitable for the direct analysis of trace REEs in the presence of high concentration matrix-REEs.

References

1. Direct measurement of trace rare earth elements (REEs) in high-purity REE oxide using the Agilent 8800 Triple Quadrupole ICP-MS with MS/MS mode, Agilent application note, 2012, 5991-0892EN
2. Routine determination of trace rare earth elements in high purity Nd_2O_3 using the Agilent 8800 ICP-QQQ, Agilent application note, 2015, 5991-5400EN

> Return to table of contents
> Search entire document

Lead Isotope Analysis: Removal of ^{204}Hg Isobaric Interference on ^{204}Pb using ICP-QQQ MS/MS Reaction Cell

Author

Glenn Woods
Agilent Technologies, UK

Keywords

lead, isotope, ratio, geochronology, dating, mercury, artifacts, precious metals, food, ammonia, on-mass

Introduction

Lead isotope ratio analysis is important as it is used for Pb-Pb dating in geochronology, and to trace the origin of artifacts, precious metals and even foodstuffs. The natural isotopic pattern of lead varies more than any other element in the periodic table, because three of its isotopes are formed from the radioactive decay of uranium ($^{235}U \rightarrow {}^{207}Pb$; $^{238}U \rightarrow {}^{206}Pb$) and thorium ($^{232}Th \rightarrow {}^{208}Pb$). The Pb isotopic pattern can therefore vary depending upon the geology of the rocks and minerals from which the lead was extracted, and the age of the material. In geochronology, the constant rate of U/Th decay allows the Pb/Pb, U/Pb and Th/Pb ratios to be used to date the age of rocks using a so-called geological clock.

When Pb ratios are measured, it is often necessary to correct for the lead naturally present in the sample, and the only non-radiogenic isotope of Pb (^{204}Pb; natural or common lead), is used for this purpose. For Pb-Pb dating, ^{204}Pb is the reference isotope against which the radiogenic isotopes are compared ($^{206}Pb/^{204}Pb$; $^{207}Pb/^{204}Pb$). Unfortunately, ^{204}Pb is directly overlapped by an isotope of Hg (^{204}Hg), which makes accurate measurement of ^{204}Pb impossible by ICP-MS. Mass resolution of ^{204}Pb from ^{204}Hg is far beyond the capability of any commercial high-resolution (HR-) ICP-MS system, and until recently there has been no reliable chemical means to remove the Hg interference, so mathematical correction has been employed, which introduces error. Mercury does however undergo a gas-phase charge-transfer reaction with ammonia gas (NH_3), a reaction that can be utilized in the collision/reaction cell of a suitably equipped ICP-MS as follows:

$$Hg^+ + NH_3 \rightarrow Hg^0 + \text{“}NH_3^+\text{”}$$

This reaction offers the potential to remove the ^{204}Hg interference from ^{204}Pb, and could be applied to either solution or laser-based ICP-MS analysis.

Experimental

Instrumentation: Agilent 8800 #100.

Plasma conditions: Preset plasma/General purpose.

Ion lens tune: Soft extraction tune: Extract 1 = 0 V, Extract 2 = -170 V.

CRC conditions: NH_3 gas (10% in He) at 1.7 mL/min, Octopole bias = -8 V, KED = -8 V.

Acquisition parameters: Three acquisition modes were compared:

- **No gas:** No reaction cell gas; Single Quad (SQ) mode with Q1 operating as an ion guide.
- **NH_3 bandpass:** Ammonia reaction gas; SQ mode with Q1 operating as a bandpass filter.
- **NH_3 MS/MS:** Ammonia reaction gas; MS/MS mode with Q1 operating as a mass filter at unit mass resolution.

Results and discussion

Removal of $^{204}Hg^+$ interference on $^{204}Pb^+$

A preliminary study showed that Pb is almost unreactive with NH_3 cell gas (<0.5% loss of Pb signal) indicating that on-mass sensitivity for Pb should be maintained. On-mass measurement of Pb in NH_3 cell gas mode was therefore investigated in the presence of Hg at 10 ppb. Figure 1 displays the spectra obtained in no gas (left) and NH_3 cell gas (right) modes. The ^{204}Hg interference on ^{204}Pb can be clearly seen in the no gas spectrum, while it has been completely removed under NH_3 reaction mode with MS/MS. A perfect isotopic pattern match was confirmed for Pb in NH_3 mode.

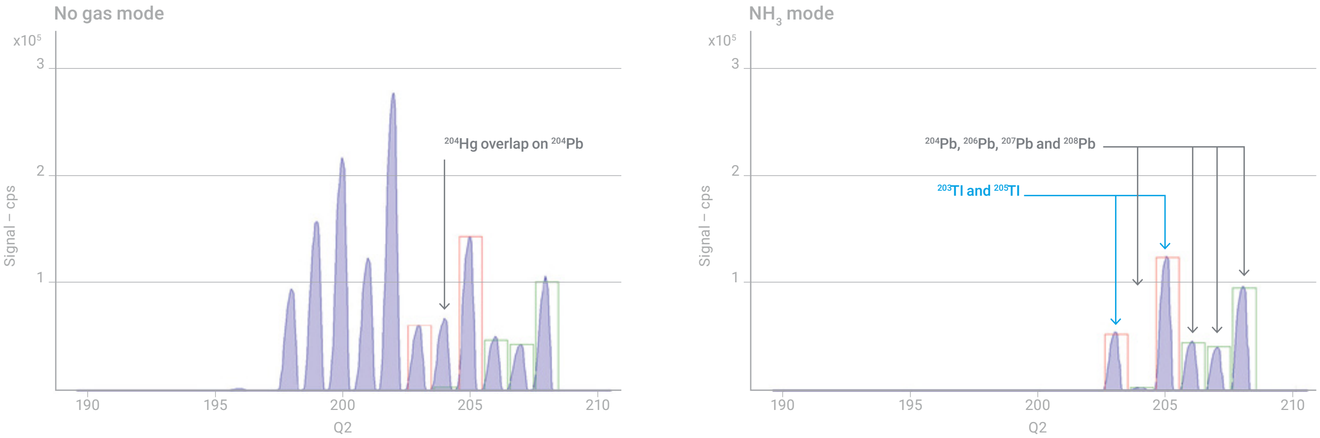

Figure 1. Standard solution (1 ppb each of Pb and Tl) spiked with 10 ppb Hg without cell gas (left) and with NH_3 (right) using MS/MS mode. Note the ^{204}Hg interference on ^{204}Pb in no gas mode.

Effectiveness of MS/MS

The NH_3 reaction that removes the ^{204}Hg interference would also work in the reaction cell of a single quadrupole ICP-MS (ICP-QMS), but ammonia is a highly reactive gas and can produce many adduct cluster ions, for example from Rare Earth Elements (REEs), see Table 1. The complex matrix composition of many natural samples means that the results obtained with NH_3 cell gas in ICP-QMS are often extremely unreliable. With the 8800 ICP-QQQ, MS/MS mode allows all the co-existing matrix elements to be rejected by Q1, so only the target ions (^{204}Pb and ^{204}Hg) enter the CRC. The NH_3 reactions are therefore controlled and consistent, and no overlapping reaction product ions are formed from other elements in the sample.

Table 1. Some possible Rare Earth Element cluster ions that can form in the CRC of an ICP-QMS when using NH_3 reaction gas – the list is by no means exhaustive.

Mass	Potential Cluster Ions of REE
204	$Eu(NH_3)_3$; $Yb(NH_3)_2$; $Ce(NH_3)_4$
205	$Yb(NH_3)_2$; $Gd(NH_3)_3$
206	$Yb(NH_3)_2$; $Lu(NH_2)_2$; $La(NH_3)_4$; $Ce(NH_3)_4$; $Gd(NH_3)_3$
207	$La(NH_3)_4$; $Yb(NH_3)_2$; $Gd(NH_3)_3$
208	$Ce(NH_3)_4$; $GdNH(NH_3)_2$; $TbNH(NH_3)_2$; $Yb(NH_3)_2$; $Gd(NH_3)_3$

To check the formation of cluster ions, the ICP-QQQ was operated with NH_3 cell gas; "Single Quad bandpass" and MS/MS modes were compared for the measurement of a 50 ppb REE mix. Figures 2a and 2b display the spectra obtained using bandpass and MS/MS conditions, respectively.

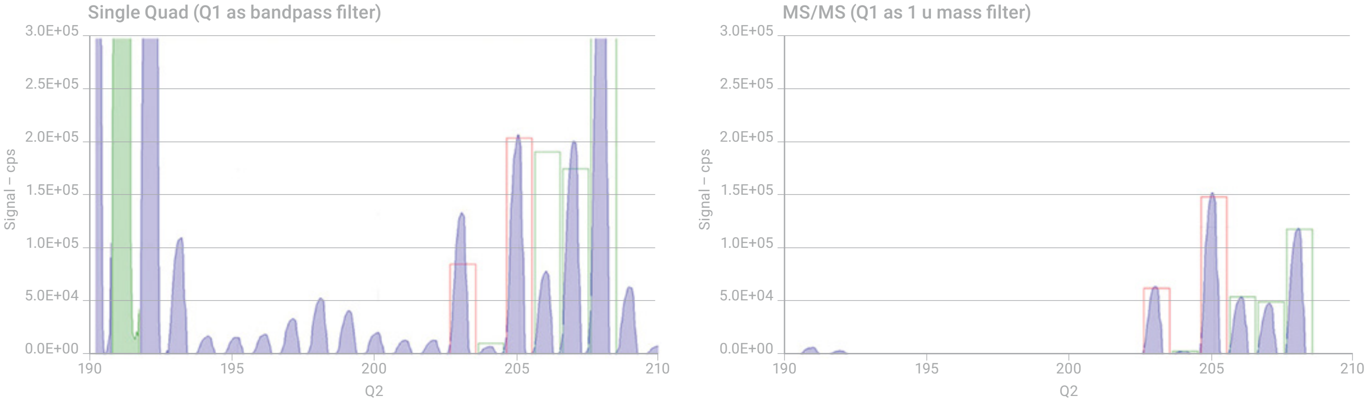

Figure 2. Cluster ion formation for 50 ppb REE standard in ammonia mode. Figure 2a (left): REE cluster ion formation using ammonia cell gas in bandpass mode; REE's are allowed into the cell if Q1 is operated as a bandpass filter. The REE cluster ions can be seen at all masses including those for Hg, Tl, Pb and Bi. Figure 2b (right): The identical sample under the same ammonia conditions but this time with Q1 operated at unit mass resolution (MS/MS mode). The REE's are removed from the ion beam before they can enter the cell and form reaction by-products.

^{204}Pb/^{208}Pb isotope ratio analysis in presence of Hg

To check the effectiveness of the ^{204}Hg removal, the ^{204}Pb/^{208}Pb ratio was measured in a 1 ppb lead solution spiked with increasing Hg concentration. Table 2 displays the measured Pb ratio results (without any mass bias correction), showing that the Pb isotope ratio remained constant, regardless of the Hg content.

Table 2. Uncorrected isotopic ratios measured in 1 ppb Pb solutions containing mercury at varying concentrations. The lead isotopic ratio 204/208 is not influenced by the presence of Hg.

	^{204}Pb	^{208}Pb	IR (204/208)
Sample		CPS	
Theoretical	NA	NA	0.02671
Pb	3518.5	136124.8	0.02585
Pb Hg 5 ppb	3510.0	139585.9	0.02515
Pb Hg 10 ppb	3439.2	132796.4	0.02590
Pb Hg 20 ppb	3464.8	134417.7	0.02578

Conclusion

With the successful removal of the ^{204}Hg interference on the natural ^{204}Pb isotope, ICP-QQQ displays great promise for Pb/Pb and U/Pb dating and for other applications where accurate measurement of ^{204}Pb is required.

> Return to table of contents
> Search entire document

Fractionation of Sulfur Isotope Ratio Analysis in Environmental Waters

Author

Naoki Sugiyama
Agilent Technologies, Japan

Keywords

sulfur, sulfur isotope ratio, isotope ratio analysis, fractionation, mass-shift

Introduction

Sulfur isotope ratio (IR) data is a useful indicator in geochemical and biochemical studies [1]. In stable sulfur isotope analysis, the variation in the $^{34}S/^{32}S$ IR is calculated and reported as a deviation or delta (δ) in ^{34}S abundance relative to a standard material, the troilite (iron sulfide) mineral from the Canyon Diablo meteorite. This standard is referred to as δVCDT (Vienna Canyon Diablo Troilite). Natural variations in ^{34}S abundance, expressed in parts per thousand or "per mil" (‰), can be of the order of -50‰ to +40‰ (and occasionally much greater), due to redox reaction [2]. In this study, triple quadrupole ICP-MS (ICP-QQQ) was investigated as a fast and simple technique for S IR analysis. ICP-QQQ is a tandem ICP-MS that can resolve spectral interferences using reaction cell technologies. Using the method described in this paper, ICP-QQQ can measure S at a low concentration (background equivalent concentration < 0.2 ppb in UPW) with high sensitivity (^{32}S > 10000 cps/ppb).

Experimental

Instrumentation: Agilent 8900 Advanced Applications configuration ICP-QQQ with PFA nebulizer. Self-aspiration mode was used for better precision.

Tuning: O_2 mass-shift method. Tuning conditions are summarized in Table 1.

Method: the following procedures were used for the accurate determination of sulfur IRs:

- **Matrix matching:** all samples were diluted by the matrix blank, which contained 50 ppm Ca and 100 ppm NaCl in 1% HNO_3.
- **Concentration matching:** each sample was diluted by the matrix blank to ~0.5 ppm S concentration. This dilution was done to remove any errors caused by signal count differences. For example, NASS 5 was diluted 2000 times and mineral water A was diluted 10 times.
- **Mass bias correction:** to correct mass bias (including mass-bias drift), sample-standard bracketing was applied. IR of 0.5 ppm IAEA-S-1 [3] was measured before and after the IR analysis of each sample. The average of the IRs for the standard was used to correct the mass-bias and the drift.

Table 1. ICP-QQQ tuning and method parameters.

	Tuning parameter	Unit	Value
Plasma	RF power	W	1550
	Sampling depth	mm	8.0
	Nebulizer gas flow rate	L/min	0.90
	Make-up gas flow rate	L/min	0.30
Lens	Extract 1	V	-80
	Extract 2	V	-150
	Omega	V	10.0
	Omega bias	V	-120
Cell	Octp Bias	V	-5.0
	Axial Acceleration	V	2.0
	KED	V	-8.0
	Cell gas		Oxygen
	Cell gas flow rate	mL/min	0.45

	Method parameter	Unit	Value
Data acquisition	Integration time	s	1 and 5 for ^{32}S and ^{34}S
	Number of sweeps	–	1000
	Number of replicates	–	10
Rinse	1% HNO_3 rinse	s	20
	50 ppm/100 ppm NaCl rinse	s	30
Sample load	Load time	s	30
	Stabilization time	s	30

Results and discussion

Figure 1 shows a spectrum of three sulfur isotopes in a blank and 10 ppb S standard measured by ICP-QQQ in O_2 mass-shift mode. The two spectra show the low BEC of sulfur in the blank, which allows accurate S IR analysis.

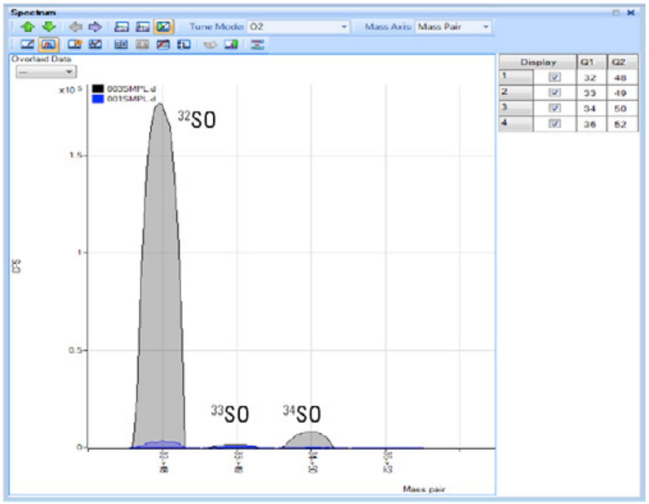

Tune Mode: O2

Mass Axis: Mass Pair

	Display	Q1	Q2
1	☑	32	48
2	☑	33	49
3	☑	34	50
4	☑	36	52

Figure 1. Spectra of S isotopes measured in O_2 mass-shift mode. The blank is indicated in blue and the 10 ppb S standard in grey. The spectra show that the BEC of the blank is < 200 ppt.

Synthetic samples were prepared and analyzed. Two standards, IAEA S-1 ($^{34}\delta$ = -0.3‰) and IAEA S-2 ($^{34}\delta$ = +22.6‰), were mixed to make four synthetic samples with a theoretical S IR of $^{34}\delta$ = -0.3, 5.4, 11.2 and 22.6 ‰. Each sample was measured six times, and the average IR and precision (as two times the standard deviation) were calculated. As shown by the linearity of Figure 2, the measured $^{34}\delta$ values were in excellent agreement with the theoretical values.

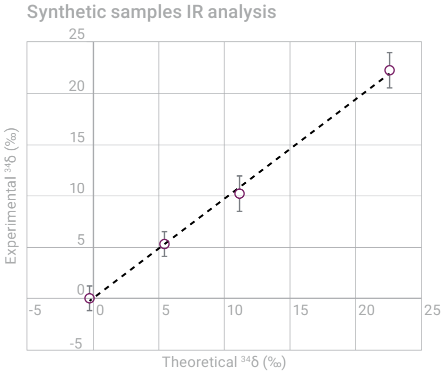

Figure 2. Sulfur IR of four synthetic samples.

The developed method was used to analyze seven samples: sulfuric acid (Tamapure AA-100); a Japan river water CRM, JSAC0301; a hot spring water, IKAHO; three mineral waters A, B, and C; and a seawater SRM, NASS-5. The concentration of S was first determined in each sample. The samples were then diluted with the matrix blank (50 ppm Ca + 100 ppm NaCl) to ~0.5 ppm of S. The IR of each sample was measured 10 times to determine the average value and precision (as two times the standard deviation). The results given in Figure 3 show ±1.2 to ±1.7 ‰ error.

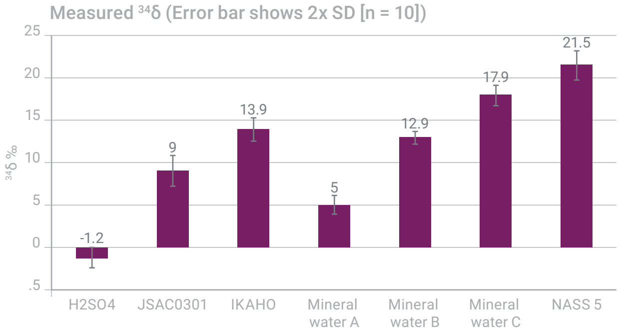

Figure 3. Measured $\delta^{34}S$ of seven samples.

Conclusion

The Agilent 8900 Advanced Applications configuration ICP-QQQ is ideally suited to $^{34}S/^{32}S$ isotope ratio analysis. The analysis can provide valuable information for sample characterization in natural systems or to monitor anthropogenic impact. The 8900 ICP-QQQ provides a low background and high sensitivity for sulfur, which enabled a method to be developed that required the sample to be diluted with the matrix blank before analysis. The precision of the IRs achieved was excellent at 1.2–1.7 ‰ (as two times the standard deviation).

References

1. J. Ryu, R.A. Zierenberg, R.A. Dahlgren et al., **2006**, *Chemical Geology* 229: 257-2722.
2. H.G. Thode, *Mineral. Soc. Amer. Spec.*, **1970**, Pap. 3: 133–144
3. National Institute of Standards and Technology certificate sheet for Reference Material 8554 -IAEA-S-1 (Sulfur Isotopes in Silver Sulfide)

More information

Sulfur isotope fractionation analysis in mineral waters using an Agilent 8900 ICP-QQQ, Agilent publication 5991-7285EN

> Return to table of contents
> Search entire document

Measurement of $^{87}Sr/^{86}Sr$ Isotope Ratios in Rocks by ICP-QQQ in Mass-Shift Mode

Authors

Xiaoming Liu[1]
Yahui Yue[1]
Yibo Yang[1]
Shuofei Dong[2]

[1] Institute of Tibetan Plateau Research, Chinese Academy of Sciences, Beijing 100085, China

[2] Agilent Technologies Co., Ltd. (China), Beijing 100102, China

The direct Agilent 8900 ICP-QQQ method removes need for chromatographic separation of ^{87}Sr and ^{87}Rb

Introduction

Triple quadrupole ICP-MS (ICP-QQQ) instrumentation is increasingly used for isotope ratio (IR) analysis studies (*1–5*). Geologists use radioactive isotopes that have long half-lives to date rocks and sediments, often with the choice of dating method dependent on the type of samples under investigation. For example, rubidium (Rb) is abundant in many potassium-containing rocks, so the Rb-strontium (Sr) β-decay scheme is used in geochronology studies of igneous, and sometimes metamorphic rocks and minerals (*5, 6*).

Strontium (Sr) has four naturally occurring isotopes: ^{84}Sr (0.56% abundance), ^{86}Sr (9.86% abundance), ^{87}Sr (7.00% abundance), and ^{88}Sr (82.58% abundance). While these are the four stable isotopes of Sr, the abundance of ^{87}Sr varies over long periods of time due to the formation of radiogenic ^{87}Sr following β-decay of ^{87}Rb. The level of ^{87}Sr compared to ^{86}Sr is dependent on the original concentration of Rb in the environmental or geological system. Therefore, $^{87}Sr/^{86}Sr$ IR measurements can also serve as a tracer of ecosystem processes (*7*).

Traditional IR measurement techniques such as thermal ionization mass spectrometry (TIMS) or multicollector inductively coupled plasma mass spectrometry (MC-ICP-MS) offer excellent accuracy and high precision for most IR studies. However, they are less efficient for the measurement of β decay product isotopes, due to isobaric interferences of the daughter isotope by their respective parent isotope. For example, ^{87}Sr must be separated from ^{87}Rb before analysis by TIMS or MC-ICP-MS to avoid the isobaric spectral overlap at mass 87. This process is labor-intensive and time consuming, especially for large sample numbers that are typical of geological and environmental survey studies. By contrast, no Rb/Sr separation is needed before analysis using ICP-MS/MS methodology, simplifying the analysis and improving sample throughput. ICP-MS/MS methods use "chemical resolution" to resolve isobaric interferences, as demonstrated in previous studies using Agilent ICP-QQQ instrumentation (*1, 5*).

In those studies, reactive gases were used in the collision/reaction cell (CRC) of the ICP-QQQ to separate the isobaric overlap from ^{87}Rb on ^{87}Sr, avoiding the need for chromatographic separation. Isobaric ion interferences can be separated using ICP-QQQ when the cell gas reacts quickly with one of the elements to form a product ion, while the other element does not react (or reacts slowly). Although reaction cell gases such as CH_3F, N_2O, and SF_6 provide a higher reaction rate with Sr^+ than O_2, O_2 is more widely available in laboratories and is more suited to routine applications.

The aim of this study was to develop a fast, high throughput, routine method suitable for the accurate determination of $^{87}Sr/^{86}Sr$ IR with precision below 0.1% RSD. To achieve the objective, an Agilent 8900 ICP-QQQ was operated in MS/MS mass-shift mode using O_2 as the cell gas.

$^{87}Sr/^{86}Sr$ IR analysis by ICP-QQQ in O_2 mass-shift mode

The Agilent 8900 Triple Quadrupole ICP-MS (ICP-QQQ) uses two identical, full-sized quadrupoles (Q1 and Q2), one before and one after the ORS[4] reaction cell. Like the analyzer mass filter, Q2, Q1 operates in a high vacuum region, so it provides excellent resolution and abundance sensitivity. This allows precise selection of which ions enter the cell, ensuring the reactions used to resolve the analyte ions from their on-mass interferences are consistent and predictable. As shown in Figure 1, by setting Q1 to *m/z* 87, only Rb-87 and Sr-87 enter the cell that is pressurized with O_2. In the cell, $^{87}Sr^+$ reacts with O_2 to form $^{87}Sr^{16}O^+$ product ion, while $^{87}Rb^+$ does not react. The second quadrupole (Q2) is set to *m/z*=103, which allows $^{87}Sr^{16}O^+$ to pass to the detector, free of interference.

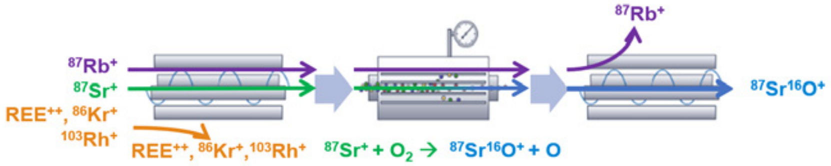

Figure 1. Determination of ^{87}Sr as $^{87}Sr^{16}O^+$ product ion using ICP-QQQ operating in mass-shift mode with O_2 cell gas.

Efficiency of using mass-shift mode to separate Sr from Rb

When Sr^+ ions react with O_2 in the cell, not all Sr^+ ions complete the reaction to form SrO^+ ions during the short transit time in the cell. To optimize the O_2 flow rate, counts per second (cps) of both $^{86}Sr^+$ (at *m/z* 86) and $^{86}Sr^{16}O^+$ (at *m/z* 102) were monitored. For the calculation, the measured cps of Q1 (*m/z* = 86) → Q2 (*m/z* = 102) was divided by the cps of Q1 (*m/z* = 86) → Q2 (*m/z* = 86). The mass-shift efficiency of Sr in O_2 reaction mode ranged between the expected range of 10 and 14% (*8*). The variation was mainly due to instrument conditions on the day of measurement.

To evaluate whether $^{87}Rb^{16}O^+$ formed in the cell sufficiently to affect the measurement of $^{87}Sr^{16}O^+$, ^{85}Rb was used as a proxy for ^{87}Rb. The signals at *m/z* 85 (for $^{85}Rb^+$) and *m/z* 101 (for $^{85}Rb^{16}O^+$) were monitored during method development. First, Q1 and Q2 were both set to *m/z* = 85. The measured cps of $^{85}Rb^+$ in the reference materials (RMs) and rock samples were between 6×10^5 and 4×10^6 (the cps of $^{85}Rb^+$ in the solution blank was typically below 1). Then Q2 was set to *m/z* 101 and the measured cps range was below 1, suggesting minimal formation of $^{85}Rb^{16}O^+$ in the cell. Using the natural abundance of ^{85}Rb (72.17%) and ^{87}Rb (27.83%), we calculated that the conversion of $^{87}Rb^+$ to $^{87}Rb^{16}O^+$ would lead to a measured cps for $^{87}Rb^{16}O^+$ at *m/z* = 103 below 0.4 cps.

In this study, the Sr concentration of the RMs and rock samples measured by ICP-QQQ were mostly around 100 ng/mL. This concentration is equivalent to over 1×10^5 cps for $^{87}Sr^+$ as $^{87}Sr^{16}O^+$ (*m/z* = 103). Therefore, the interference effect of $^{87}Rb^{16}O^+$ (*m/z* = 103) on $^{87}Sr^{16}O^+$ (*m/z* = 103) is negligible in this study.

Experimental

Standards and sample preparation

To determine the accuracy and precision of the method, three US Geological Survey (USGS) RMs were used: Basalt, Columbia River (BCR-2), Basalt, Hawaiian Volcanic Observatory (BHVO-2), and Andesite (AGV-2). Twenty-three rock samples were analyzed in the study, including basalt (Rb/Sr concentration ratio 0.02–0.12), dolerite (Rb/Sr concentration ratio 0.04–0.10), andesite (Rb/Sr concentration ratio 0.76–0.87), and rhyolite (Rb/Sr concentration ratio 5.6–9.1).

All RMs and samples were prepared at the Institute of Tibetan Plateau Research, Chinese Academy of Sciences (ITP-CAS) using a classic pressurized acid digestion method for trace element measurements. Approximately 50 mg of each sample was digested using 1 mL each of purified HNO_3 and HF in a closed vessel oven, heated at 190 °C for 36 hours. Following the addition of 0.25 mL of $HClO_4$, the sample was evaporated to incipient dryness on a hot plate at 130 °C. This procedure was repeated with the addition of 0.5 mL of HNO_3. The sample was further heated at 170 °C until white fumes were seen. 0.5 mL of 40% HNO_3 was added, and the sample was oven-heated at 130 °C for 3 h. After cooling, 49.5 mL of de-ionized water was added to the sample, ready for analysis by ICP-QQQ.

Instrumentation

An Agilent 8900 ICP-QQQ was used. The sample introduction system consisted of a quartz torch with 2.5 mm i.d. injector, a quartz spray chamber, glass concentric nebulizer, and nickel-tipped interface cones. Samples were introduced into the ICP-QQQ using a standard peristaltic pump and Agilent SPS 4 autosampler.

^{87}Sr and ^{86}Sr were determined in mass-shift mode using O_2 as the cell gas. The isobaric interference on ^{87}Sr by ^{87}Rb was avoided by measuring the Sr product ions $^{87}Sr^{16}O^+$ and $^{86}Sr^{16}O^+$ at m/z=103 and m/z=102, respectively. Typical instrument operating parameters are listed in Table 1.

Throughout the analytical workflow, a BCR-2 RM sample solution containing 100 ng/mL Sr was measured after every two or three samples to ensure that the mass bias calibration was up to date. Instrument mass bias occurs when ions of different element masses transmit through the ICP-MS with different efficiencies, resulting in inaccurate IR measurements. The Agilent ICP-MS MassHunter software automatically updates the mass bias.

Table 1. ICP-QQQ operating parameters and acquisition settings for $^{87}Sr/^{86}Sr$ IR analysis.

Parameter	Setting
RF Power (W)	1550
Sampling Depth (mm)	8.0
Nebulizer Gas Flow Rate (L/min)	1.15
KED (V)	–6.0
Cell Gas Flow Rate (mL/min)	0.45 (30% of full scale)
Axial Acceleration (V)	1.0
Q1→Q2 Masses (*m/z*)	86→ 102 87→ 103
Q2 Peak Pattern	1 point
Replicates	7
Sweeps	1000
Integration Time of Each Mass (s)	9

Results and discussion

Determination of $^{87}Sr/^{86}Sr$ IRs in the RMs

$^{87}Sr/^{86}Sr$ IRs were measured in BCR-2 and BHVO-2 RMs using the ICP-QQQ mass-shift method with O_2 cell gas. To confirm that chromatographic separation of Sr wasn't needed for successful ICP-QQQ analysis, data was acquired with and without the Sr purification stage. Each RM was measured seven times in different batches or on different days, with seven replicate measurements.

The $^{87}Sr/^{86}Sr$ ratio results in Figure 2 show that there was no significant difference in the results for BCR-2 and BHVO-2 with and without Sr purification. Both sets of measured data are within the literature reported values that were obtained using TIMS and MC-ICP-MS (*9*). The ICP-QQQ method is accurate enough to study $^{87}Sr/^{86}Sr$ ratios in natural samples/systems with a wide range of $^{87}Sr/^{86}Sr$ distributions. Also, the sample preparation procedure doesn't affect the precision of the ICP-QQQ measurements.

The error bars show two times the standard deviation (SD) of the average of seven separate measurements of the two RMs, which range between 0.0003 and 0.0005 (n=7) or between 0.02 and 0.04% RSD. This deviation is significantly higher than the RSD of the MC-ICP-MS method. However, the results show that ICP-QQQ can distinguish $^{87}Sr/^{86}Sr$ ratios of materials within 0.001 (i.e. 0.1%) precision.

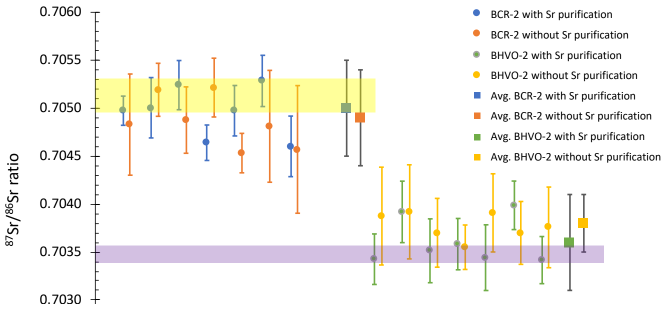

Figure 2. Comparison of the measured $^{87}Sr/^{86}Sr$ ratios of BCR-2 and BHVO-2 with and without Sr purification column chemistry by ICP-QQQ with literature values (*9*) represented by the shaded bands. Circle symbols: average value of each measurement, the error bar is 1SD of the seven replicates of each measurement. Square symbols: the average value of the seven measurements of BCR-2 and BHVO-2, the error bar represents 2SD of the seven measurements.

The effect of the Sr concentration in the samples

To optimize the level of sample dilution of the sample digests, we investigated the effects of the concentration of Sr in the rock samples on the analysis. Three fully digested rock samples (andesite, dolerite, and basalt) were diluted to give a Sr concentration between 60 and 350 ng/mL. A BCR-2 solution containing 100 ng/mL of Sr was used for online instrumental mass bias correction.

The results in Table 2 show that, within the measured concentration range, the Sr concentration doesn't significantly affect the $^{87}Sr/^{86}Sr$ ratios of each type of sample. Therefore, the digested samples could potentially be diluted into a certain range, such as from 60 to 350 ng/mL, according to a standard operation procedure, simplifying the analysis.

Table 2. Measured $^{87}Sr/^{86}Sr$ IRs of three different rock samples (one sample of each type of rock) with four different Sr concentrations.

Sample	Sr Concentration (ng/mL)	$^{87}Sr/^{86}Sr$ Ratio	2SD (n=3)
Basalt	70	0.7036	0.0009
	100	0.7055	0.0002
	175	0.7043	0.0008
	350	0.7060	0.0009
Dolerite	70	0.7035	0.0015
	100	0.7047	0.0009
	170	0.7039	0.0016
	340	0.7046	0.0008
Andesite	60	0.7114	0.0013
	100	0.7126	0.0006
	140	0.7120	0.0015
	280	0.7126	0.0014

Analysis of Sr IRs of rock samples by ICP-QQQ

The 23 rock samples were analyzed in triplicate (n=3) using the ICP-QQQ mass-shift method, without Sr purification. As shown in Figure 3, the samples cover a large $^{87}Sr/^{86}Sr$ ratio range from 0.705 to 0.748. This range is typical of common rocks (Figure 3), as well as minerals, waters, and plants (*4*).

The accuracy of the $^{87}Sr/^{86}Sr$ ratio measurements obtained by ICP-QQQ was compared with data obtained by MC-ICP-MS. There was good agreement between the two methods (*4*), with a variation of between 0.00001 and 0.0016 of the mean of the $^{87}Sr/^{86}Sr$ ratio. The variation wasn't dependent on the $^{87}Sr/^{86}Sr$ ratio range.

The precision of the $^{87}Sr/^{86}Sr$ ratio measured by ICP-QQQ varied between 0.0001 and 0.0019 (2SD, n=3) or between 0.01 and 0.13% (RSD, n=3). While this precision is lower than the precision of the MC-ICP-MS method, it is sufficient for applications with large $^{87}Sr/^{86}Sr$ ratio differences, such as the identification of $^{87}Sr/^{86}Sr$ ratio in between certain rock types. Andesite, rhyolite, and dolerite rock samples have significant $^{87}Sr/^{86}Sr$ ratio variations, as shown in Figure 3. However, distinguishing rock types within a narrow range of $^{87}Sr/^{86}Sr$ ratios, e.g., low $^{87}Sr/^{86}Sr$ basalts, could be challenging.

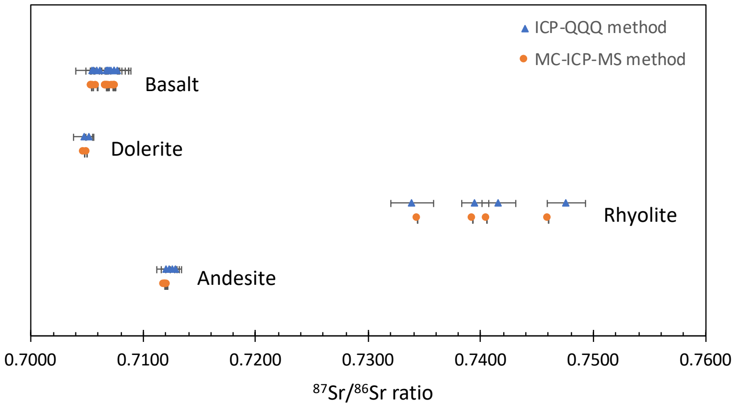

Figure 3. $^{87}Sr/^{86}Sr$ IR distribution for typical rocks. Triangle symbol: $^{87}Sr/^{86}Sr$ IR of ICP-QQQ method, error bar in 2SD (n=3). Circle symbol: $^{87}Sr/^{86}Sr$ IR of MC-ICP-MS method, error bar in 2SD (n=3) which falls within the circle mark.

Conclusion

The study has shown that the Agilent 8900 ICP-QQQ can be used for the accurate measurement of $^{87}Sr/^{86}Sr$ isotope ratios in a range of rock samples. The isobaric interference of ^{87}Rb on ^{87}Sr was resolved using a mass-shift method with O_2 cell gas. Because Sr reacts with oxygen at a much faster rate than Rb, ^{87}Sr was measured as $^{87}Sr^{16}O^+$, free from interference from ^{87}Rb. This method is simpler, faster, and less costly than TIMS or MC-ICP-MS methods, as both TIMS and MC-ICP-MS require chromatographic separation of Sr from Rb before analysis. The ICP-QQQ mass-shift method is also suited to nonspecialist laboratories that aren't equipped with TIMS or MC-ICP-MS.

The distribution of $^{87}Sr/^{86}Sr$ IRs of natural samples is generally between 0.70 and 0.77, although it can range from 0.700 to 0.943 (*4*). The accuracy and precision of the ICP-MS/MS method is sufficient to differentiate between various sources when the $^{87}Sr/^{86}Sr$ ratio varies by more than 0.001. Therefore, this method has the potential to be used in applications that require source identification, such as environmental pollutant source tracing, large-scale geological surveys, and agricultural product authenticity studies.

More information

For detailed information, please see Liu, X, Dong, S, Yue, Y, et al. $^{87}Sr/^{86}Sr$ isotope ratios in rocks determined by ICP-MS/MS in O_2 mode without prior Sr purification. *Rapid Commun Mass Spectrom*. 2020, https://doi.org/10.1002/rcm.8690

References

1. E. Bolea-Fernandez, L. Balcaen, M. Resano, F. Vanhaecke, Tandem ICP-mass spectrometry for Sr isotopic analysis without prior Rb/Sr separation. *J Anal At Spectrom*., **2016**, 31, 303-310
2. Glenn Woods, Resolution of ^{176}Yb and ^{176}Lu interferences on ^{176}Hf to enable accurate $^{176}Hf/^{177}Hf$ isotope ratio analysis using an Agilent 8800 ICP-QQQ with MS/MS, Agilent publication, 5991-6752EN
3. Glenn Woods, Lead isotope analysis: Removal of ^{204}Hg isobaric interference from ^{204}Pb using ICP-QQQ in MS/MS mode, Agilent publication, 5991- 5270EN
4. X. Liu, S. Dong, Y. Yue, et al. $^{87}Sr/^{86}Sr$ isotope ratios in rocks determined by ICP-MS/MS in O_2 mode without prior Sr purification. *Rapid Commun Mass Spectrom*., **2020**, accessed May 2020, https://doi.org/10.1002/rcm.8690
5. T. Zack, K. J. Hogmalm, Laser ablation Rb/Sr dating by online chemical separation of Rb and Sr in an oxygen-filled reaction cell. *Chem Geol*. **2016**, 437, 120–133
6. G. Faure, J. L. Powell, Strontium Isotope Geology. *Springer-Verlag*, New York, **1972**
7. R. C. Capo, B. W. Stewart, O. A. Chadwick, Strontium isotopes as tracers of ecosystem processes: theory and methods. *Geoderma*. **1998**, 82, 197-225
8. Naoki Sugiyama and Kazumi Nakano, Reaction data for 70 elements using O_2, NH_3 and H_2 gases with the Agilent 8800 Triple Quadrupole ICP-MS; Agilent publication, 5991-4585EN
9. K.P. Jochum, U. Nohl, K. Herwig, E. Lammel, B. Stoll, A. W. Hofmann, GeoReM: A new geochemical database for reference materials and isotopic standards. *Geostand Geoanal Res*. **2005**, 29, 333–338

Direct Strontium Isotopic Analysis of Solid Samples by LA-ICP-MS/MS

Authors

Eduardo Bolea-Fernandez, Stijn J. M. Van Malderen, Lieve Balcaen, and Frank Vanhaecke, Ghent University, Belgium

Martín Resano,
University of Zaragoza, Spain

Keywords

isotopic analysis, LA-ICP-MS/MS, LA-ICP-QQQ, strontium, geology

Introduction

Strontium has four stable isotopes: ^{84}Sr (0.56%), ^{86}Sr (9.86%), ^{87}Sr (7.0%), and ^{88}Sr (82.58%). ^{87}Sr is either formed during nucleosynthesis with other stable Sr isotopes or via beta decay from ^{87}Rb (half-life of 4.88 x 10^{10} years): $^{87}\text{Rb} \rightarrow {}^{87}\text{Sr} + \beta^{-} + \bar{\upsilon}$. Consequently, a high ^{87}Sr/^{86}Sr ratio is observed in rocks that are geologically old or which contain a high concentration of Rb (high Rb/Sr ratio). The ^{87}Sr/^{86}Sr ratio has been widely studied and reported in geological studies [1].

Measuring the ^{87}Sr/^{86}Sr ratio using mass spectrometry techniques is challenging because of the isobaric overlap of the signals from ^{87}Rb and ^{87}Sr. Chemical separation can be used to isolate Sr from Rb before analysis by ICP-MS. However, a simpler method uses triple quadrupole ICP-MS (ICP-QQQ) and chemical reaction in the CRC with a reactive gas. In this study, Laser Ablation coupled to ICP-QQQ (LA-ICP-QQQ) in MS/MS mode with CH_3F/He reaction gas was used to resolve the ^{87}Rb interference on ^{87}Sr. This approach allowed the direct Sr isotopic analysis of solid samples [2].

Experimental

A preliminary study showed that better precision was obtained using wet plasma conditions. The experimental setup shown in Figure 1 was used throughout. De-ionized water was continuously aspirated using a standard nebulizer.
The sample aerosol that was generated by the LA system was carried by helium gas. Before being delivered to the plasma, the dry aerosol was combined with the liquid aerosol in the spray chamber, which was chilled to 2 °C.

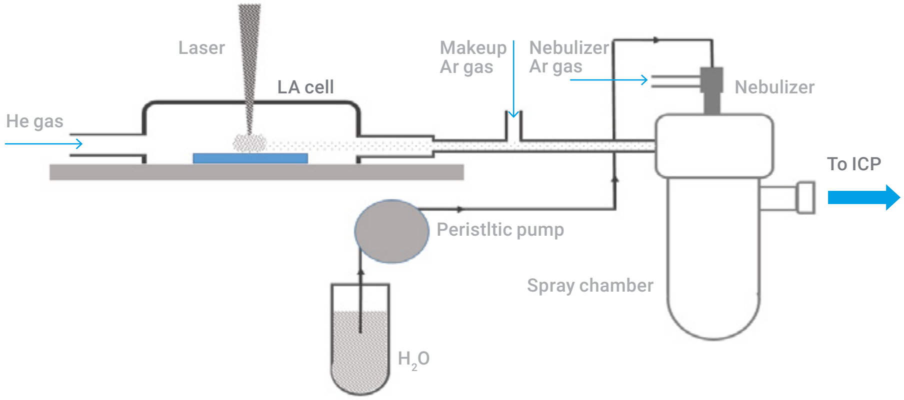

Figure 1. Schematic diagram of LA-ICP-QQQ using wet plasma conditions.

Instrumentation: An Analyte G2 193 nm ArF*excimer-based LA-unit (Teledyne CETAC Technologies, USA) equipped with a HELEX 2 ablation cell was coupled to an Agilent 8800 #100. The ICP-QQQ was fitted with a standard sample introduction system.

Method: Tuning conditions and method parameters are given in Table 1.

Reaction cell method: The CH_3F/He (1:9) cell gas was introduced via the ICP-QQQ's fourth cell gas mass flow channel (0-1 mL/min as O_2). Rb^+ ions do not react with CH_3F, whereas Sr^+ reacts with CH_3F to form SrF^+. Thus $^{86}Sr^+$, $^{87}Sr^+$, and $^{88}Sr^+$ can be measured as the corresponding $^{86}SrF^+$, $^{87}SrF^+$ and $^{88}SrF^+$ reaction product ions, free from interference.

Mass bias correction: The instrumental mass bias was corrected for using a double correction approach: internal correction assuming a constant $^{88}Sr/^{86}Sr$ isotope ratio (Russell's law, given below), followed by external correction in a sample-standard bracketing (SSB) approach using NIST 612 glass SRM.

$$R^{87Sr/86Sr}{}_{\text{sample, corrected}} = R^{87Sr/86Sr}{}_{\text{sample, measured}} \text{ x } (m^{87Sr}/m^{86Sr})^{f}$$

$$f = \ln\,[R^{88Sr/86Sr}{}_{\text{true}} \,/\, R^{88Sr/86Sr}{}_{\text{measured}}] \,/\, \ln\,[m^{88Sr}/m^{86Sr}]$$

Samples: Seven geological reference materials (RMs) were analyzed for their Sr isotopic composition. The RMs were selected to cover a wide range of matrix composition, Sr concentration, and Rb/Sr elemental ratio, as summarized in Table 2.

Table 1. LA-ICP-QQQ tuning conditions.

Laser Ablation		
Energy density	J/cm^2	3.54
Repetition rate	Hz	40
Scan speed	µm/s	15
Beam size	µm	20-85
He carrier gas flow	L/min	0.42

ICP-QQQ		
RF power	W	1550
Sampling depth	mm	3.5
Nebulizer gas flow	L/min	1.0
Make-up gas flow	L/min	0.33
CH_3F/He cell gas flow	mL/min	0.90
Dwell time per acquisition point	ms	300
Acquisition time per replicate	s	60
Number of replicates		12
Total analysis time per sample	min	15.55

Results and discussion

Removal of ^{87}Rb overlap using MS/MS mass-shift mode with CH_3F/He cell gas

Seven RMs were selected to cover a wide range of Rb/Sr ratios. The $^{87}Sr/^{86}Sr$ ratio was measured in each RM. For comparison purposes, the analysis was done using a no gas on-mass method and the CH_3F/He mass-shift method. Figure 2 shows the measured $^{87}Sr/^{86}Sr$ and $^{88}Sr/^{86}Sr$ ratios obtained with the two methods as a function of the Rb/Sr ratio.

With both methods, a constant $^{88}Sr/^{86}Sr$ ratio was obtained regardless of the sample type. However, the measured $^{87}Sr/^{86}Sr$ ratio increased in no gas mode, indicating an interference from ^{87}Rb on ^{87}Sr. In contrast, the $^{87}Sr/^{86}Sr$ ratio measured in CH_3F/He mode remained constant, regardless of the Rb/Sr ratio, showing that the method was effective at removing the ^{87}Rb isobaric overlap on ^{87}Sr.

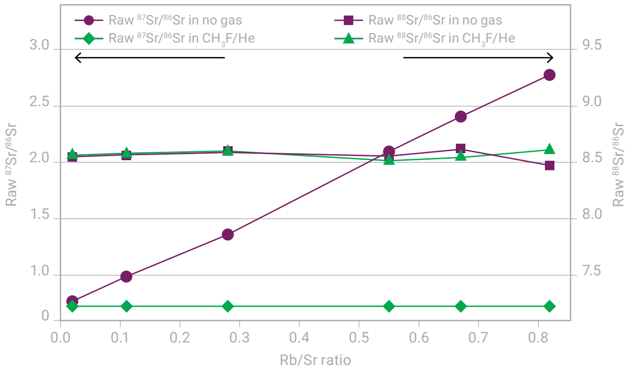

Figure 2. $^{87}Sr/^{86}Sr$ and $^{88}Sr/^{86}Sr$ isotope ratios measured using LA-ICP-QQQ in no gas and CH_3F/He cell gas modes. *Reproduced from J. Anal. At. Spectrom., 2016, 31, 464–472 with permission from the Royal Society of Chemistry.*

Determination of $^{87}Sr/^{86}Sr$ ratio in seven RMs

The method was used to determine the $^{87}Sr/^{86}Sr$ ratio in seven RMs. The results are summarized in Table 2. After mass bias correction, excellent agreement was obtained between the measured $^{87}Sr/^{86}Sr$ ratios and the recommended reference values, even in samples with a high Rb content.

Table 2. $^{87}Sr/^{86}Sr$ isotope ratio results in seven reference materials.

Reference material	Type	Rb/Sr ratio	Chemical composition of the reference materials (%)								$^{87}Sr/^{86}Sr$ ratio				
			Al_2O_3	CaO	FeO	K_2O	MgO	MnO	Na_2O	SiO_2	Experimental		Recommended		Error (%)
USGS BHVO-2G	Basalt	0.02	13.6	11.4	11.3	0.51	7.13	0.17	2.4	49.3	0.70351	±0.00034	0.703469	±0.000007	0.006
USGS NKT-1G	Nephelinite	0.03	10.5	13.4	12.2	1.27	14.2	0.24	3.85	38.9	0.70363	±0.00017	0.703509	±0.000019	0.017
USGS TB-1G	Basalt	0.11	17.12	6.7	8.67	4.52	3.51	0.18	3.56	54.29	0.70576	±0.00030	0.705580	±0.000023	0.026
USGS GSD-1G	Basalt	0.55	13.4	7.2	13.3	3	3.6		3.6	53.2	0.70924	±0.00029	0.709416	±0.000050	-0.025
USGS BCR-2G	Basalt	0.14	13.4	7.06	12.4	1.74	3.56	0.19	3.23	54.4	0.70486	±0.00038	0.705003	±0.000004	-0.020
MPI-DING T1-G	Diorite	0.28	17.1	7.1	6.44	1.96	3.75	0.127	3.13	58.6	0.70990	±0.00035	0.710093	±0.000017	-0.027
MPI-DING ATHO-G	Rhyolite	0.67	12.2	1.7	3.27	2.64	0.103	0.106	3.75	75.6	0.70310	±0.00026	0.703271	±0.000015	-0.024

Reproduced from J. Anal. At. Spectrom., 2016, 31, 464–472 with permission from the Royal Society of Chemistry.

Conclusion

LA-ICP-QQQ with wet plasma conditions can be used for the direct determination of the $^{87}Sr/^{86}Sr$ isotope ratio in geological samples. The isobaric interference from ^{87}Rb on ^{87}Sr was overcome using MS/MS mass-shift mode with CH_3F/He cell gas. The Sr^+ ions react in the CRC to form SrF^+ reaction product ions, while Rb^+ ions do not react. $^{87}Sr/^{86}Sr$ ratios were accurately determined in seven reference materials, regardless of the matrix composition, Sr concentration, and Rb/Sr elemental ratio.

References

1. R. A. Bentley, *J. Archaeol. Meth. Theor.,* **2006**, 13, 135–187.
2. E. Bolea-Fernandez, S. Van Malderen, L. Balcaen, M. Resano, and F. Vanhaecke, Laser ablation-tandem ICP-mass spectrometry (LA-ICP-MS/MS) for direct Sr isotopic analysis of solid samples with high Rb/Sr ratios, *J. Anal. At. Spectrom*., **2016**, 31, 464–472

Resolution of ^{176}Yb and ^{176}Lu interferences on ^{176}Hf to enable accurate ^{176}Hf/^{177}Hf isotope ratio analysis using ICP-QQQ with MS/MS

Author

Glenn Woods
Agilent Technologies, UK

Keywords

Hafnium, Hf, geology, dating studies, rock dating, isotopic abundance

Introduction

Hafnium ^{176}Hf to ^{177}Hf isotope ratio analysis can provide insight into the different geological events and processes that a mineral underwent during its formation/metamorphosis; ^{176}Hf/^{177}Hf ratios are also used for geochronology dating studies. Isotope geochronology is a dating technique in which the age of a rock or mineral is derived from differences in the abundance of two isotopes of an element. Changes in isotopic abundance may be caused by isotopic (mass) fractionation, or by radioactive decay; in each case, the ratio acts as a geological clock, allowing the time that the mineral was formed to be estimated. Hf has lower mobility than lead (Pb) in metamict minerals such as zircon, xenotime, euxenite etc., so Hf isotope ratios can offer an alternative to Pb/Pb or Pb/U ratios for dating these minerals.

Of the Hf isotopes of interest, ^{177}Hf is free from direct isobaric overlap from any other element and does not typically suffer from polyatomic interference from other co-existing elements. However, the second Hf isotope used in the isotope ratio calculation, ^{176}Hf, suffers isobaric overlap from ^{176}Lu and ^{176}Yb, as shown in Figure 1. In order to obtain accurate Hf ratios, it is therefore necessary to separate the ^{176}Hf signal from the overlapping Lu and Yb signals.

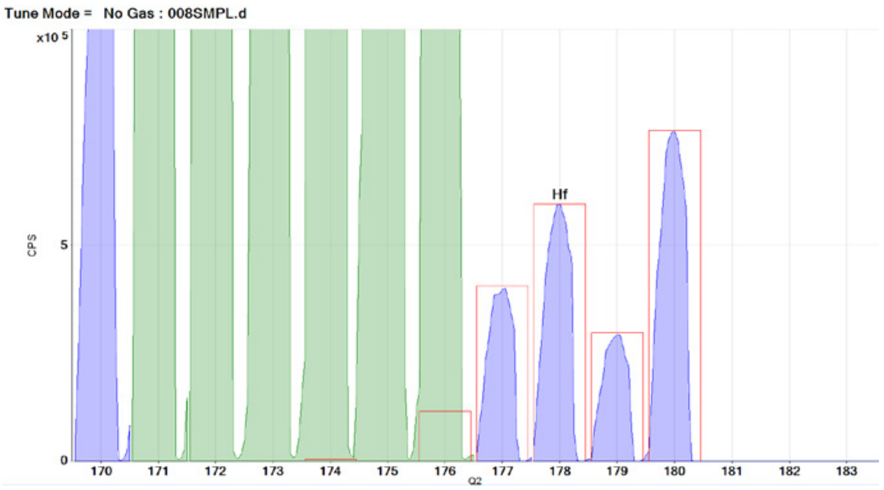

Figure 1. Hf (red peak template) in the presence of Lu and Yb matrix. The poor template fit for ^{176}Hf (highlighted in blue outline) is due to the contribution from ^{176}Lu and ^{176}Yb to the signal at *m/z* 176.

The mass resolution required to separate ^{176}Hf from the Lu and Yb isobaric interferences (M/ΔM of ~140,000 for ^{176}Lu and >150,000 for ^{176}Yb) is far beyond the capability of commercial High Resolution Sector Field ICP-MS (SF-ICP-MS), so sample preparation (chemical separation) is required prior to analysis. In cases where chemical separation cannot be performed, for example in-situ measurement by Laser Ablation (LA), the Lu/Yb overlaps mean that accurate Hf isotope ratio analysis is not possible or must rely on mathematical corrections (and the errors they can introduce).

An alternative direct approach is “chemical” resolution within a collision/reaction cell (CRC), using specific gas phase ion-molecule reaction(s) that will either:

- React with the interfering ion to neutralize it or move it to a new mass.
- React with the analyte to create a new product ion at a different, non-interfered mass.

In this study, the second approach, known as “mass-shift”, was used. Hf reacts efficiently with ammonia cell gas to form Hf-ammonia cluster ions, while Lu and Yb are relatively unreactive. However, ammonia will react with the other Hf isotopes and other co-existing ions present in a typical sample matrix. These other ions also form ammonia-adduct ions, creating new interferences that vary depending on the matrix composition. These ammonia-adduct ions would interfere with the original Hf isotope pattern, making Hf isotope analysis unreliable, so control over the reaction process is essential.

The solution to this problem is to use a tandem mass spectrometer, which has an additional mass filter before the CRC. This extra mass filter prevents all ions apart from the target mass from entering the CRC, so the reaction chemistry is precisely controlled and unwanted side-reactions are avoided. This double mass filter approach is only possible with a tandem MS (or MS/MS) configuration, which provides unprecedented control of the ion/molecule reaction chemistry used in CRC-ICP-MS methods.

The Agilent 8800 and 8900 Triple Quadrupole ICP-MS (ICP-QQQ) instruments have an additional quadrupole mass filter (Q1), positioned in front of the CRC, with the capability of operating at unit mass resolution (MS/MS mode). In MS/MS operation, only a single mass-to-charge ratio (*m/z*) is transmitted through Q1, so the other Hf isotopes and any co-existing elements are rejected before they can enter the CRC. Unwanted side-reactions and potentially overlapping product ions are therefore eliminated. This method was used to measure Hf isotope ratios in a variety of samples containing Lu, Yb and mixed rare earth elements (REE). For this proof of concept, all work was performed using solution sample introduction, which allowed a greater flexibility to test interference removal. However, the same cell gas and MS/MS method can also be applied successfully to sample analysis using laser ablation (LA-ICP-QQQ).

Experimental

Instrumentation

The Agilent 8800* ICP-QQQ was configured with an SPS 4 autosampler and the standard sample introduction system consisting of a Micromist nebulizer (free aspiration), quartz spray chamber and torch, and Ni interface cones. Table 1 shows the key instrument parameters used for the analysis.

Table 1. Instrument parameters.

Parameter	Value
RF power	1550 W
Sampling depth	7.0 mm
Nebulizer gas	1.15 L/min
Spray chamber temp	2 °C
Ammonia (10% in He) cell gas	22% of full scale (~2.2 mL/min)
Octopole bias	-6.0 V
Energy discrimination	-8.0 V

Samples and sample preparation

Due to the reactivity of ammonia, its use as a cell gas leads to a complex population of product ions, even in a simple sample matrix. However, selection of the most appropriate adduct ion is relatively simple with ICP-QQQ, by performing a Product Ion Scan. Unique to the MS/MS mode of operation, a Product Ion Scan uses a fixed mass setting for Q1, combined with a Q2 scan across the selected mass range. To identify useful ^{176}Hf- ammonia product ions, Q1 was fixed to mass (*m/z*) 176 u, and Q2 was scanned across the mass range from *m/z* 170 to *m/z* 260, while aspirating a solution of 5 µg/L Hf. The resulting mass spectrum can be seen in Figure 2. Initially, the reaction product ion spectra may appear complex, but it should be noted that the use of a fixed mass setting for Q1 means that all these ammonia product ions are derived from the ^{176}Hf isotope. The most abundant ammonia adduct ion was $Hf(NH)(NH_2)(NH_3)_3^+$, which occurs at M + 82 u (*m/z* 258 for the ^{176}Hf isotope); this adduct was selected as the preferred mass transition.

It should be noted that the Hf adduct ion used is sensitive to CRC conditions, particularly the acceleration voltage applied from the Octopole Bias. This parameter was optimized to a lower value than is typically used, in order to favor the preferred transition and maximize the yield of the desired product ion. The cell gas flow rate was then re-optimized using the ICP-MS MassHunter autotune routines to further improve the product ion signal.

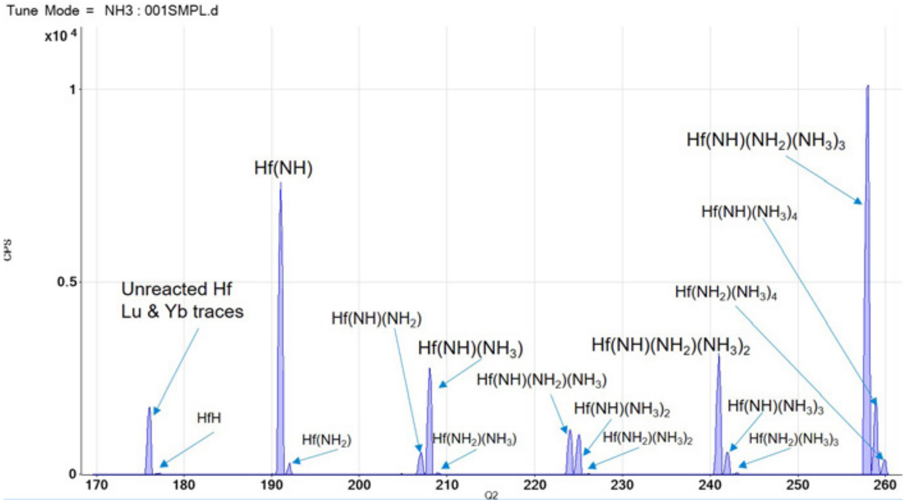

Figure 2. Product Ion Scan from *m/z* 170 to *m/z* 260 showing ammonia adduct reaction product ions formed from ^{176}Hf precursor ion (Q1 set to *m/z* 176).

A graphical representation of the ^{176}Hf transition can be seen in Figure 3; this schematic illustrates how Q1 (set to *m/z* 176) eliminates all ions apart from those at *m/z* 176, and Q2 (set to *m/z* 258) eliminates the unreacted ^{176}Lu and ^{176}Yb isotopes. The same mass transition is used for the other isotope of interest, ^{177}Hf, using Q1 and Q2 settings of *m/z* 177 and *m/z* 259, respectively.

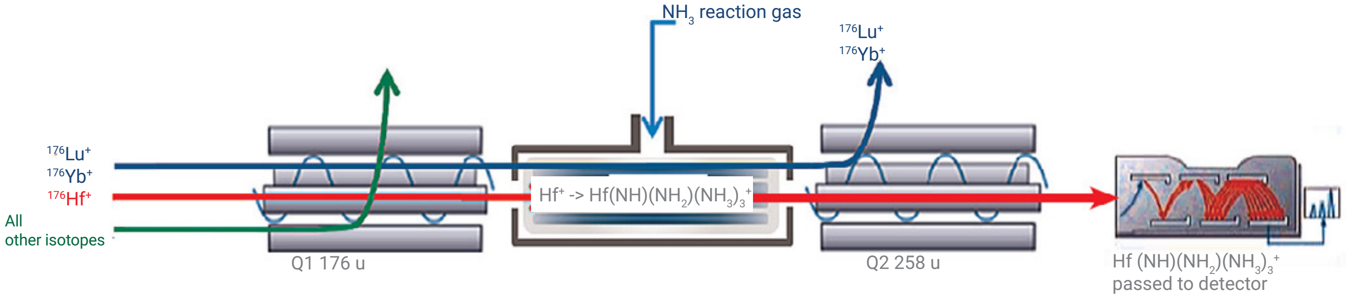

Figure 3. Schematic of the ^{176}Hf isotope reaction with ammonia cell gas in MS/MS mode.

To check that the Hf isotope pattern was maintained, a Neutral Gain Scan was performed where both Q1 and Q2 were scanned together, with a fixed mass difference of +82 u applied to Q2. Figure 4 shows the resultant spectrum, confirming that the Hf-ammonia product ions match the overlay of the theoretical Hf isotopic abundances. This spectrum demonstrates the unique benefit of MS/MS mode, which ensures that inter-isotope overlaps cannot occur, as only one Hf isotope mass is present in the cell at any given time.

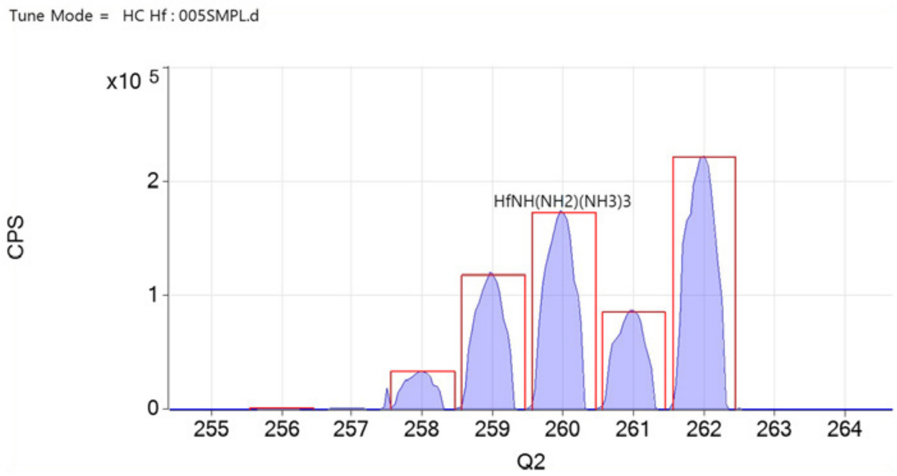

Figure 4. Neutral Gain Scan of the Hf isotopes as Hf(NH)(NH$_2$)(NH$_3$)$_3^+$ clusters; theoretical Hf isotopic abundances are shown in red, confirming that the isotope ratios are preserved in the product ion spectrum.

To simulate real-world sample analysis, several potential sources of interference were introduced to assess whether bias or new interferences were created.

The test solutions included:

- Hf standard (5 ppb) – also used for Mass Bias Calibration
- 100 ppb Yb and 5 ppb Hf
- 100 ppb Lu and 5 ppb Hf
- 100 ppb Yb + Lu and 5 ppb Hf
- Mixed 100 ppb “REE[1]” standard and 5 ppb Hf
- Mineral[2] sample with 100 ppb “REE[1]” and 5 ppb Hf

Hf isotope ratio measurement

In order to provide comparative performance data, the ICP-QQQ was set to measure $^{176/177}$Hf isotope ratios in three separate acquisition modes:

- No cell gas, “Single Quad” mode
  “Base” ICP-MS data not utilizing any mechanism to reduce isobaric overlaps
- NH$_3$ reaction gas, Single Quad Bandpass mode
  Non-MS/MS operation, allowing a limited mass range “window” into the CRC
- NH$_3$ reaction gas, MS/MS mode
  Q1 operating as a mass filter with unit mass resolution, allowing only a single *m/z* into the CRC

Table 2 displays the Hf isotope ratio (IR) data for each of the test solutions in each instrument mode. It can be seen that there was a large positive deviation from the expected ratio (i.e. the ^{176}Hf signal was high relative to its theoretical abundance) in both of the Single Quad modes of operation (no gas mode and ammonia mode with bandpass filtering). This indicates that “Single Quad” operation did not resolve the Yb and Lu isobars at *m/z* 176, or stop the formation of new reaction product ion interferences.

---

[1] *Agilent Standard 8500-6944 containing La, Ce, Pr, Nd, Sm, Eu, Gd, Tb, Dy, Ho, Er, Tm, Yb, Lu, plus Sc, Y, Th.*

[2] *Natural mineral sample containing approximately 500 ppm Ca, 120 ppm Mg, 15 ppm Na, 5 ppm K, 1500 ppm SO$_4$*

By contrast, MS/MS mode with NH_3 cell gas gave consistent, accurate Hf IR data in all the sample matrices.

To visualize and further investigate the potential overlaps that could have caused the poor Hf isotope ratio performance in Single Quad mode, a mass scan of the mineral sample was performed using Single Quadrupole Bandpass mode with NH_3 reaction gas. The spectrum can be observed in Figure 5. The measured Hf isotopic pattern (far right of the spectrum) does not match the theoretical abundance template, showing that the Hf isotopes suffer overlap from new cell-formed cluster ions, due to the lack of control over the reaction processes. In a complex sample matrix, numerous cell-formed interferences are created, precluding the accurate analysis of many target product ions.

Table 2. $^{176/177}$Hf isotope ratio (IR) data measured in samples containing various sources of interferences, using three different ICP-QQQ operating modes. The "deviation" is the error in the measured ratio relative to the true ratio of 0.282796.

	No gas Single Quad		NH_3 Single Quad bandpass		NH_3 MS/MS	
Sample	IR	Deviation	IR	Deviation	IR	Deviation
Hf 5 ppb	0.27981	0.989	0.28252	0.999	0.28196	0.997
Hf 5 ppb, Yb 100 ppb	15.25251	53.935	0.30461	1.077	0.28370	1.003
Hf 5 ppb, Lu 100 ppb	3.18739	11.271	1.06062	3.750	0.28051	0.992
Hf 5 ppb, Yb, Lu 100 ppb	18.51262	65.463	1.06267	3.758	0.28099	0.994
Hf 5 ppb, REE mix 100 ppb	15.26995	53.996	0.64603	2.284	0.28139	0.995
Hf 5 ppb, Mineral REE mix 100 ppb	16.16150	57.149	0.63479	2.245	0.28230	0.998

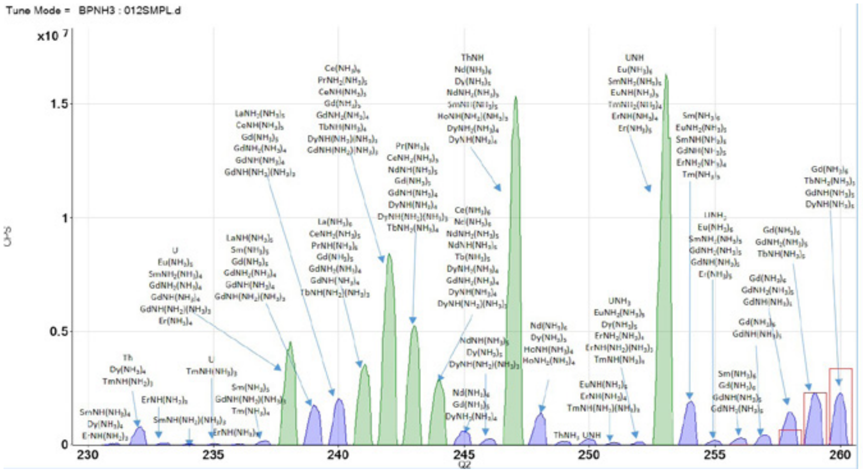

Figure 5. Mass spectrum of the mineral sample acquired under Single Quad Bandpass mode using ammonia as the reaction gas. The poor fit of the measured Hf isotopic pattern (far right) illustrates the interferences that occur in Single Quad mode. Some examples of cell-formed ammonia cluster ions are shown.

Many matrix elements and other analytes can react with ammonia to produce higher order reaction products, so MS/MS mode is essential to remove these precursor ions before they enter the cell and form new interferences.

The 8800 and 8900 ICP-QQQ use an additional quadrupole mass filter, operating at unit mass resolution and positioned before the CRC, to control which ions enter the reaction cell. This ensures unprecedented levels of control over the reaction processes that occur within the cell. MS/MS mode can quickly switch between on-mass measurement and off-mass measurement within a single acquisition, supporting multi-element analysis in each gas mode. Figure 6 shows the Hf isotopes measured using off-mass mode (Q2=Q1 + 82 u) and the other masses measured on-mass (Q1=Q2). The small, residual peaks for unreacted Th and U can be seen, along with ThO and UO. Most of the Th and U would have reacted with ammonia cell gas, forming adduct species that are not measured in MS/MS on-mass mode. Any undesired side reactions are eliminated before they can proceed, so the underlying analyte isotope ratios are preserved in the product ion spectrum.

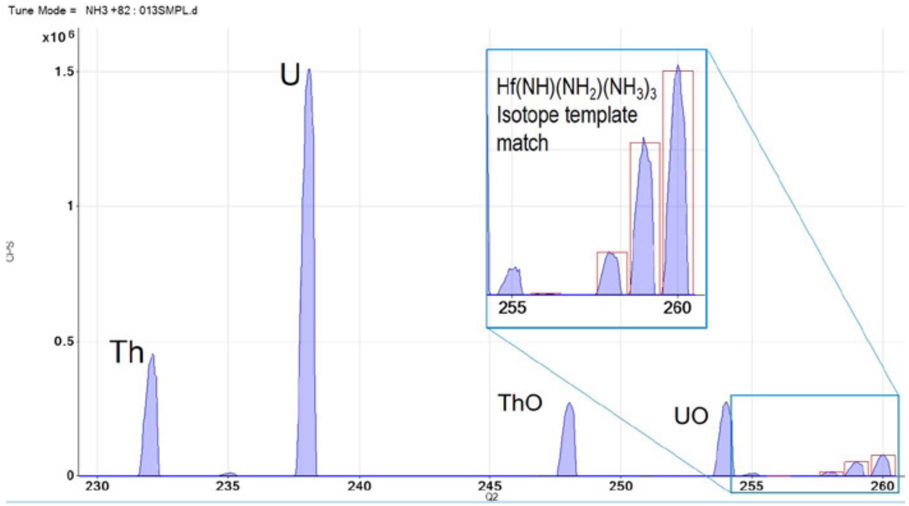

Figure 6. Mass spectrum of the mineral sample measured using NH_3 mass-shift mode for Hf and on-mass mode for all other isotopes. The Hf isotopic pattern illustrates that all of the interferences that occurred in Single Quad mode (shown in Figure 5) have been resolved.

Conclusion

The MS/MS capabilities of Agilent's ICP-QQQ measured Hf isotope ratios with excellent accuracy—even in samples containing high levels of co-existing and potentially interfering matrix elements.

The isobaric overlaps from ^{176}Lu and ^{176}Yb on ^{176}Hf were eliminated using NH_3 as the reaction gas. The reaction chemistry was controlled in the cell by operating the first quadrupole mass filter at unit mass resolution set to *m/z* 176. This excluded all ions apart from those at *m/z* 176 (^{176}Lu, ^{176}Yb and ^{176}Hf). Since only Hf reacts readily with NH_3, ^{176}Hf was free to be measured via its most appropriate cluster ion at *m/z* 258, effectively avoiding the isobaric overlaps from Lu and Yb. Together with the corresponding ammonia cluster ion formed from the ^{177}Hf isotope, this method allowed accurate Hf isotope analysis to be performed in a range of complex synthetic sample matrices.

In summary:

Chemical resolution using a reaction gas offers a powerful alternative to mass resolution, allowing access to isobars beyond the maximum resolution available with commercial High Resolution SF-ICP-MS.

Control over the reaction processes is essential to avoid new, unexpected interferences forming from the sample matrix and other coexisting elements and isotopes.

MS/MS technology affords unprecedented control over the reaction processes, greatly simplifying methodology regardless of the process or sample matrix.

Crucially, MS/MS operation allows access to higher order reaction product (cluster) ions, while still preserving the analyte's original isotopic information.

> Return to table of contents
> Search entire document

Removal of Complex Spectral Interferences on Noble Metal Isotopes

Author

Naoki Sugiyama
Agilent Technologies, Japan

Keywords

Platinum Group Elements, gold, silver, ore exploration, geochemical, environmental, catalytic converter, ammonia

Introduction

The precise determination of the noble metals, comprising the Platinum Group Elements (PGEs: Ru, Rh, Pd, Os, Ir and Pt), Au and Ag, is of great interest in areas such as ore exploration and geochemical studies, and these metals are increasingly used for industrial applications including advanced materials and alloys, medical devices, and catalysts for pharmaceutical manufacturing. Environmental monitoring is also required as some of these elements are used in automobile catalytic converters. ICP-MS is widely used for these applications due to its high sensitivity and multi-element capability. However, the analysis is challenging because the metal concentrations are often low and they are subject to severe spectral overlaps.

Table 1 summarizes the interferences and abundance (%) of each isotope of the elements (the isotopes highlighted in yellow represent the recommended isotope for determination by ICP-MS). Several methods have been developed to resolve the interferences, such as mathematical correction, matrix removal and high-resolution magnetic sector (HR-)ICP-MS. However, the mass resolution required to separate some of the interferences is beyond the capability of current commercial HR-ICP-MS. For example, separation of $^{103}Rh^+$ from $^{87}Sr^{16}O^+$, $^{105}Pd^+$ from $^{89}Y^{16}O^+$, and $^{109}Ag^+$ from $^{93}Nb^{16}O^+$ requires mass resolution (M/ΔM) of 102900, 27600 and 31500, respectively; commercial HR-ICP-MS instruments are limited to a maximum resolution of 10,000. To remove the multiple, complex interferences on noble elements, the Agilent 8800 ICP-QQQ was used in MS/MS mode, using ammonia as the reaction gas.

Experimental

Instrumentation: Agilent 8800 #100.

Plasma conditions: Preset plasma/Low matrix.

Ion lens tune: Soft extraction tune: Extract 1 = -3 V, Extract 2 = -200 V.

CRC conditions: NH_3 (10% NH_3 in He) was used as CRC gas in MS/MS mode.

Following a preliminary optimization study, three different NH_3 gas flow rates (low (L), medium (M) and high (H)) were used. Cell conditions are given in Table 2. No gas mode was also applied for comparison purposes.

> Return to table of contents

Table 1. Abundance (%) of each isotope of noble metals and the interference on each isotope.

m		96	97	98	99	100	101	102	103	104	105	106	107	108	109	110
Element	Ru	5.54		1.87	12.76	12.6	17.06	31.55		8.62						
	Rh								100							
	Pd							1.02		11.14	22.33	27.33		26.46		11.72
	Ag												51.84		48.16	
Interference	Atomic	Zr, Nb, Mo		Mo		Mo						Cd		Cd		Cd
	MH			MoH	MoH		MoH									
	MO, MOH	SeO, BrOH		SeO		SrO	RbO	SrO	SrO, RbO	SrO	YO, SrOH	YOH, ZrO	ZrO	ZrO, MoO	NbO	ZrO, MoO
	Argide			NiAr		NiAr	NiAr	NiAr	CuAr	ZnAr	CuAr	ZnAr	ZnAr	ZnAr		
	Others			CuCl	ZnCl	CuCl	ZnCl	CuCl, ZnCl	ZnCl, Pb^{++}	ZnCl	ZnCl					

m		**184**	**185**	**186**	**187**	**188**	**189**	**190**	**191**	**192**	**193**	**194**	**195**	**196**	**197**	**198**
Element	**Os**	0.02		1.59	1.96	13.24	16.15	26.26		40.78						
	Ir								37.3		62.7					
	Pt							0.014		0.782		32.97	33.83	25.24		7.163
	Au														100	
Interference	Atomic	W		W	Re									Hg		Hg
	MH				WH											
	MO, MOH			YbO	YbO	YbO	YbO	YbO	LuO	YbO, LuD, HfO	HfO	HfO	HfO	HfO	TaO, HfOH	Wo, TaOH
	Argide	NdAr	NdAr	NdAr	SmAr	SmAr, NdAr	SmAr	SmAr, NdAr	EuAr	SmAr	EuAr	SmAr, GdAr	GdAr	GdAr	GdAr	GdAr
	Others															

> Return to table of contents

Table 2. CRC conditions.

	No gas	NH_3-L	NH_3-M	NH_3-H
Cell gas	na	NH_3	NH_3	NH_3
Gas flow rate (mL/min)	na	2.0	3.0	5.0
Octopole bias (V)	-8	-5	-10	-12
KED (V)	+5	-8		
Cell exit (V)	-90			
Deflect lens (V)	20	10	6	2
Plate lens (V)	-110			

Method

The BECs of the noble metals were determined in a series of synthetic-matrix samples, using an external calibration method. Indium (In) internal standard (ISTD) was mixed online with the sample via the standard ISTD mixing T-connector. An integration time of 1 s per isotope was used with 3 replicates (7 replicates for blank).

Samples and sample preparation

Standards and matrix samples were prepared from single element stock solutions purchased from Kanto Chemical Co., Inc. (Saitama, Japan) and a REE mixture standard, XSTC-1 purchased from Spex certiPrep. All solutions were diluted into a final acid mix of 1% HNO_3 and 3% HCl.

Results and discussion

Matrix interference study

Tables 3 and 4 summarize the results of the spectral interference study obtained by analyzing individual synthetic matrix blank solutions. Table 3 shows the observed interferences, expressed as BEC (ppb), in each matrix blank measured using no gas mode. As expected from Table 1, the synthetic matrices caused significantly elevated BECs (>> 1 ppb) on all the primary and secondary isotopes of all the analytes except for Ru; Rh suffered a relatively minor increase in BEC of ~0.5 ppb in the 10 ppm Pb/1 ppm Hg matrix.

Table 4 shows the results obtained using NH_3 reaction mode. The optimum gas flow rate for NH_3 for each element was investigated and three gas flow rates (Low: 2.0, Medium: 3.0, and High: 5.0 mL/min) were used. The best isotope and method is highlighted in bold in the Table. It can clearly be seen that NH_3 reaction mode effectively removes the interferences on all the analytes, giving BECs of << 0.1 ppb for the preferred isotope/cell mode in all the matrices. The mechanism for the removal of each interference using the MS/MS capability of the 8800 ICP-QQQ is as follows:

- **Ru:** slight interferences from Zn and Mo were resolved using on-mass method with NH_3-M.
- **Rh:** Pb^{++} interference was resolved using on-mass method with NH_3-M.
- **Pd:** significant interferences from $SrOH^+$ and YO^+ were seen on ^{105}Pd, the only isotope free from atomic isobar. On-mass method with NH_3-H removed the interferences.
- **Ag:** significant ZrO^+ interference on both ^{107}Ag and ^{109}Ag was resolved using on-mass method with NH_3-H.

- **Os:** YbO$^+$ interference was observed on both ^{188}Os$^+$ and ^{189}Os$^+$. Since Os$^+$ sensitivity in NH$_3$ mode is low, but Os$^+$ forms a product ion of OsNH$^+$, NH$_3$-L with mass-shift gave the best result.
- **Ir:** LuO$^+$ and HfO$^+$ interfere with ^{191}Ir$^+$ and ^{193}Ir$^+$ respectively. NH$_3$-M with mass-shift method worked for ^{191}Ir$^+$ as Ir$^+$ forms a product ion of IrNH$^+$.
- **Pt:** ^{195}Pt$^+$ suffers a significant interference from HfO$^+$. While the overlap is less significant on ^{198}Pt$^+$, ^{198}Pt$^+$ suffers an atomic isobar interference from ^{198}Hg$^+$. However, Hg$^+$ is effectively neutralized by NH$_3$ so ^{198}Pt$^+$ can be measured free from interference.
- **Au:** significant interferences by TaO$^+$ and HfOH$^+$ are resolved by mass-shift method with NH$_3$-M. Au$^+$ forms a product ion of Au(NH$_3$)$_2^+$.

Table 3. Summary of spectral interferences in no gas mode, showing analyte BECs (ppb) in each matrix blank. Matrix overlaps that made a significant contribution to the analyte BECs are indicated in red (BEC > 10 ppb) and orange (BEC > 1 ppb).

	Ru		Rh	Pd	Ag		Os	
Isotope	99	101	103	105	107	109	188	189
NH$_3$ flow rate mL/min	NA							
Method	on-mass	on-mass	on-mass	on-mass	on-mass	on-mass	on-mass	on-mass
Mass pair	99-99	101-101	103-103	105-105	107-107	109-109	188-188	189-189
10 ppm Cu Zn	0.058	0.041	0.138	0.328	0.064	0.061	0.000	0.000
10 ppm Sr Rb	0.000	0.034	0.150	4.39	0.005	0.001	0.000	0.000
10 ppm Ni	0.007	0.019	0.000	0.022	0.012	0.016	0.000	0.000
10 ppm Mo	0.059	0.018	0.000	0.004	0.000	0.018	0.000	0.000
10 ppm Pb, 1 ppm Hg	0.000	0.000	0.472	0.002	0.033	0.034	0.000	0.000
10 ppm Zr Nb	0.000	0.000	0.000	0.022	21.9	1.59	0.000	0.000
10 ppm REE	0.004	0.000	0.009	165	0.147	0.005	2.78	2.99
10 ppm Ta	0.008	0.000	0.000	0.004	0.003	0.000	0.000	0.000
10 ppm Hf	0.000	0.000	0.000	0.004	0.312	0.026	0.000	0.000
10 ppm W	0.000	0.000	0.000	0.003	0.001	0.001	0.000	0.000

	Ir		Pt		Au
Isotope	191	193	195	198	197
NH$_3$ flow rate mL/min	NA				
Method	on-mass	on-mass	on-mass	on-mass	on-mass
Mass pair	191-191	193-193	195-195	198-198	197-197
10 ppm Cu Zn	0.003	0.002	0.000	0.279	0.001
10 ppm Sr Rb	0.002	0.000	0.001	0.310	0.004
10 ppm Ni	0.009	0.004	0.002	0.444	0.011
10 ppm Mo	0.000	0.000	0.000	0.295	0.000
10 ppm Pb, 1 ppm Hg	0.002	0.002	0.000	1293	0.000
10 ppm Zr Nb	0.002	0.775	1.98	3.17	0.417
10 ppm REE	123	0.712	0.788	2.17	0.138
10 ppm Ta	0.000	0.000	0.244	114	284
10 ppm Hf	0.071	28.1	70.9	2.34	14.1
10 ppm W	0.001	0.000	0.000	19.6	0.002

> Return to table of contents

Table 4. Summary of spectral interferences in MS/MS NH_3 reaction cell mode, showing analyte BECs (ppb) in each matrix blank. Matrix overlaps that made a significant contribution to the analyte BECs are indicated in red (> 10 ppb) and orange (> 1 ppb).

t	Ru		Rh	Pd	Ag		Os			
Isotope	99	101	103	105	107	109	188		189	
NH_3 flow rate mL/min	3.0		3.0	5.0	5.0		2.0			
Method	on-mass	on-mass	on-mass	on-mass	on-mass	on-mass	on-mass	mass-shift	on-mass	mass-shift
Mass pair	99-99	101-101	103-103	105-105	107-107	109-109	188-188	188-203	189-189	189-204
10 ppm Cu Zn	0.000	0.000	0.000	0.001	0.061	0.057	0.000	0.000	0.001	0.002
10 ppm Sr Rb	0.000	0.005	0.016	0.033	0.000	0.000	0.000	0.000	0.002	0.000
10 ppm Ni	0.000	0.000	0.000	0.000	0.010	0.009	0.000	0.000	0.000	0.000
10 ppm Mo	0.005	0.001	0.000	0.000	0.001	0.000	0.000	0.000	0.001	0.000
10 ppm Pb, 1 ppm Hg	0.000	0.000	0.000	0.001	0.033	0.035	0.000	0.000	0.001	0.000
10 ppm Zr Nb	0.000	0.000	0.000	0.000	0.003	0.000	0.000	0.000	0.002	0.001
10 ppm REE	0.000	0.000	0.000	0.014	0.004	0.004	2.79	0.003	5.85	0.010
10 ppm Ta	0.000	0.000	0.000	0.000	0.000	0.000	0.000	0.001	0.003	0.000
10 ppm Hf	0.000	0.000	0.000	0.000	0.000	0.000	0.000	0.001	0.058	0.000
10 ppm W	0.000	0.000	0.000	0.001	0.001	0.001	0.000	0.000	0.000	0.000

	Ir				Pt				Au	
Isotope	191		193		195		198		197	
NH_3 flow rate mL/min	3.0				5.0		3.0		3.0	
Method	on-mass	mass-shift	on-mass	mass-shift	on-mass	mass-shift	on-mass	mass-shift	on-mass	mass-shift
Mass pair	191-191	191-206	193-193	193-208	195-195	195-229	198-198	198-232	197-197	197-231
10 ppm Cu Zn	0.004	0.000	0.003	0.004	0.003	0.000	0.002	0.000	0.000	0.000
10 ppm Sr Rb	0.002	0.000	0.001	0.001	0.000	0.000	0.000	0.000	0.000	0.000
10 ppm Ni	0.004	0.000	0.001	0.004	0.000	0.000	0.000	0.002	0.000	0.000
10 ppm Mo	0.000	0.000	0.000	0.000	0.000	0.000	0.003	0.000	0.000	0.000
10 ppm Pb, 1 ppm Hg	0.002	0.001	0.000	0.000	0.000	0.000	0.005	0.001	0.000	0.000
10 ppm Zr Nb	0.017	0.000	0.679	0.066	0.031	0.009	0.003	0.001	0.000	0.000
10 ppm REE	44.3	0.019	1.56	0.019	0.031	0.002	0.000	0.000	0.044	0.003
10 ppm Ta	0.000	0.000	0.000	0.000	0.004	0.000	0.261	0.009	4.11	0.046
10 ppm Hf	0.690	0.095	21.4	2.40	0.904	0.115	0.141	0.070	0.070	0.003
10 ppm W	0.001	0.000	0.000	0.000	0.001	0.000	0.479	0.000	0.001	0.000

Analysis of complex synthetic matrix sample using optimized NH_3 reaction mode

A complex synthetic matrix sample containing 10 ppm each of Cu, Zn, Sr, Rb, Ni, Mo, Pb, Zr, Nb, REEs, Ta, Hf, W and 1 ppm Hg was prepared, and this matrix was spiked with 1 ppb each of Ru, Rh, Pd, Ag, Os, Ir, Pt and Au as analytes. The concentration of the noble metals was determined in two modes: No gas mode and NH_3 reaction cell mode, and the spike recovery results are displayed in Figure 1 for each mode. The results demonstrate that MS/MS mode with NH_3 reaction cell gas successfully removes multiple interferences on all the noble metals, providing accurate results for these analytes even in a complex and challenging matrix.

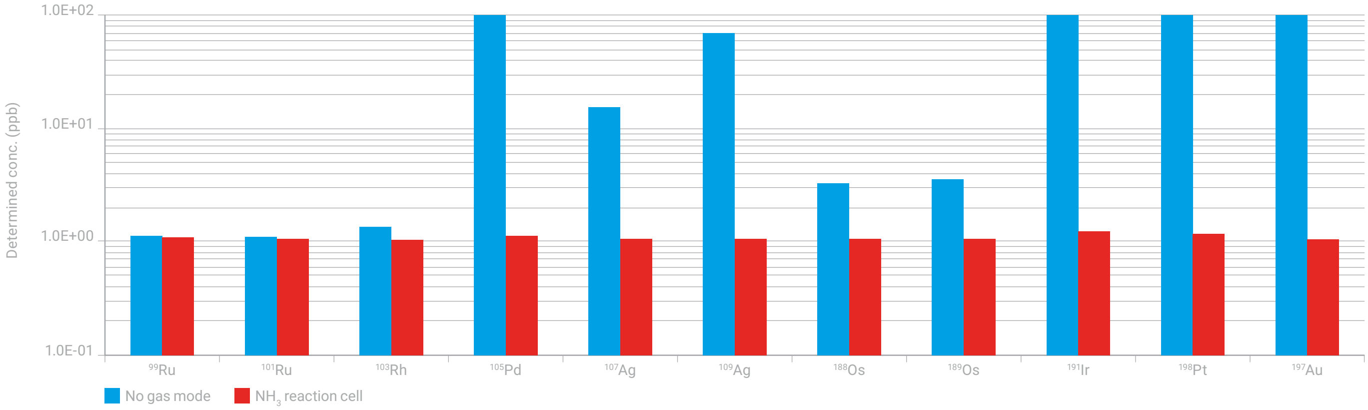

Figure 1. Result of synthetic matrix sample test. 1 ppb noble metals were measured in a multi-matrix sample containing 10 ppm of each Cu, Zn, Sr, Rb, Ni, Mo, Pb, Zr, Nb, REEs, Ta, Hf, W and 1 ppm Hg.

> Return to table of contents
> Search entire document

Analysis of Platinum Group Elements (PGEs), Silver, and Gold in Roadside Dust using Triple Quadrupole ICP-MS

Authors

Dominique Demare and
Liliane Jean-Soro,
Université Gustave Eiffel (IFSTTAR),
Nantes, France

Alain Desprez,
Agilent Technologies Ltd, France

Glenn Woods and Ed McCurdy,
Agilent Technologies LDA (UK) Ltd

Accurate, interference-free measurement of sub-ppb levels of the PGEs using the Agilent 8900 ICP-QQQ

Introduction

There is increasing interest in monitoring the noble metals—that is the Platinum Group Elements (PGEs), Ru, Rh, Pd, Os, Ir, and Pt, together with Ag and Au—in the environment. The levels of these elements have increased due to deposition arising from automobile catalytic converters *(1, 2)*. Precious metals are also used in healthcare and pharmaceuticals and in advanced technologies such as industrial catalysts, fuel cells, and electrodes, capacitors, and magnetic storage for consumer electronics. Production, use, and disposal of these products leads to wider release of the PGEs into the environment, which increases the need for routine monitoring of the metals in environmental samples. ICP-MS is widely used for analysis of trace levels of metals and metalloids, due to the technique's high sensitivity and multi-element capability. However, determination of the PGEs in samples such as soil and roadside dust is challenging for conventional single quadrupole ICP-MS because of the low concentration of the elements. Also, there is the potential for intense spectral overlaps from several common matrix elements, as shown in Table 1.

Many different approaches have been employed in an attempt to avoid, correct, or resolve matrix-based spectral overlaps in ICP-MS, including mathematical correction, matrix removal, and magnetic sector High-Resolution (HR)-ICP-MS. However, mathematical corrections are often unreliable, and matrix elimination is time-consuming, expensive, and prone to errors and contamination. HR-ICP-MS seems an attractive option, as it should give certainty that the analyte has been resolved from the overlapping ion on the mass scale. But many common spectral interferences require mass resolution far beyond the capability of commercial HR-ICP-MS instruments. For example, resolving $^{103}Rh^+$ from $^{87}Sr^{16}O^+$ requires mass resolution (M/ΔM) of 102,900; resolving $^{105}Pd^+$ from $^{89}Y^{16}O^+$, requires resolution of 27,600; and resolving $^{109}Ag^+$ from $^{93}Nb^{16}O^+$ requires resolution of 31,500. Current HR-ICP-MS instruments have a maximum mass resolution of 10,000, so are unable to separate any of these spectral overlaps.

The most widely used approach to resolve the common polyatomic ion overlaps that occur in quadrupole ICP-MS is to use a Collision/Reaction Cell (CRC) pressurized with helium (He) cell gas. He mode enables selective attenuation of polyatomic ions using a process called kinetic energy discrimination (KED). However, some of the matrix-based interferences on the trace PGEs are at too high intensity to be completely removed using He KED mode. Also, some interferences, such as $^{206}Pb^{++}$ on Rh at mass 103, are caused by spectral overlaps that are not polyatomic ions, so He mode cannot remove them effectively.

Table 1. Noble metal isotopic abundances (%) and potential spectral interferences on each isotope. Preferred isotopes for ICP-MS analysis are highlighted in yellow, secondary isotopes may be useful for data confirmation.

Mass	Analyte Isotope Abundance (%)				Potential Spectral Interferences				
	Ru	Rh	Pd	Ag	Isobaric	Hydride	Oxide/ Hydroxide	Argide	Other
96	5.54				Zr, Nb, Mo		SeO, BrOH		
98	1.87				Mo	MoH	SeO	NiAr	CuCl
99	12.76					MoH			ZnCl
100	12.6				Mo		SrO	NiAr	CuCl
101	17.06					MoH	RbO	NiAr	ZnCl
102	31.55		1.02				SrO	NiAr	CuCl, ZnCl
103		100					SrO, RbO	CuAr	ZnCl, Pb^{++}
104	8.62		11.14				SrO	ZnAr	ZnCl, Pb^{++}
105			22.33				YO, SrOH	CuAr	ZnCl
106			27.33		Cd		YOH, ZrO	ZnAr	
107				51.84			ZrO	ZnAr	
108			26.46		Cd		ZrO, MoO	ZnAr	
109				48.16			NbO		
110			11.72		Cd		ZrO, MoO		
	Os	Ir	Pt	Au					
184	0.02				W			NdAr	
186	1.59				W		YbO	NdAr	
187	1.96				Re	WH	YbO	SmAr	
188	13.24						YbO	SmAr, NdAr	
189	16.15						YbO	SmAr	
190	26.26		0.014				YbO	SmAr, NdAr	
191		37.3					LuO	EuAr	
192	40.78		0.782				YbO, LuO, HfO	SmAr	
193		62.7					HfO	EuAr	
194			32.97				HfO	SmAr, GdAr	
195			33.83				HfO	GdAr	
196			25.24		Hg		HfO	GdAr	
197				100			TaO, HfOH	GdAr	
198			7.163		Hg		WO, TaOH	GdAr	

In this work, an alternative approach to He KED was investigated, using an Agilent 8900 Triple Quadrupole ICP-MS (ICP-QQQ) to resolve the multiple, matrix-based interferences that affect analysis of the PGEs (*1*). The 8900 ICP-QQQ is a tandem mass spectrometer with two high performance, hyperbolic, quadrupole mass filters, one before (Q1) and one after (Q2) the ORS^4 CRC. The tandem (MS/MS) configuration gives the possibility to use the additional quadrupole—Q1, before the CRC—to select the ions that can enter the cell. This allows the ion/molecule reaction chemistry to be precisely controlled, even when highly reactive cell gases such as ammonia (NH$_3$) are used in the CRC. Reaction chemistry processes happen much faster than He KED, so can provide more effective separation of trace analytes that are overlapped by intense spectral interferences.

The 8900 ICP-QQQ includes UHMI (Ultra High Matrix Introduction) aerosol dilution technology, which increases plasma robustness and allows samples with higher Total Dissolved Solids (TDS) to be analyzed routinely. The 8900 with UHMI improves trace level analysis, as samples can be analyzed with minimal dilution, which reduces the risk of errors and contamination from the dilution step. Use of a more robust (hotter) plasma also increases ionization, improving sensitivity for poorly ionized noble metals such as Ir, Pt, and Au.

A series of synthetic matrix element mixes and a certified reference material (CRM) of road dust were used to evaluate the effectiveness and accuracy of the 8900 ICP-MS/MS method.

This work was performed in collaboration with the Université Gustave Eiffel, formerly IFSTTAR, Institut Français des Sciences et Technologies des Transports, de l'Aménagement et des Réseaux (the French Institute of Science and Technology for Transport, Development and Networks).

Experimental

Instrumentation

An Agilent 8800 ICP-QQQ was used for initial measurements, with later work being performed using an Agilent 8900 ICP-QQQ model. Both instruments were operated in the standard configuration, which includes Ni interface cones and standard "x" type ion lens. The standard sample introduction system was used, consisting of a MicroMist nebulizer, Peltier-cooled quartz double-pass Scott-type spray chamber, and quartz torch with 2.5 mm injector. Preset plasma condition UHMI-4 (aerosol dilution factor of approximately 4) was selected for the analysis.

The interference removal capability of NH_3 reaction gas in MS/MS mode (both quadrupoles functioning as true mass filters) was assessed. Results acquired with NH_3 in MS/MS mode were compared to the data collected with no cell gas and in He KED mode, as typically used on single quadrupole ICP-MS. Three different NH_3 gas flow rates (Low (NH_3-L), Medium (NH_3-M), and High (NH_3-H)) were used. The NH_3 cell modes used a cell gas of 10% NH_3 in He buffer gas, which controls the in-cell formation of unwanted reaction gas product ions. Details of all the cell gas modes and other acquisition conditions are given in Table 2.

Table 2. Agilent 8900 ICP-QQQ acquisition and CRC conditions.

	No Gas	He	NH_3-L	NH_3-M	NH_3-H
Acquisition Mode	SQ	SQ	MS/MS	MS/MS	MS/MS
Cell Gas	N/A	He	NH_3	NH_3	NH_3
Gas Flow (mL/min)	N/A	5.0	2.0	3.0	5.0
Octopole Bias (V)	−8	−18	−5	−10	−12
KED (V)	+5		−8		
Cell Exit (V)	−90				
Deflect Lens (V)	20	0	10	6	2
Integration Time/Mass (s)	0.2	0.3	1	1	1

Method

The Background Equivalent Concentrations (BECs) of the PGEs were quantified in a series of synthetic interference solutions containing several potentially interfering matrix elements, either individually or in various combinations. The BECs for the PGEs were calibrated against simple, synthetic, non-matrix-matched calibration standards.

Spike recoveries were measured for a spike containing 1 µg/L (ppb) of each of the PGEs, Ag, and Au in the highest, most complex synthetic matrix (all individual matrix components in one solution). To check the accuracy of the method for real sample analysis, the PGEs were also quantified in a digested CRM (BCR 723 Road Dust, IRMM, Geel, Belgium). The CRM has certified values for Rh, Pd, and Pt.

Data was acquired for all three cell gas modes during one visit to the sample vial, and three replicate measurements were acquired for each sample. The no gas and He mode conditions used Single Quad (SQ) mode (Q1 not operating as a mass filter) to replicate the interference removal performance achievable with single quadrupole ICP-MS. The NH_3 cell gas conditions used MS/MS mode with either on-mass measurement of the analyte ion, or mass-shift measurement where an analyte reaction product ion is measured. The indium (In) internal standard (ISTD) was added to the sample solutions online via the standard ISTD mixing T-connector.

Standards and sample preparation

Standards and interference matrices—most elements at 10 mg/L (ppm)—were prepared from single element 1000 or 10,000 mg/L stock solutions. The single and multiple matrix element mixes analyzed are shown in Table 3. All synthetic solutions were acidified to 4% HNO_3 and 12% HCl. This matrix is typical of the final acid concentration resulting from digestion of soil, dust, and mineral ore samples using aqua regia (a 1:3 mix of concentrated HNO_3/HCl).

The acid concentration in the synthetic samples matched the acid mix in the digested CRM. The CRM was prepared by mineralization of 0.5084 g of BCR 723 in 2 mL of concentrated HNO_3 and 6 mL of concentrated HCl. The volume was then brought up to 50 mL by addition of ultrapure water, giving a final matrix containing approximately 1% TDS in 16% aqua regia.

Results and discussion

Interference removal in complex synthetic matrices

The BEC results obtained in the study of matrix-based spectral interferences in the synthetic matrix solutions are shown in Table 3. The BECs for the PGEs in each of the matrix solutions are compared for no gas, He, and the optimum NH_3 mode (low, medium, or high NH_3 flow). The colored cells in Table 3 indicate the level of contribution that the matrix interferences made to the PGE BEC. For example, a matrix interference contribution causing a BEC of between 0.1 ppb and 1 ppb is indicated by the yellow shading. As can be seen from Table 3, Ru did not suffer significant interference in any of the synthetic matrices, even when measured in no gas mode. However, the other PGEs all suffered moderate or severe interference (up to 996 ppb BEC) in no gas mode. Interference contributions were higher than 10 ppb for Pd, Ag, Ir, Pt, and Au. The BECs for Rh and Os were lower, but still in the 100s of ng/L (ppt) or low ppb range.

The He mode data in Table 3 was evaluated to assess the relative performance of the standard single quadrupole ICP-MS approach to controlling polyatomic ions. Compared to no gas mode, He KED mode gave lower BECs for many of the PGEs, some improved by several orders of magnitude. But He mode was not able to completely resolve all the overlaps to a low enough level for trace analysis of all the PGEs. In He mode, the contribution of the spectral interferences from some of the matrix combinations was still in the ppb range for Pd, Ag, and Os and above 10 ppb for Ir, Pt, and Au.

By contrast, the optimum NH_3 mode significantly reduced the interference contributions on the PGEs in all the matrix solutions, including the most complex interference mix. BECs were lower than single or low 10s ppt for all the PGEs except Ir and Pt-195. The BECs for Ir and Pt in NH_3 mode remained a little higher at 0.1 to 0.2 ppb. But these BECs are still around 100x lower than was achieved in He mode and up to 1000x lower than in no gas mode. The improved interference removal capability provided by NH_3 in MS/MS mode allows the reliable quantitation of PGEs at ultra-trace levels in a complex environmental matrix such as roadside dust.

Spike recoveries, detection limits (DLs) and BECs in a complex matrix mix

To evaluate more specifically the accuracy of the ICP-MS/MS method, a 1 µg/L (ppb) PGE spike was measured in the highest and most complex synthetic interference solution. The mix contained 10 ppm of all interfering elements (listed in Table 3) except for Hg, which was present at 1 ppm. The PGE spike concentrations were quantified in no gas, He, and the optimum NH_3 cell gas mode. As shown in Figure 1, the PGE spike concentrations measured in no gas mode were strongly affected by spectral overlaps formed from the matrix elements. The matrix interferences in He mode were lower, but several of the measured results were still far above the true spike concentrations. The NH_3 mode results are all free from significant overlap, with measured PGE spike concentrations close to the true value of 1 ppb.

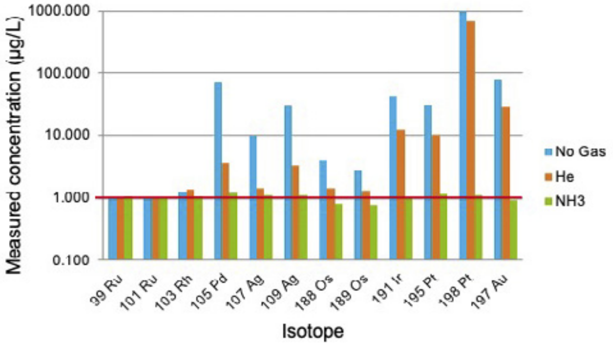

Figure 1. Reported concentrations of the PGEs spiked at 1 ppb in the most complex mixed matrix, measured in three different gas modes.

Table 4 shows the DL and BEC for each PGE in the optimum NH_3 cell gas mode. The DLs were calculated from three times the standard deviation of a low standard (10 ppt) divided by the slope of the calibration. The BECs were calculated from the blank intensity divided by the sensitivity. The DLs and BECs for the PGEs measured in NH_3 mode were all in the low or sub-ppt range despite the reduction in sensitivity that occurs due to the use of aerosol dilution with UHMI. The low DLs and BECs indicate that the 8900 ICP-QQQ can achieve excellent detection capability, even when combined with the very robust plasma conditions needed for routine analysis of high matrix sample digests.

Table 3. PGE Background Equivalent Concentrations (BECs) in µg/L (ppb) due to matrix-based spectral overlaps measured in no gas, He, and NH_3 cell gas modes. Significant matrix interferences are indicated by colored cells: Yellow (BEC >0.1 ppb), orange (BEC >1 ppb), and red (BEC >10 ppb). MS/MS mode with NH_3 cell gas resolves interferences on all analytes. Note, some PGEs have two usable isotopes.

No cell gas, SQ mode BEC results (µg/L)

Element	Ruthenium		Rhodium	Palladium	Silver		Osmium		Iridium	Platinum		Gold
Isotope	99	101	103	105	107	109	188	189	191	195	198	197
10 ppm Cu Zn	0.035	0.028	0.036	0.069	0.014	0.004	0.001	0.002	0.005	0.000	0.000	0.002
10 ppm Sr Rb	0.001	0.021	0.096	2.957	0.004	0.001	0.001	0.001	0.002	0.000	0.000	0.002
10 ppm Ni	0.001	0.004	0.002	0.020	0.007	0.008	0.001	0.003	0.005	0.000	0.000	0.001
10 ppm Mo	0.016	0.005	0.001	0.006	0.001	0.006	0.004	0.005	0.001	0.000	0.000	0.001
10 ppm Pb, 1 ppm Hg	0.000	0.000	0.254	0.004	0.002	0.004	0.011	0.012	0.006	0.000	666.924	0.001
10 ppm Zr Nb	0.000	0.000	0.001	0.829	10.436	34.858	0.018	0.018	0.004	0.005	5.270	0.127
10 ppm REE, Sc, Y	0.012	0.030	0.014	78.040	0.098	0.008	3.793	2.229	45.307	1.004	4.540	0.390
10 ppm Ta	0.000	0.001	0.000	0.004	0.001	0.001	0.001	0.001	0.001	0.090	45.386	62.760
10 ppm Hf	0.000	0.000	0.000	0.001	0.001	0.002	0.001	0.016	0.325	29.337	1.062	5.095
10 ppm W	0.001	0.000	0.000	0.001	0.000	0.002	0.004	0.001	0.001	0.005	104.237	0.614
10 ppm all, 1 ppm Hg	0.081	0.078	0.347	75.342	9.210	30.395	3.314	1.936	43.256	31.971	996.057	81.912

He cell gas, SQ mode BEC results (µg/L)

Element	Ruthenium		Rhodium	Palladium	Silver		Osmium		Iridium	Platinum		Gold
Isotope	99	101	103	105	107	109	188	189	191	195	198	197
10 ppm Cu Zn	0.001	0.001	0.001	0.001	0.005	0.004	0.004	0.002	0.005	0.001	0.000	0.002
10 ppm Sr Rb	0.000	0.001	0.002	0.058	0.001	0.001	0.003	0.002	0.001	0.001	0.000	0.001
10 ppm Ni	0.001	0.000	0.000	0.004	0.005	0.007	0.004	0.003	0.004	0.000	0.000	0.000
10 ppm Mo	0.005	0.001	0.000	0.001	0.000	0.001	0.008	0.005	0.001	0.000	0.000	0.001
10 ppm Pb, 1 ppm Hg	0.000	0.000	0.468	0.001	0.004	0.003	0.016	0.013	0.007	0.000	602.063	0.000
10 ppm Zr Nb	0.000	0.000	0.000	0.038	0.479	0.155	0.023	0.019	0.002	0.004	3.969	0.041
10 ppm REE, Sc, Y	0.000	0.001	0.010	2.692	0.010	0.005	0.543	0.366	11.157	0.064	1.578	0.020
10 ppm Ta	0.002	0.000	0.000	0.002	0.001	0.000	0.002	0.002	0.001	0.055	16.102	25.002
10 ppm Hf	0.000	0.000	0.000	0.001	0.001	0.000	0.004	0.006	0.082	8.937	0.627	1.122
10 ppm W	0.001	0.000	0.000	0.000	0.001	0.001	0.007	0.003	0.001	0.002	36.586	0.199
10 ppm all, 1 ppm Hg	0.016	0.003	0.399	2.748	0.510	0.169	0.489	0.320	11.158	9.264	669.894	27.554

NH_3 cell gas, MS/MS mode BEC results (µg/L)

Element	Ruthenium		Rhodium	Palladium	Silver		Osmium		Iridium	Platinum		Gold
Isotope	99	101	103	105	107	109	188	189	191	195	198	197
NH_3 flow rate (mL/min)	3.0	3.0	3.0	5.0	5.0	5.0	2.0	2.0	3.0	5.0	5.0	5.0
MS/MS mode	On-mass	On-mass	On-mass	On-mass	On-mass	On-mass	Mass-shift	Mass-shift	Mass-shift	Mass-shift	Mass-shift	Mass-shift
Mass Pair (Q1 - Q2)	99 - 99	101 - 101	103 - 103	105 - 105	107 - 107	109 - 109	188 - 203	189 - 204	191 - 206	195 - 229	198 - 232	197 - 231
10 ppm Cu Zn	0.002	0.001	0.000	0.000	0.004	0.004	0.002	0.004	0.003	0.000	0.000	0.001
10 ppm Sr Rb	0.000	0.003	0.009	0.012	0.000	0.001	0.002	0.003	0.003	0.000	0.000	0.000
10 ppm Ni	0.001	0.001	0.000	0.003	0.005	0.008	0.004	0.003	0.005	0.000	0.000	0.000
10 ppm Mo	0.001	0.001	0.000	0.001	0.000	0.001	0.004	0.008	0.003	0.001	0.003	0.000
10 ppm Pb, 1 ppm Hg	0.000	0.000	0.000	0.001	0.002	0.003	0.010	0.011	0.010	0.000	0.004	0.001
10 ppm Zr Nb	0.000	0.000	0.000	0.002	0.004	0.006	0.020	0.018	0.005	0.001	0.002	0.000
10 ppm REE, Sc, Y	0.000	0.001	0.009	0.017	0.002	0.006	0.050	0.046	0.105	0.008	0.031	0.001
10 ppm Ta	0.000	0.000	0.000	0.000	0.000	0.002	0.004	0.007	0.003	0.001	0.000	0.000
10 ppm Hf	0.001	0.000	0.000	0.000	0.000	0.001	0.007	0.009	0.036	0.113	0.003	0.000
10 ppm W	0.000	0.000	0.000	0.000	0.000	0.002	0.009	0.007	0.006	0.000	0.000	0.000
10 ppm all, 1 ppm Hg	0.002	0.004	0.020	0.044	0.022	0.023	0.030	0.017	0.183	0.137	0.023	0.002

The low DLs and BEC are partly due to the optimized configuration of the 8900 ICP-QQQ, which gives extremely low background signals. For example, 0 cps were measured in the calibration blank for Os, Ir, and Au in NH_3 mode. A second factor is the highly selective reaction chemistry in the CRC when the 8900 is operated in MS/MS mode with NH_3 cell gas. The MS/MS configuration uses Q1 to select the specific mass of ions that are allowed to enter the CRC and react. Q1 ensures that only the selected analyte ions and on-mass interfering ions enter the CRC, so the reactions are controlled and predictable, leading to very effective resolution of the interfering ions. No new potentially overlapping product ions can form from ions at other masses, because all other masses are excluded from the CRC when Q1 is operating as a true mass filter.

Table 4 also shows the percent recoveries for the 1 ppb PGE spike in the highest, most complex mixed matrix solution. All recoveries in NH_3 mode were within 10% of the target value, with the exception of Os, which suffers from chemical instability in the presence of HNO_3. Osmium stability can be improved by reducing the HNO_3 concentration in the solutions and increasing the HCl concentration.

Table 4. PGE DLs, BECs, and recoveries of a 1 ppb spike in a complex synthetic interference matrix.

Element	Mass Pair (Q1 - Q2)	DL (ng/L)	BEC (ng/L)	1 ppb Spike Recovery (%)
Ru	99 - 99	1.691	1.123	104
Ru	101 - 101	0.67	0.129	101
Rh	103 - 103	0.653	0.126	101
Pd	105 - 105	5.541	2.133	108
Ag	107 - 107	3.78	5.288	106
Ag	109 - 109	0.849	0.327	107
Os	188 - 203	6.245	3.704	81
Os	189 - 204	6.558	3.571	78
Ir	191 - 206	8.566	5.882	103
Pt	195 - 229	6.247	1.202	102
Pt	198 - 232	2.232	0.918	109
Au	197 - 231	7.592	4.348	91

Recovery of PGEs in CRM BCR 723 Road Dust

The aqua regia digestion of CRM BCR 723 Road Dust was analyzed to evaluate the accuracy of the ICP-MS/MS method for quantitative analysis of the PGEs in a representative complex sample matrix. BCR 723 Road Dust has certified values for Rh, Pd, and Pt, and the recoveries for these elements in NH_3 mode on the 8900 ICP-QQQ are shown in Figure 2.

For all three certified elements, the values measured using the 8900 ICP-QQQ in NH_3 mode were in good agreement with the certified values. For Rh and Pt, the 8900 mean measured concentrations were almost identical to the certified mean values, and the measured precision (n=3) was less than 2% RSD. For Pd, the 8900 result was a little higher than the certified mean value, but still within the 95% confidence limits. The Pd result measured by the 8900 method is close to the limit of quantification (LOQ), as indicated by the relatively high RSD of 7%. However, note that the uncertainly of the certified value is also high at 31% (6.1 ± 1.9 µg/kg), due to the low concentration of the element. The certified value for Pd is also based on results from only 8 of the 20 labs that participated in the CRM certification exercise, further illustrating the difficulty of measuring this element at the low levels present in BCR 723.

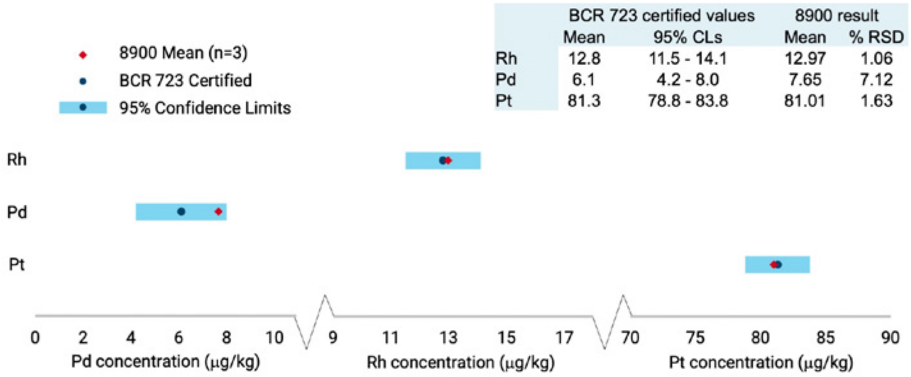

	BCR 723 certified values		8900 result	
	Mean	95% CLs	Mean	% RSD
Rh	12.8	11.5 - 14.1	12.97	1.06
Pd	6.1	4.2 - 8.0	7.65	7.12
Pt	81.3	78.8 - 83.8	81.01	1.63

Figure 2. Agilent 8900 ICP-MS/MS measured results compared to certified mean values and uncertainly ranges (95% confidence limits) for Rh, Pd, and Pt in CRM BCR 723 Road Dust.

Conclusion

A method has been developed for the routine analysis of the PGEs and other noble metals in high and complex matrices using the Agilent 8900 ICP-QQQ in MS/MS mode with NH_3 cell gas. Using the UHMI aerosol dilution system, the ICP-MS was able to tolerate the high levels of TDS (~10 g/L, 1%) in an aqua regia digest of a Road Dust CRM sample. UHMI enables high matrix sample digests such as soil, roadside dust, and mining samples to be analyzed with minimal dilution, avoiding potential problems of dilution errors or contamination from the diluent.

The 8900 ICP-QQQ method used MS/MS mode with NH_3 cell gas to resolve matrix-based interferences on the noble metals. The ability of ICP-MS/MS to resolve severe spectral interferences on the PGEs was shown by the low BECs obtained in a range of complex synthetic matrices. The method was further validated by demonstrating accurate spike recovery of the PGEs in the most complex matrix mix and accurate recovery of the certified elements in a Road Dust CRM sample. Potential matrix-based spectral interferences that cannot be addressed either by He KED mode on single quadrupole ICP-MS or by High Resolution ICP-MS were resolved successfully using the ICP-MS/MS method with NH_3 cell gas.

The 8900 ICP-QQQ offers a unique combination of exceptional matrix tolerance due to the robust UHMI plasma conditions, together with the low background and effective control of NH_3 reactions due to the MS/MS configuration. This combination allowed the development of a method that enables the accurate, interference-free measurement of sub-ppb levels of the PGEs with good precision in complex sample matrices.

The method is suitable for routine environmental monitoring of trace PGEs, as well as other applications such as mineral prospecting, extraction, and processing/reprocessing of the PGEs.

References

1. M. Omrani, M. Goriaux, Y. Liu, S. Martinet, L. Jean-Soro, V. Ruban, *Environ. Pollut.*, 257 (**2020**) 113477
2. M. Omrani, M. Goriaux, L. Jean-Soro, V. Ruban, Environ. Sci. *Pollut. Res.* 28 (**2021**) 33231–33240
3. Handbook of ICP-QQQ Applications using the Agilent 8800 and 8900, 4th Edition, Agilent publication 5991-2802EN, 2020

> Return to table of contents
> Search entire document

Direct Analysis of Ultratrace Rare Earth Elements in Environmental Waters by ICP-QQQ

Author

Naoki Sugiyama,
Agilent Technologies Inc.

Measure emerging pollutants in river water using the Agilent 8900 ICP-QQQ in MS/MS mass-shift mode

Introduction

The Rare Earth Elements (REEs)—also known as the lanthanides—range from lanthanum to lutetium. Scandium and yttrium are also commonly considered to be REEs. REEs are used in a wide range of applications from the glass industry, phosphors, permanent magnets, and lasers to clean energy, defense technologies, and batteries (*1–3*). With their increasing importance in high tech applications, there is growing concern about the migration of REEs into the environment during mining, processing, use, discarding, or recycling. More evidence is required to understand the effects of REEs on the environment, ecosystems, and from dietary intake. Depending on the findings that emerge from the research, regulations may be introduced to limit the disposal of REEs into water courses. In support of both research and routine monitoring purposes, quick, reliable, and sensitive analytical methods are needed to measure these emerging pollutants at low concentrations in a range of sample-types.

While ICP-MS is suited to the measurement of REEs at trace levels, the direct measurement of REEs in waste and natural waters remains challenging for two main reasons. Typically, the natural background concentration of the REEs is very low in environmental waters, often at or below the detection capabilities of conventional single quadrupole ICP-MS. Also, the analysis may be hindered by spectral interferences such as BaO^+ on Eu^+, BaH^+ on La^+, or low mass REE-oxide ions overlapping high mass REEs. A chelating resin can be used to preconcentrate the REEs and separate them from Ba, which is usually present at a much higher concentration. But this approach must be optimized for each sample matrix, requiring time, skill, and resources that may not be available in routine labs.

Triple quadrupole ICP-MS (ICP-QQQ) is a simpler, faster, direct method for the analysis of REEs in environmental waters at the ultratrace level. Compared to single quadrupole ICP-MS, ICP-QQQ offers greater sensitivity and advanced interference removal using controlled reaction chemistry in the collision/reaction cell (CRC). Agilent ICP-QQQ instruments feature two quadrupoles (Q1 and Q2), one either side of the CRC, enabling double mass selection (MS/MS). Q1 rejects all nontarget ions before they enter the cell, allowing only analyte ions and on-mass interference ions to pass to the cell. These ions can then be separated using predictable, consistent, and reproducible reaction chemistry (*4*). Q2 then ensures that only the analyte ions (on mass mode) or analyte-product ions (mass-shift mode) pass to the detector, free of interferences.

In this study, an Agilent 8900 ICP-QQQ was used for the direct analysis of REEs in water that was collected at four different points along a Japanese river. Using an MS/MS mass-shift method with nitrous oxide (N_2O) as a reaction cell gas, any interferences were resolved quickly and effectively.

> Return to table of contents

Experimental

Instrumentation

An Agilent 8900 ICP-QQQ (model #100 for advanced applications) was used in this study. The instrument was fitted with a quartz double-pass spray chamber, quartz torch with 2.5 mm id injector, and Ni interface cones. Sample delivery was via a peristaltic pump and PFA microflow nebulizer (G3139-65100 nebulizer) with a small dead volume. The samples were clean, natural waters, so `low-matrix' preset plasma conditions were selected in the Agilent ICP-MS MassHunter software. The preset plasma setting automatically optimizes the plasma conditions for the routine analysis of samples with total dissolved solids < 0.1%.

Selection of reactive cell gas

Oxygen (O_2) and N_2O were investigated as reaction cell gases to remove spectral interferences on REEs using a MS/MS mass-shift method. The potential spectral interferences include BaO^+ on Eu^+, BaH^+ on La^+, or low mass REE-oxide ions on high mass REE ions.

Since the O atom transfer reaction of REE^+ with N_2O ($REE^+ + N_2O \longrightarrow REEO^+ + N_2$) is exothermic for all REEs, good sensitivity was expected with N_2O. As shown in Figure 1, comparable or greater sensitivity was achieved for all REEs using N_2O compared to O_2 cell gas. Based on these results, N_2O was used as the reaction cell gas in this study.

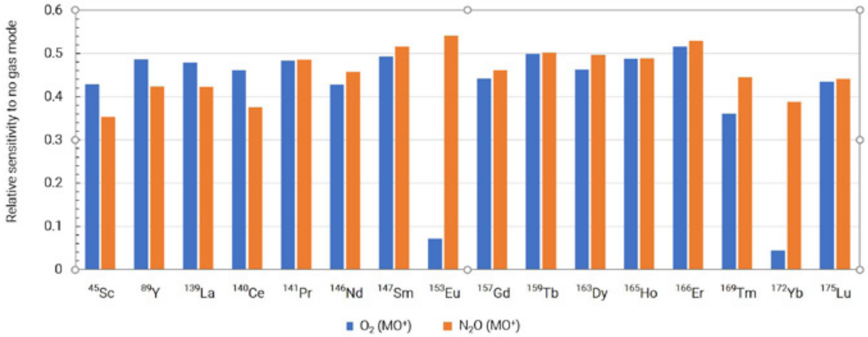

Figure 1. Comparison of the sensitivity of ICP-QQQ MS/MS mass-shift method with O_2 and N_2O cell gas.

All 8900 ICP-QQQ operating and tuning conditions are summarized in Table 1.

Table 1. ICP-QQQ tuning and operating conditions.

Parameter	Setting
RF Power (W)	1550
Sampling Depth (mm)	8.0
Nebulizer Gas Flow Rate (mL/min)	1.05
Makeup Gas Flow Rate (mL/min)	0.0
Extraction 1 Lens (V)	−5.0
Extraction 2 Lens (V)	−200
Omega Lens (V)	7.0
Omega Bias Lens (V)	−110
Octopole Bias (V)	−3.0
Cell Gas Flow Rate (% of full scale)	20
Axial Acceleration (V)	1.0

Method detection limits (MDLs)

MDLs for the REEs were calculated from three times the standard deviation of nine replicate measurements of a low-level standard (0.3 ppt each REE in 1% HNO_3). The results are summarized in Table 2. All the MDLs are sub ppt, confirming the suitability of the method for the determination of REEs at background levels in environmental waters.

Certified reference material analysis

A river water certified reference material (CRM), SLRS-6 (NRC-CNRC, Ottawa, Canada) was analyzed using the ICP-QQQ in MS/MS mode with N_2O. All REEs were measured as oxide ions, with a mass-shift of 16 u, as indicated in the Q1/Q2 settings provided in Table 2.

There is good agreement between the CRM reported values (*5*) and measured concentrations for all elements except for Sc (Table 2). To investigate the discrepancy, Sc was analyzed in the CRM using no gas and helium (He) collision (kinetic energy discrimination) mode. The measured concentrations were 367 and 33.3 ppt, respectively. No detailed information is given for the reported value for Sc on the CRM certificate. Since the reported concentration (333.0 ppt) agrees with the measured value obtained in no gas mode (367 ppt), the author suspects the CRM reported value provided for Sc is not correct. Because the CRM contains Si at the ppm level, a spectral interference on Sc^+ by SiO^+ or $SiOH^+$ may account for the high reported value.

Using the ICP-QQQ method, any Si-based interferences on Sc^+ would be avoided. In MS/MS mode, Q1 operates as a single (1 u) mass filter so that only ions with the targeted *m/z* enter the CRC and react with the cell gas. Q1 rejects all other masses (including Si ions), avoiding any subsequent interferences by SiO^+ or $SiOH^+$ on Sc^+.

River water analysis

River water samples were collected at four points (A to D) of the Tama River, Japan. Two of the samples were collected at wastewater treatment plant (WWTP) discharge points (C and D), as shown in Figure 2. Three samples were collected from each sampling point, then filtered through a 0.45 µm filter, and acidified to 1% HNO_3.

Table 2. MDLs and SLRS-6 river water CRM reported values (*5*) and ICP-QQQ measured results.

Element	Q1/Q2	Integration Time (s)	MDL (ppt)	SLRS-6 Reported (ppt)	SLRS-6 This Study (ppt)
Sc	45/61	1.0	0.127	333.0	16.3
Y	89/105	1.0	0.053	128.0	125.7
La	139/155	1.0	0.062	248.3	241.3
Ce	140/156	1.0	0.061	292.7	288.5
Pr	141/157	1.0	0.057	59.1	57.3
Nd	146/162	3.0	0.066	227.8	221.3
Sm	147/163	3.0	0.096	39.5	37.8
Eu	153/169	1.0	0.082	7.26	6.50
Gd	157/173	3.0	0.078	31.6	29.9
Tb	159/175	1.0	0.059	4.07	3.75
Dy	163/179	3.0	0.073	21.9	21.1
Ho	165/181	1.0	0.100	4.30	4.14
Er	166/182	1.0	0.092	12.4	11.7
Tm	169/185	1.0	0.079	1.79	1.63
Yb	172/188	3.0	0.096	11.2	10.7
Lu	175/191	1.0	0.052	1.91	1.74

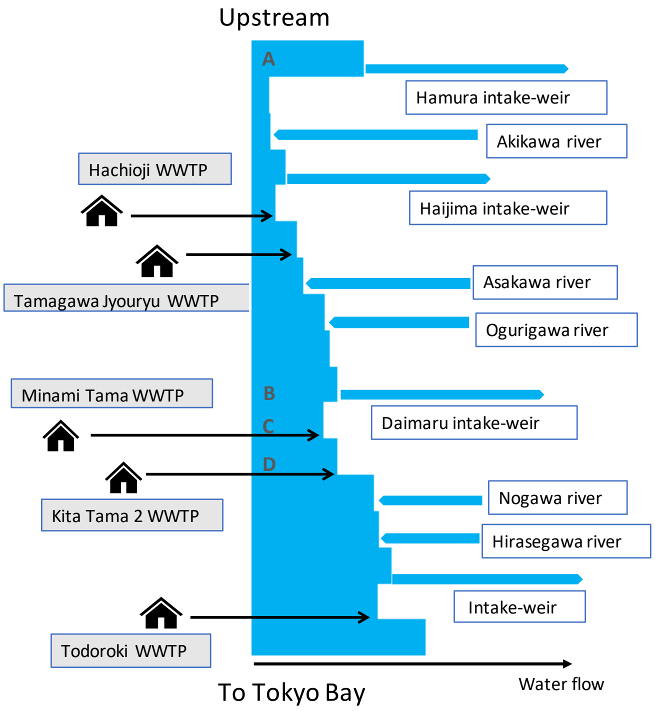

Figure 2. Tama River water flow balance and sample collection points A to D. The water flow balance is based on data provided by the Japanese Ministry of Land, Infrastructure, Transport, and Tourism, 1999.

Results and discussion

Each water sample was analyzed in triplicate using the 8900 ICP-QQQ method, and the average REE concentration for each site is shown in Figure 3 (left). The REEs are a chemically similar group of elements, so tend to behave consistently. However, in most natural materials, the REEs alternate between high and low concentrations, giving a saw-tooth profile which makes it difficult to see anomalies. For this reason, geochemists often normalize REE data by dividing the concentration of each REE measured in the sample by that element's value in a reference material. In this case, the reference material used was Post-Archean Australian Shales (PAAS) (6), as shown in Figure 3 (right).

Apart from gadolinium (Gd), the normalized REE results for waters from different points on the river gave consistent, smooth profiles, despite the low concentrations. Gd was consistent with the other REEs in the river water collected at the upstream location (Mitake). But there was a spike in the Gd concentration in the samples taken at the other three sites. The results indicate contamination by Gd compounds, which were not removed by WWTP and so were discharged into the river. A possible source is widely used Gd-based magnetic resonance imaging (MRI) contrast agents.

The plots in Figure 3 also suggest that the light REEs were depleted in the WWTP effluents, but the higher mass REEs were somewhat enriched. There is also a suggestion that Ce might be anomalously high in the water from the Kita Tama WWTP, as this element lies above the smooth line formed by the other light REEs.

These patterns may indicate other sources of REE contamination from local industry, although most REE concentrations apart from Gd were at the single ppt level or below.

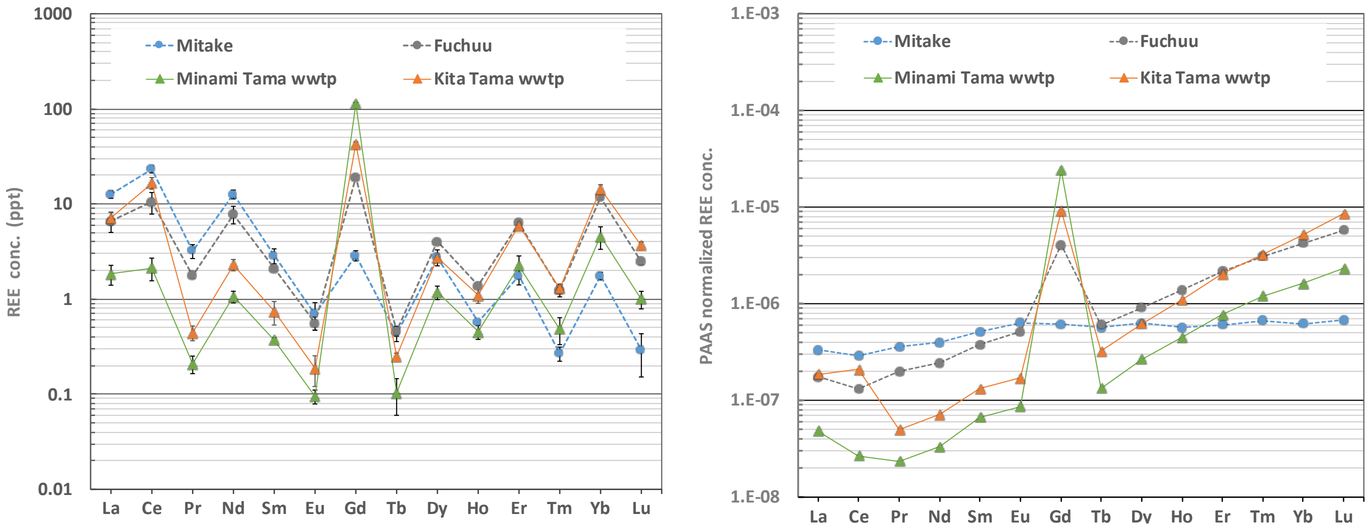

Figure 3. Concentrations of REEs in Tama River water samples by ICP-QQQ. Left: Average of three samples from each site with error bars showing two times the standard deviation. Right: Same REE results normalized to PAAS values.

Conclusion

The study demonstrates the suitability of the Agilent 8900 ICP-QQQ with MS/MS mode for the direct measurement of 16 REEs in river water. All potential polyatomic interferences arising from Ba oxide or low mass REE-based hydride, oxide, and hydroxide polyatomic interferences were resolved using the N_2O mass-shift method.

Sub ppt MDLs were achieved for all the REEs using the MS/MS method. The high sensitivity and low background provided by the 8900 are needed for the determination of emerging pollutants in environmental samples, which are typically present at ultratrace concentrations.

The results from the analysis of the Japanese river water samples collected at different points along the river highlighted an interesting finding for Gd. While all the other REEs were measured below 50 ppt in all samples, there was a spike in the Gd concentration in samples collected at or near to wastewater discharge points. Gd MRI reagents may be the source of the contamination.

References

1. US Geological Survey Mineral Resources Program
   The Rare-Earth Elements—Vital to Modern Technologies and Lifestyles,
   Fact Sheet 2014–3078, November 2014
2. Naoki Sugiyama and Glenn Woods, Direct measurement of trace rare earth elements (REEs) in high-purity REE oxide using the Agilent 8800 Triple Quadrupole ICP-MS with MS/MS mode, Agilent publication, 5991-0892EN
3. Juane Song, Xiang-Cheng Zeng, Dong Yan, and Wei-ming Wu, Routine determination of trace rare earth elements in high purity Nd_2O_3 using the Agilent 8800 ICP-QQQ, Agilent publication, 5991-5400EN
4. Reaction data for 70 elements using O_2, NH_3 and H_2 with the Agilent 8800 Triple Quadrupole ICP-MS, Agilent publication, 5991-4585EN
5. Delphine Yeghicheyan et al, A New Interlaboratory Characterisation of Silicon, Rare Earth Elements and Twenty-Two Other Trace Element Concentrations in the Natural River Water Certified Reference Material SLRS-6 (NRC-CNRC), *Geostandards and Geoanalytical Research*, Vol. 43 issue 3, **2019**, 475–4
6. W.B Nance and S.R Taylor, Rare earth element patterns and crustal evolution—I. Australian post-Archean sedimentary rocks, *Geochimica et Cosmochimica Acta*, Vol. 40, issue 12, **1976**, 1539-1551

> Return to table of contents
> Search entire document

Analysis of Radioactive Iodine-129 Using MS/MS with Oxygen Reaction Mode

Authors

Yasuyuki Shikamori, Kazumi Nakano and Naoki Sugiyama
Agilent Technologies, Japan

Keywords

radionuclide, iodine, ^{129}I, environmental, nuclear, xenon, NIST 3231 Level I and II, abundance sensitivity, oxygen on-mass

Introduction

Iodine-129 is a long-lived radionuclide (half-life of 15.7 My) which has been released into the environment as a result of human activities such as nuclear weapons testing, accidents at nuclear power plants and especially by emissions from spent nuclear fuel reprocessing plants. The determination of iodine-129 in environmental samples is very difficult by ICP-MS due to the element's relatively low sensitivity, the very low concentrations at which ^{129}I must be determined, relative to potentially high levels of ^{127}I, the high background caused by ^{129}Xe impurities in the argon plasma gas, and possible polyatomic interference from $^{127}IH_2^+$. Iodine analysis is further complicated by the fact that it is rapidly volatilized from samples prepared using the acid digestions that are normal for ICP-MS analysis, so an alternative, alkaline sample solubilization and stabilization strategy is required. The isobaric interference from $^{129}Xe^+$ can be significantly reduced using ICP-QMS with an Octopole Reaction Cell operated in O_2 reaction mode, resulting in a measured ratio for $^{129}I/^{127}I$ of 10^{-7} in NIST 3231 SRM Level I (*1*). However, the problem of potential overlap due to tailing from ^{127}I and ^{127}IH remains, as the relative abundance of the ^{129}I to ^{127}I will typically exceed 10^{-7}, which is of the same order as the abundance sensitivity (ability to separate adjacent peaks) of quadrupole ICP-MS (ICP-QMS). In order to overcome these challenges, ICP-QQQ operating in MS/MS mode with O_2 reaction gas was applied to determine ultratrace levels of iodine-129 in aqueous samples.

Experimental

Instrumentation: Agilent 8800 #100.

Plasma conditions: Preset plasma/Low matrix.

Ion lens tune: Soft extraction tune: Extract 1 = 0 V, Extract 2 = -190 V.

CRC conditions: O_2 gas at 0.8 mL/min,
Octopole bias = -18 V and KED = -1.5V. MS/MS O_2 on-mass mode was applied to measure iodine-127 and iodine-129 (Q1 = Q2 = 127 for iodine-127; Q1 = Q2 = 129 for iodine-129).

Reference materials and calibration standards: Calibration standards were prepared by diluting ^{129}I isotopic standards NIST SRM 3231 Level I and II (NIST, Gaithersburg MD, USA) with 0.5% TMAH in deionized water. The Level I Certified Value for $^{129}I/^{127}I = 0.981 \times 10^{-6} \pm 0.012 \times 10^{-6}$, Level II = $0.982 \times 10^{-8} \pm 0.012 \times 10^{-8}$. These reference materials were used to check the calibration linearity of the iodine isotopes and to validate the isotopic ratio of iodine-129 and iodine-127.

Results and discussion

Optimization of oxygen cell gas flow

The oxygen gas flow rate was optimized by varying the O_2 flow over the full range of the mass flow controller (0–1.12 mL/min), while monitoring the $^{127,129}I$ signal and blank intensity, as shown in Figure 1. As the flow rate of O_2 increases, the background signal (due to ^{129}Xe) at *m/z* = 129 decreases rapidly, and the iodine signal remains high, dramatically improving the DL for ^{129}I.

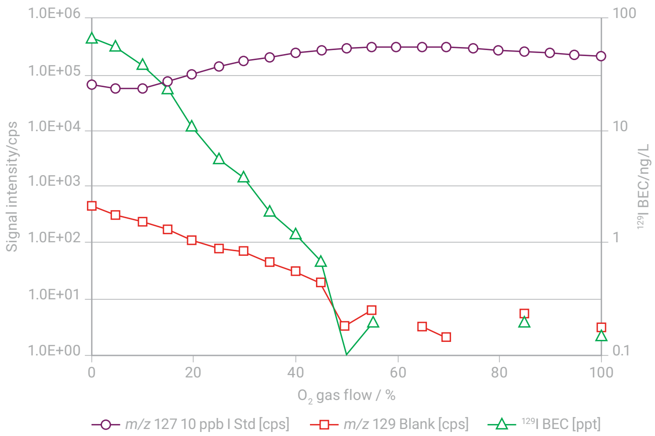

Figure 1. Profile of $^{127}I^+$, $^{129}Xe^+$ signals and estimated ^{129}I BEC. For the BEC calculation, the sensitivity of ^{129}I was assumed to be the same as ^{127}I. Scale of O_2 flow: 100% = 1.12 mL/min.

Abundance sensitivity

Scan spectra over the mass range 127 to 129, covering both ^{127}I and ^{129}I, were acquired for the two SRMs, NIST 3231 Level I and II, using the Agilent 8800 ICP-QQQ in MS/MS on-mass mode with O_2 reaction gas. The overlaid spectra are shown in Figure 2. Excellent abundance sensitivity can be seen, with the sides of the intense (>10^9 cps) ^{127}I peak reaching baseline with no tailing of $^{127}I^+$ or $^{127}IH^+$ on $^{129}I^+$.

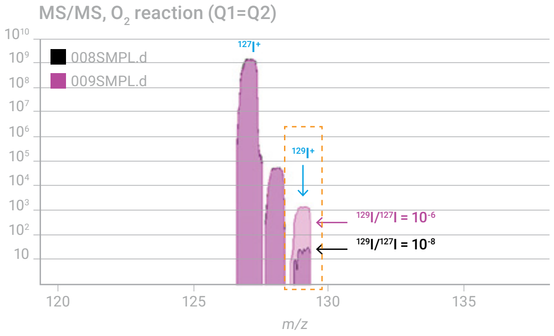

Figure 2. Iodine spectra showing both ^{127}I and ^{129}I acquired using MS/ MS on-mass mode with O_2 cell gas. $^{127}IH^+$ remains to some extent while $^{127}IH_2^+$ is completely removed, as noted later.

Calibration curves for ^{127}I and ^{129}I

In order to check the linearity of both iodine isotopes, different concentration solutions of NIST 3231 SRM Level I were prepared in 0.5% TMAH and analyzed as calibration standards, as shown in Figure 3. The BECs for ^{127}I and ^{129}I were 2.9 µg/L and 0.04 ng/L respectively, and the detection limits (3σ, n=10) were 0.26 µg/L for ^{127}I and 0.07 ng/L for ^{129}I.

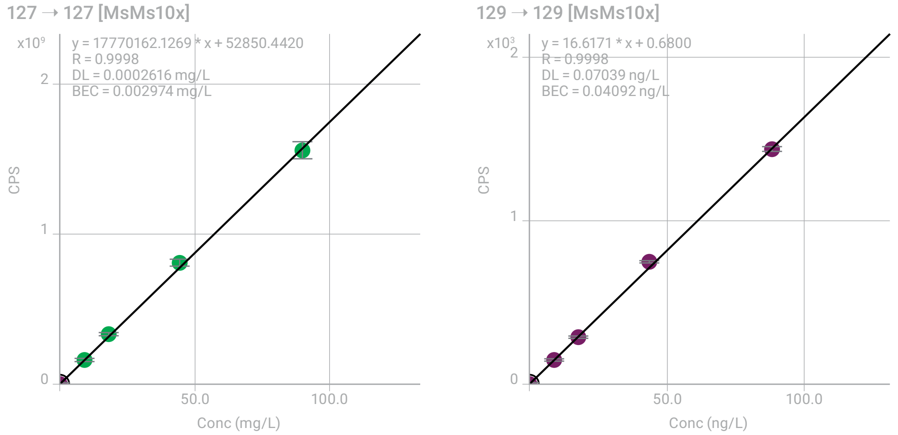

Figure 3. Calibration curve for iodine-127 (top) and iodine-129 (bottom) obtained from multiple dilutions of NIST 3231 SRM.

Analysis of NIST 3231 SRM Level I and Level II

The ^{129}I/^{127}I ratio in 10x diluted NIST 3231 SRM Levels I (^{129}I/^{127}I = 0.981 x 10^{-6}) and II (^{129}I/^{127}I = 0.982 x 10^{-8}) was measured using ICP-QQQ in MS/MS on-mass mode with O_2 cell gas. The results are summarized in Table 1. After subtracting the ^{129}I blank, the measured ^{129}I/^{127}I ratio of NIST 3231 SRM Levels I and II corresponded well with the certified values of 0.981x10^{-6} and 0.982x10^{-8} respectively. The good agreement with the certified ratio indicates that the potential interference of $^{127}IH_2^+$ on $^{129}I^+$ is completely removed by O_2 reaction with MS/MS mode.

Table 1. Analytical results for NIST 3231 Level I and Level II.

Sample name	Dilution factor	Q1=Q2=127 CPS	Q1=Q2=129 CPS	^{129}I/^{127}I	^{129}I/^{127}I (average n = 5)	RSD (%)
NIST 3231 10^{-6} (^{129}I/^{127}I = 0.981 x 10^{-6})	10	594,277,896	585.6	0.971 x 10^{-6}	0.981 x 10^{-6}	0.8
		592,633,576	597.4	0.994 x 10^{-6}		
		590,000,723	586.5	0.980 x 10^{-6}		
		593,387,443	588.5	0.978 x 10^{-6}		
		592,834,056	588.9	0.979 x 10^{-6}		
NIST 3231 10^{-8} (^{129}I/^{127}I = 0.982 x 10^{-8})	10	608,737,949	15.1	1.12 x 10^{-8}	1.02 x 10^{-8}	7.2
		608,536,242	14.8	1.07 x 10^{-8}		
		602,626,536	14.2	0.979 x 10^{-8}		
		603,091,763	13.9	0.929 x 10^{-8}		
		603,250,003	14.5	1.03 x 10^{-8}		
NIST Blank	10	600,444,851	8.3	—	—	—

Reference

1. The ultratrace determination of iodine 129 in aqueous samples using the 7700x ICP-MS with oxygen reaction mode, Agilent application note, 5990-8171EN.

More information

The ultratrace determination of iodine 129 using the Agilent 8800 Triple Quadrupole ICP MS in MS/MS mode, Agilent publication, 5991-0321EN

> Return to table of contents
> Search entire document

Feasibility Study on the Analysis of Radioisotopes: Sr-90 and Cs-137

Authors

Yasuyuki Shikamori and
Kazumi Nakano
Agilent Technologies, Japan

Keywords

radioisotopes, radioactive, environmental, nuclear, strontium, ^{90}Sr, zirconium, cesium, ^{137}Cs, barium, abundance sensitivity, oxygen and hydrogen on-mass, nitrous oxide on-mass

Introduction

ICP-MS can be an effective analytical tool for the analysis of long half-life radioisotopes due to its high sensitivity, speed of analysis, low sample consumption, and ease of sample preparation. The challenge for ICP-MS analysis of radioisotopes arises from interferences; not only by polyatomic ions but also atomic isobar ions that cannot be separated even by high-resolution (HR-) ICP-MS.

Trace analysis of the radionuclide ^{90}Sr (half-life = 28.74 years) in environmental samples is of great interest. ^{90}Sr is a main fission product that may be present in the environment following accidental releases from nuclear power plants. Geiger-Muller (GM) detectors or Liquid Scintillation Counters (LSC) are used to measure ^{90}Sr, though both techniques require complex chemical separation prior to analysis, or long integration times. ICP-MS is also used to measure ^{90}Sr, especially when a quick turn-around time is desired. However, detection limits of quadrupole ICP-MS are compromised by a spectral overlap from ^{90}Zr; in common with all direct isobaric interferences, the ^{90}Zr overlap is too close in mass to the ^{90}Sr to be resolved using sector field HR-ICP-MS, which is limited to a maximum resolution ($M/\Delta M$) of 10,000. This note describes a method for measuring trace ^{90}Sr in the presence of ^{90}Zr using ICP-QQQ in MS/MS reaction mode. Since it isn't possible to obtain ^{90}Sr, a natural isotope of strontium (^{88}Sr) was used to estimate the DL for ^{90}Sr. A similar approach was applied to ^{137}Cs (half-life = 30.0 years).

Experimental

Instrumentation: Agilent 8800 #100.

Plasma conditions: Preset plasma/Low matrix.

Ion lens tune: Soft extraction tune: Extract 1 = 0 V, Extract 2 = -190 V.

CRC and acquisition conditions: The following conditions were used for the analysis of ^{90}Sr and ^{137}Cs:

- For ^{90}Sr: MS/MS on-mass mode (Q1 = Q2 = 90) with O_2 + H_2 cell gas: 1 mL/min of O_2 and 10 mL/min of H_2, Octopole bias = -5 V and KED = -13 V.
- For ^{137}Cs: MS/MS on-mass mode (Q1 = Q2 = 137) with N_2O cell gas: 7 mL/min of N_2O (10% N_2O balanced in He, introduced via the 3rd cell gas flow line), Octopole bias = -5 V and KED = -13 V.

Results and discussion

Radioactive Sr-90 ($O_2 + H_2$ on-mass mode)

Figure 1 shows spectra of a solution containing Sr and Zr (natural isotopes) acquired on the 8800 ICP-QQQ operated in Single Quad mode (Q1 operated as an ion guide to emulate conventional quadrupole ICP-MS) with no cell gas (left), and in MS/MS mode with $O_2 + H_2$ cell gas (right). As can be seen in the left hand spectrum, the overlap of $^{90}Zr^+$ on $^{90}Sr^+$ precludes the low-level determination of ^{90}Sr by conventional quadrupole ICP-MS. The spectrum on the right indicates that $^{90}Sr^+$ could be measured on-mass at *m/z* = 90 free from interference by $^{90}Zr^+$, since Zr^+ reacts readily with the $O_2 + H_2$ gas to form ZrO^+ and ZrO_2^+. The signal-to-noise ratio for ^{90}Sr was improved by six orders of magnitude using MS/MS $O_2 + H_2$ reaction cell mode.

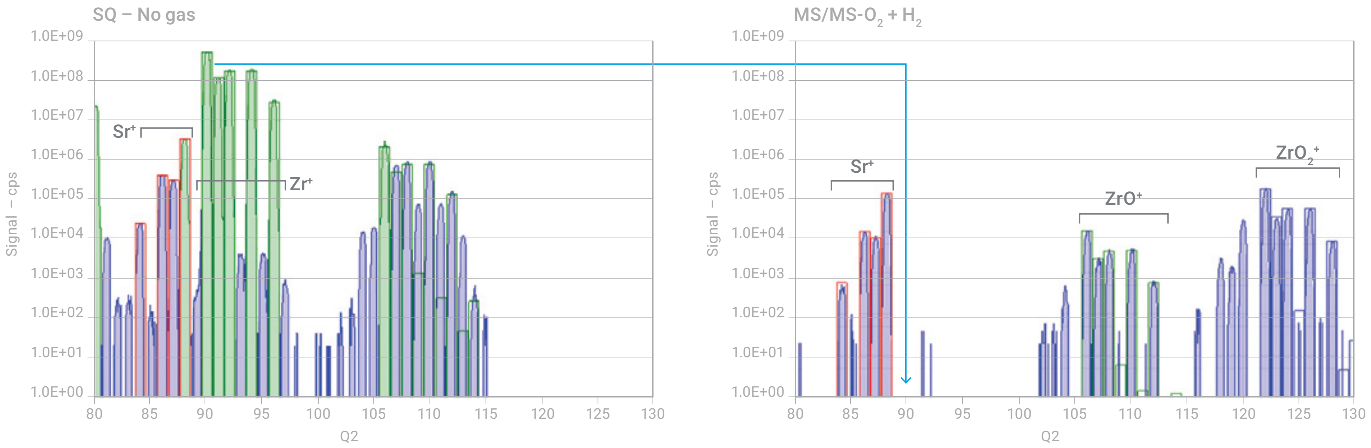

Figure 1. Mass spectra of a solution containing 20 ppb Sr + 5 ppm Zr: (left) SQ no gas mode and (right) MS/MS $O_2 + H_2$ reaction mode.

Figure 2 is a spectrum of 100 ppm Sr acquired using MS/MS on-mass mode with $O_2 + H_2$ reaction gas. The excellent abundance sensitivity (peak separation) of MS/MS mode can be confirmed. The peak sides reach the baseline with no tailing from the intense peak of the natural isotope of $^{88}Sr^+$. In addition, no $^{88}SrHH^+$ at *m/z* = 90 is formed in cell, even in a solution containing 100 ppm natural Sr.

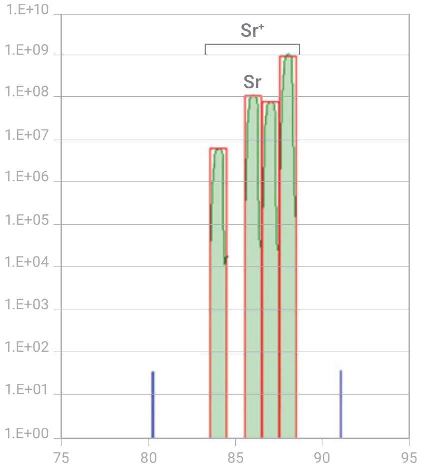

Figure 2. Spectrum of 100 ppm Sr solution acquired using MS/MS $O_2 + H_2$ on-mass mode.

Radioactive Cs-137 (N_2O on-mass mode)

Figure 3 shows spectra of a solution containing Cs and Ba (natural isotopes) acquired on the 8800 ICP-QQQ operated in Single Quad mode with no gas mode (left), and in MS/MS mode with N_2O cell gas (right). As can be seen in the left hand spectrum, the $^{137}Ba^+$ overlap on $^{137}Cs^+$ is a problem in conventional quadrupole ICP-MS. As with ^{90}Sr, the right hand spectrum shows that $^{137}Cs^+$ could be measured on mass at *m/z* = 137, free from the $^{137}Ba^+$ interference. Ba^+ reacts readily with N_2O to form BaO^+ and $BaOH^+$ while a part of the Cs^+ analyte ion signal remains at its original mass (as shown by the substantial peak for ^{133}Cs in the right-hand spectrum).

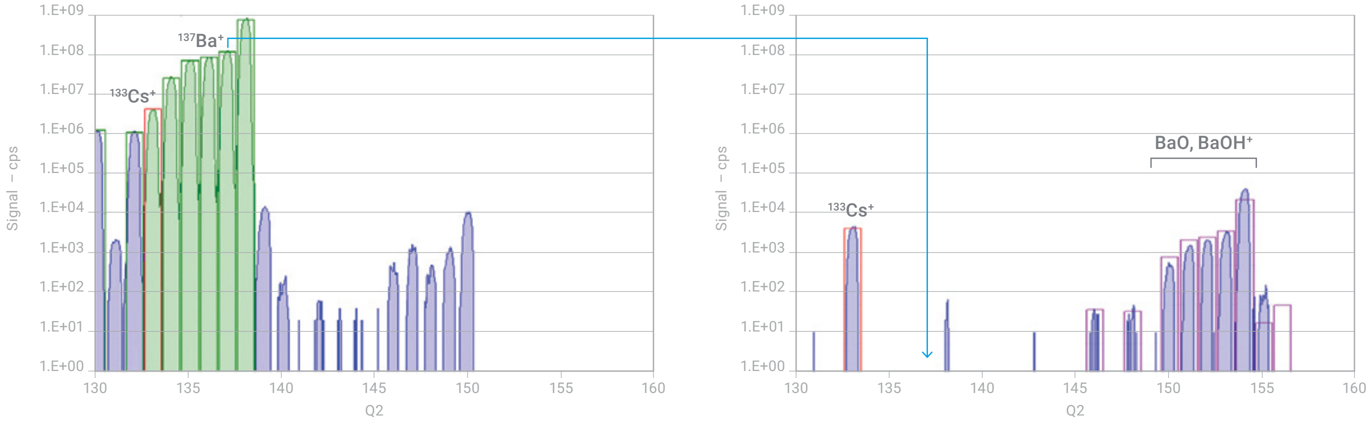

Figure 3. Mass spectra of a solution containing 20 ppb Cs + 5 ppm Ba: (left) SQ no gas and (right) MS/MS N_2O reaction mode.

Estimated BEC and DL for Sr-90 and Cs-137

The BEC and DL for two radioisotopes, ^{90}Sr and ^{137}Cs, were estimated from these spectra as summarized in Table 1. This feasibility study demonstrates the potential of ICP-QQQ for the measurement of radioisotopes such as ^{90}Sr and ^{137}Cs.

Table 1. Estimated BEC and DL for ^{90}Sr and ^{137}Cs.

Radioisotope	BEC (ng/L)	DL (ng/L)
^{90}Sr	0.08	0.23
^{137}Cs	2.9	15

Determination of Trace ^{236}U as UOO^+ using ICP-QQQ Oxygen Mass-shift Method

Author

Naoki Sugiyama
Agilent Technologies, Japan

Keywords

uranium, uranium-236, O_2 cell gas, mass-shift, extended mass range

Introduction

Uranium-236 is a long-lived radionuclide that is created from the naturally occurring trace isotope ^{235}U (0.72% abundance) by thermal neutron capture. This process leads to a natural abundance of ^{236}U in the range from 10^{-14} to 10^{-13} relative to the major ^{238}U isotope ($^{236}U/^{238}U$). ^{236}U is also created during the process of uranium enrichment for nuclear fuel or weapons. The $^{236}U/^{238}U$ ratio is increased up to 10^{-3} in spent nuclear fuel, with background levels in the environment at around 10^{-7} to 10^{-8} as a result of global fallout. The $^{236}U/^{238}U$ isotope ratio can therefore be used as a sensitive method to trace the accidental release of enriched uranium fuel, spent fuel, and nuclear waste.

The challenges for ICP-MS for this application are the interference on $^{236}U^+$ by the hydride ion $^{235}UH^+$, and the contribution at *m/z* 236 from tailing of the $^{235}U^+$ and $^{238}U^+$ peaks. The hydride overlap and peak tailing are more problematic in samples that have been enriched, as these samples contain a higher proportion of ^{235}U. Uranium was measured via its dioxide ion, UO_2^+, due to the efficient conversion (almost 100%) of U^+ to UO_2^+ with O_2 cell gas.

Experimental

Instrumentation: Agilent 8900 Advanced Applications configuration ICP-QQQ with PFA nebulizer (p/n G3139-65100).

Plasma tuning: RF power = 1550 W, sampling depth = 8.0 mm, nebulizer gas flow rate = 0.80 L/min, make-up gas flow rate = 0.30 L/min, and peristaltic pump = 0.1 rps.

Cell tuning: Octopole bias = 0 V, KED = -10 V, O_2 cell gas flow = 0 to 35% of full scale (0 to 0.53 mL/min).

Sample preparation: Uranium solutions were prepared at suitable concentrations by diluting SPEX multi element standard XSTC-331 (SPEX CertiPrep, Metuchen, NJ, USA) with de-ionized water. All samples, blank, and rinse solutions were spiked with high purity TAMAPURE 100 HNO_3 (Tama Kagaku, Saitama, Japan) to a concentration of 1%.

Results and discussion

UO$^+$ and UOO$^+$ formation as a function of O_2 cell gas flow rate

The rate of formation of UO$^+$ and UO_2^+ was studied as a function of O_2 cell gas flow rate. A solution containing 10 ppb uranium (1000x dilution of XSTC-331) was introduced into the ICP-QQQ. The signals of $^{238}U^+$, $^{238}U^{16}O^+$, and $^{238}U^{16}O^{16}O^+$ were measured via three mass pairs (Q1➞Q2) = (238➞238), (238➞254), and (238➞270), and plotted against the O_2 cell gas flow rate. The octopole bias (Octp Bias) voltage was optimized to give the maximum UO_2^+ signal (0 V). Figure 1 shows that UO$^+$ formation reaches a maximum at an O_2 flow rate of 5% of full scale (equivalent to 0.074 mL/min as O_2). Above 0.075 mL/min flow rate, the formation of UO$^+$ decreased, while the formation of UO_2^+ increased, reaching a maximum at an O_2 flow of 22% of full scale (0.33 mL/min). This indicates the conversion of UO$^+$ to UO_2^+ via a chain reaction. The 8900 ICP-QQQ was optimized for highest sensitivity for the UO_2^+ product ion.

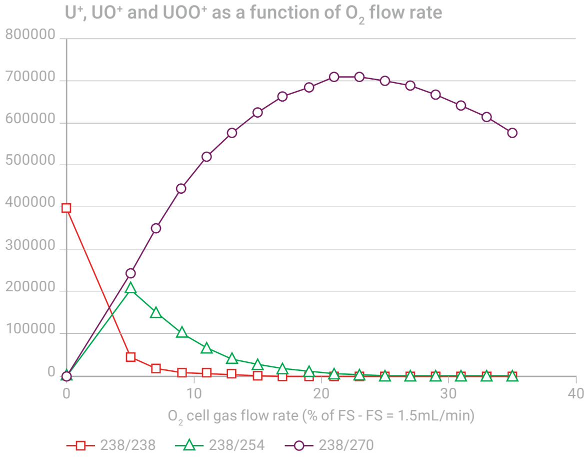

Figure 1. U$^+$ (238 ⟶ 238), UO$^+$ (238 ⟶ 254), and UO_2^+ (238 ⟶ 270) as a function of O_2 cell gas flow rate.

Effect of product ion selection on hydride ion formation rate

The hydride ratio was measured at the optimal O_2 flow rate for U$^+$ and each of the U-oxide product ions: $^{238}UH^+/^{238}U^+$, $^{238}UOH^+/^{238}UO^+$, and $^{238}UO_2H^+/^{238}UO_2^+$.

A sample containing 50 ppb U (200x diluted XSTC- 331) was introduced for the measurement of the hydride formation ratio. Ten replicate measurements were made, with integration times of 1 s and 10 s for the analyte and hydride ions respectively. The results are summarized in Table 1. The data shows that measuring UO$^+$ decreases the hydride ratio by a factor of ~20, while measuring UO_2^+ leads to more than a three orders of magnitude improvement, reducing the hydride ratio to 10^{-8}.

Uranium detection limit

The detection limit (DL) of U was estimated using the UO_2^+ method. A blank solution was introduced and the signal of the mass pairs (236→268 and 238→270) corresponding to $^{236}U^+ \rightarrow {}^{236}UO_2^+$ and $^{238}U^+ \rightarrow {}^{238}UO_2^+$ were measured using an integration time of 10 s. The results in Table 2 are based on 10 replicate measurements. The DL for ^{236}U was calculated from the concentration equivalent to three times the standard deviation of the background, using the sensitivity of $^{238}UO_2^+$ given in Table 1 and the background for mass pair 236→268 in Table 2. The DL for uranium-236 was calculated to be 0.50 ppq (fg/g).

Table 1. UH^+/U^+ ratios obtained by measuring uranium as U^+, UO^+, and UO_2^+.

	O_2 cell gas flow rate (%)	**U^+ analysis**			**UH^+ analysis**			**UH^+/U^+**
		Mass pair for U^+	**Counts**	**RSD**	**Mass pair for UH^+**	**Counts**	**RSD**	
		Q1/Q2	**cps**	**%**	**Q1/Q2**	**cps**	**%**	
as U^+	0	238/238	24168974	2.8	239/239	1578.5	0.6	6.53E-05
as UO^+	5	238/254	14152816	4.2	239/255	48.9	4.3	3.46E-06
as UOO^+	22	238/270	40527770	2.0	239/271	2.3	20.8	5.68E-08

Table 2. Uranium background noise.

236/268		238/270	
Counts	RSD	Counts	RSD
cps	%	cps	%
0.15	90.3	0.18	51.1

Conclusion

The Agilent 8900 ICP-QQQ operating in MS/MS mode with O_2 cell gas is suitable for the measurement of U via its reaction product ion UO_2^+. This approach was successful in reducing the contribution from the hydride ion (i.e. ^{235}UH overlap on ^{236}U). The formation of ^{235}UH was decreased by three orders of magnitude compared to direct, on-mass measurement of U^+. MS/MS mode with O_2 cell gas gave a UO_2H^+/UO_2^+ ratio in the 10^{-8} range, without the use of a desolvation system. The results suggest that the approach could be successful in reducing the interference of $^{235}UH^+$ on $^{236}U^+$, even in samples containing enriched U.

More information

Using ICP-QQQ for UO_2^+ product ion measurement to reduce uranium hydride ion interference and enable trace ^{236}U isotopic analysis, Agilent publication 5991-6553EN

Measurement of Neptunium in the Presence of Uranium: Benefits of Low Abundance Sensitivity and Oxygen Reaction Mode

Author

Glenn Woods
Agilent Technologies, UK

Keywords

neptunium, radiochemistry, abundance sensitivity, oxygen reaction mode

Introduction

Neptunium is present in the environment at ultratrace levels due to natural neutron capture, nuclear bomb testing, and as a decay product of ^{241}Am. ^{241}Am is used in ionizing smoke detectors, radiography, and a neutron source, among other uses. By far the greatest quantity of Np is formed during energy production within uranium fission reactors. The predominant isotope formed is ^{237}Np, with approximately 50 metric tonnes per annum being produced in nuclear waste. As the half-life of ^{237}Np is ~2.14 billion years, ^{237}Np in existence today is solely from the previously mentioned processes rather than remaining from the formation of the earth. However, the relatively long half-life ensures its persistence. Np will readily form aqueous solutions (more so than any other actinide element). It also attaches to particles and colloids rather than getting trapped in humic media (such as soil and peat). These properties mean that Np is fairly mobile once in the environment. Its high affinity for calcium-rich media causes it to concentrate within concrete, shells, etc.

Trace and ultratrace measurement of ^{237}Np is hindered by the presence of uranium within the sample. The biggest potential interference comes from peak broadening of the adjacent ^{238}U isotope. This Abundance Sensitivity (AS) interference is difficult to overcome. AS depends on the fundamental design of the spectrometer – such as the mass separation process (e.g. quadrupole or magnets), vacuum system, and electronics. Furthermore, minor but important polyatomic interferences from the hydrides of lighter U isotopes; $^{236}U^{1}H$, $^{235}U^{1}H_2$, $^{235}U^{2}H$, $^{234}U^{1}H^{2}H$ hinder the measurement of ^{237}Np. Regardless of the interference source, its affect will vary depending on the concentration of uranium (and its isotope ratio), potentially causing false and variable measurements.

Experimental

Instrumentation: An Agilent 8900 Advanced Applications configuration ICP-QQQ was used. The instrument version features Axial Acceleration across the ORS^4 collision/reaction cell that gives a higher product ion yield when using reaction chemistry.

Tuning: Np was measured under two sets of MS/MS conditions: on-mass (using no gas) and mass-shift (using O_2 reaction gas). In the latter mode, ^{237}Np is shifted away from the UH_x interferences allowing Np to be measured as the product ion NpO_2^+, free from interference, at *m/z* 269.

Calibration: Np was spiked into a 10 mg/L (ppm) U matrix to produce a set of calibration standards at 0.0, 0.19, 0.95, 1.9, 19.0, 95.0 ng/L (ppt).

Results and discussion

The Single Quad mass scan in Figure 1 shows the problem associated with AS when the U concentration is relatively high. As can be seen, the ^{238}U peak overlaps the ^{237}Np peak, impeding the trace level measurement of Np. Conversely when operating the ICP-QQQ in MS/MS mode, the peak overlap on Np is eliminated. This improvement is due to two separate mass separations taking place, improving the AS from ~10^{-7} to <<10^{-10}. The background is significantly reduced under MS/MS mode but not eliminated. Uranium can form various hydride interferences that are not related to (or removed by) AS. However, reaction chemistry can be used to remove interference-based background levels.

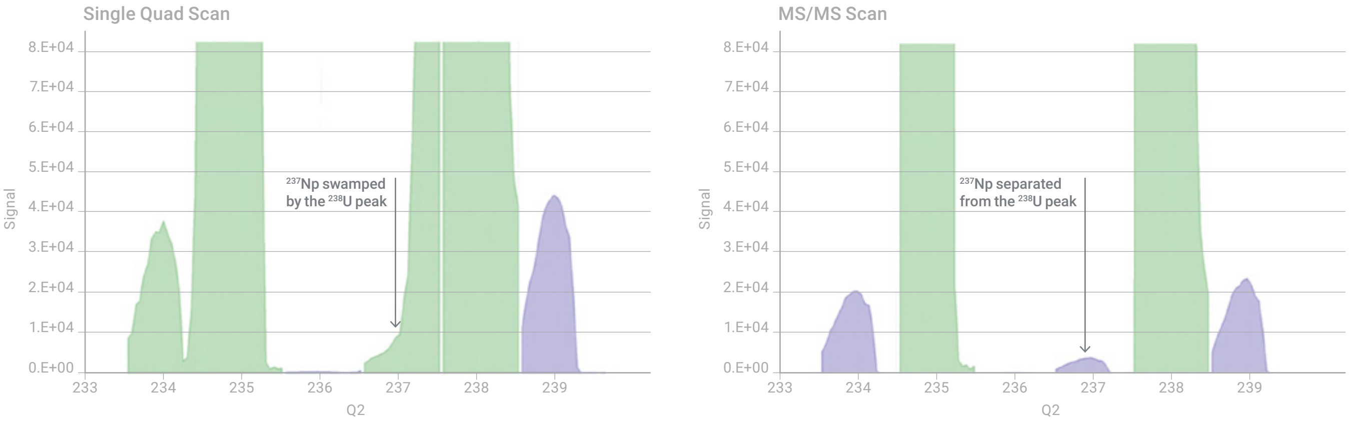

Figure 1. Spectrum of ^{237}Np in presence of 10 ppm U. Left: Single Quad scan and Right: MS/MS mode. MS/MS mode eliminates the peak tail on the low mass side of the intense ^{238}U peak.

To check the reaction efficiency of oxygen as a cell gas for this study, a spiked U matrix was measured under MS/MS mass-shift mode with O_2 reaction gas. The Np spike was 1000x lower than the previous scans at 950 ppq (0.95 ng/L). Figure 2 shows the mass scan of the NpO_2 (and UO_2) product ions. It is worth noting that during quantitative analysis (rather than scanning, as shown in Figure 2), all the U isotopes would be eliminated by Q1, which would be set to *m/z* 237. The conversion efficiency of Np to NpO_2 was found to be 99%. Only 1% of total Np signal converted to NpO.

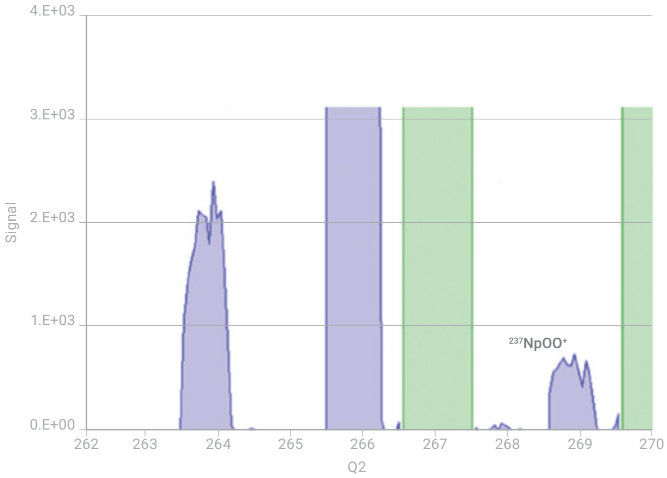

Figure 2. 950 ppt Np in 10 ppm U measured in MS/MS mass-shift mode with O_2 cell gas.

Figure 3 shows the calibration graphs for Np in a 10 ppm U matrix generated in no gas mode (left) and oxygen reaction gas mode (right). Identical solutions were analyzed in both cases. The improvement in BEC and DL can be clearly seen in oxygen mass-shift mode. The DL and BEC under no gas conditions were 1.9 ppq and 2.4 ppq. Using O_2 mode and measuring Np as NpO_2 improved the DL to 0.56 ppq and the BEC to 0.32 ppq (pg/L).

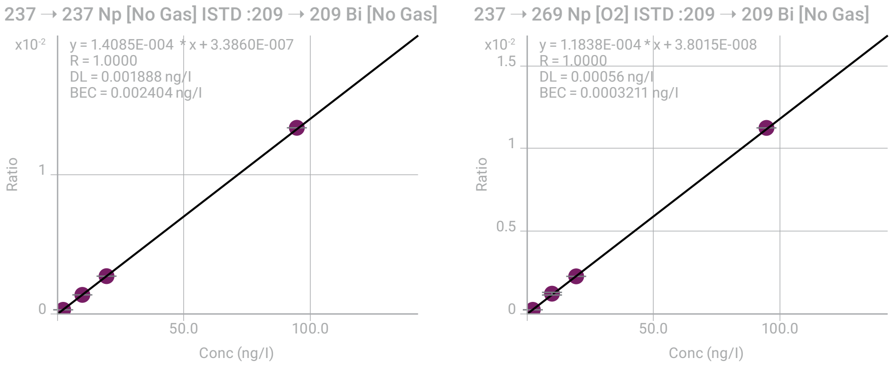

Figure 3. Np calibration in a 10 ppm U matrix. Left: no gas mode. Right: O_2 reaction gas mode – showing a 7.5x reduction in BEC. All UH-based interferences were avoided by measuring ^{237}N as $^{237}Np^{16}O_2$.

Conclusion

The Agilent 8900 ICP-QQQ in MS/MS mode performs two mass selection steps, increasing the abundance sensitivity performance and allowing an ultratrace element to be measured in the proximity of a major matrix isotope. For the determination of Np, the removal of uranium-based interferences is essential, as U is present within the environment at significantly higher concentrations than Np. The unique MS/MS capability of the 8900 ICP-QQQ removes peak overlaps and uranium hydride-based interferences.

> Return to table of contents
> Search entire document

Direct Analysis of Zirconium-93 in Nuclear Site Decommissioning Samples by ICP-QQQ

Author

Heather Thompkins[1]
Ben Russell[1]
Sharon Goddard[2]
[1]Nuclear Metrology Group and
[2]Gas and Particle Metrology Group,
National Physical Laboratory,
Teddington, UK

Using MS/MS mass-shift mode to resolve ^{93}Zr from ^{93}Nb without chemical separation

Introduction

Zirconium-93 is a long-lived radionuclide that is produced by nuclear fission of uranium and plutonium. It is also formed by neutron activation of stable zirconium in nuclear fuel cladding in pressurized water reactors. Therefore, ^{93}Zr is an important element to monitor during the decommissioning of nuclear sites. The long half-life of ^{93}Zr (1.61×10^6 years (*1*)) means it is a significant contributor to the total waste inventory over long timescales. Clearly, there is a need to accurately quantify ^{93}Zr in various complex decommissioning wastes as part of the initial site characterization process. Also, monitoring of waste repositories and the environment around nuclear sites following decommissioning is needed.

Zirconium-93 decays to stable ^{93}Nb by beta emission, but with a low decay energy that makes measurement by decay counting methods challenging. With its long-half-life, ^{93}Zr is well suited to measurement by ICP-MS (1 Bq/g is equivalent to 1.1×10^4 pg/g), which offers a high throughput alternative to decay counting techniques. However, accurate measurement by ICP-MS is affected by the isobaric interference from ^{93}Nb (100% abundance), as well as potential radioactive ^{93}Mo, and polyatomic ion interference from ^{92}Mo^{1}H$^+$ and ^{92}Zr^{1}H$^+$. The removal of these interferences traditionally requires time-consuming, multistage extraction and/or chromatographic separation before measurement, using a significant number of reagents and materials (*2, 3*). Also, since ^{93}Nb is monoisotopic, it is challenging for the analyst to be confident that complete interference removal has been achieved before measurement.

In this study, triple quadrupole ICP-MS (ICP-QQQ) was used for the rapid and direct low-level measurement of ^{93}Zr in decommissioning samples below International Atomic Energy Agency (IAEA) regulatory limits (*4*). Reactive gases were used in the collision/reaction cell (CRC) of the ICP-QQQ to separate the isobaric overlap from ^{93}Nb on ^{93}Zr, eliminating the need for chromatographic separation. Isobaric ion interferences can be separated using ICP-QQQ when the cell gas reacts quickly with one of the elements to form a product ion, while the other element does not react (or reacts slowly). This “chemical” resolution method significantly reduces the procedural time and secondary waste associated with decay counting and alternative mass spectrometric procedures. With its fast analysis times, ICP-QQQ offers a cost-effective method for the analysis of nuclear decommissioning samples.

ICP-QQQ with MS/MS mode

ICP-QQQ is a well-established technique that is especially suitable for improved control of spectral, doubly charged ion, and isobaric interferences using reactive cell gas methods (*5*). Compared to conventional single quadrupole ICP-MS, ICP-QQQ has an additional mass filter before the CRC. This extra mass filter prevents all ions apart from the target mass from entering the CRC, so the reaction chemistry in the cell can be controlled. This double mass filter approach is only possible with a tandem MS (or MS/MS) configuration, which provides unprecedented control of the ion-molecule reaction chemistry used in CRC-ICP-MS methods.

Experimental

Standards and sample preparation

Calibration standards were prepared by diluting an NPL-standardized ^{93}Zr stock solution in 0.3 M HNO_3 over a concentration range of 53.8 to 1.1 × 10^5 pg/g (equivalent to 5.0 × 10^{-3} to 10.0 Bq/g). To provide matrix matched calibration standards, the same standards were also prepared in dissolved steel and aqueous decommissioning waste solutions. To determine the separation factor of ^{93}Zr and ^{93}Nb, increasing concentrations of ^{93}Nb were spiked into 0.3 M HNO_3 and steel solutions which contained the same concentration of ^{93}Zr.

Instrumentation

An Agilent 8800 Triple Quadrupole ICP-MS (ICP-QQQ) was used for all work on active samples containing ^{93}Zr. The sample introduction system consisted of a quartz torch with 2.5 mm i.d. injector, a quartz spray chamber, glass concentric nebulizer, and nickel-tipped interface cones.

To separate ^{93}Zr and ^{93}Nb using ICP-QQQ, both O_2 and NH_3 cell gases were investigated. Helium was added as a buffer gas and H_2 was also added to the cell to see if it enhanced product ion formation.

Instrument operating conditions were established using stable isotope standards. A 10 ng/g mixed stable element standard containing ^{90}Zr and ^{93}Nb was analyzed and product ion scans were obtained for each precursor ion mass. Q1 was first set to *m/z* 90 (for Zr) and then *m/z* 93 (for Nb), while Q2 was scanned to identify the most abundant product ions formed from reactions of ^{90}Zr and ^{93}Nb with each cell gas. The optimal cell gas for interference removal was found to be NH_3 with He and H_2. The instrument conditions were then optimized for sensitivity, focusing on cell gas flow rate, octopole bias, and energy discrimination.
The operating conditions (Table 1) were validated using active samples.

Table 1. 8800 ICP-QQQ operating conditions.

Parameter	Setting	
	Stainless Steel	Aqueous Waste Samples
Scan Mode	MS/MS (Q1=93, Q2=195)	
Plasma Conditions	HMI	General Purpose
Integration Time (s)	0.1	
Carrier Gas (L/min)	0.60	0.95
Dilution Gas (L/min)	0.35	0.00
Helium Flow Rate (mL/min)	2.0	
Hydrogen Flow Rate (mL/min)	3.0	
Ammonia Flow Rate (% of maximum flow rate)	15 (1.5 mL/min)	
Octopole Bias (V)	−2.8	
Energy Discrimination (V)	−9.0	
Octopole RF (V)	180	

Results and discussion

Calibration

The zirconium-93 calibration standards were analyzed using the 8800 ICP-QQQ using the General Purpose parameters in Table 1. The detection limit was calculated as 6.5 pg/g (0.6 mBq/g).

Instrument sensitivity and interference removal

During method optimization using a 10 ng/g mixed stable element standard, different product ions were monitored to assess interference removal efficiency. The product ion scans identified multiple product ions using both O_2 and NH_3 as reaction gases. A Zr/Nb separation factor of > 5×10^3 was achieved using Zr-NH_3 product ions: $Zr(NH_3)_2NH_2^+$ (mass-shift of 50) and $Zr(NH_3)_5^+$ (mass-shift of 85), and Zr-O_2 product ions: ZrO_3^+ (mass-shift of 48), and $Zr(OH)_3^+$ (mass-shift of 51). However, the optimal Zr/Nb separation was achieved with a mass shift of 102, measuring the product ion $Zr(NH_3)_6^+$. This finding agrees with a previous study that first demonstrated measurement of ^{93}Zr by ICP-QQQ (*6*).

Figure 1 shows that, if ^{93}Zr was measured on mass, Nb concentrations of 10 pg/g and above would contribute to the signal at *m/z* 93, leading to interference on ^{93}Zr (blue bars). By comparison, when mass 195 ($^{93}Zr(NH_3)_6$) was monitored in MS/MS mass-shift mode, the background counts from Nb remained below 10 cps at concentrations up to 5×10^4 pg/g Nb (white bars). The results show the successful removal of the ^{93}Nb isobaric interference on ^{93}Zr up to 5×10^4 pg/g Nb, using the MS/MS mass-shift method.

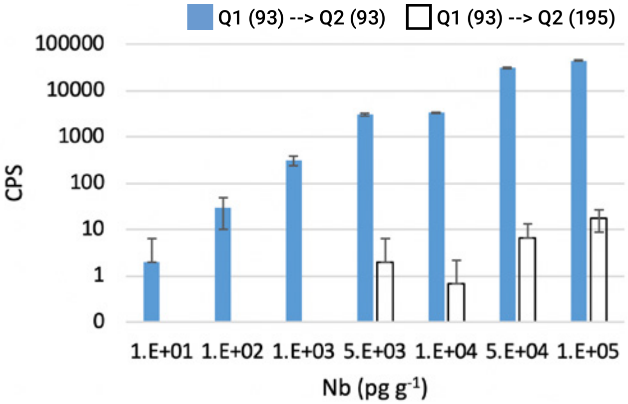

Figure 1. Background at *m/z* = 93 and 195 with increasing Nb concentration (Q1 set to *m/z* = 93 in both cases).

Measurement of decommissioning samples

Spiked stainless steel

Inactive stainless steel dissolved in concentrated nitric acid was provided as part of a European Metrology Research Program (EMRP) project. Samples were evaporated to near-dryness and made up in an equal volume of 0.3 M HNO_3. A further 1 in 10 dilution was made, giving approximately 20x total dilution (5% total dissolved solids, TDS). A semiquantitative scan of the sample was performed using the 8800 ICP-QQQ to determine the sample composition. The most abundant elements detected in the diluted solution were Fe (out of range), Cr (2 µg/g), Mg (20 µg/g), Ni (2.5 µg/g), Cu (10 µg/g), Mo and Sn (both 1 µg/g). The Nb concentration in the diluted steel samples ranged from 0.5 to 1.4

× 10^4 pg/g. The steel samples were run using the optimized operating conditions for the measurement of ^{93}Zr (Table 1). No background was measured at *m/z*=195, which also demonstrates removal of any potential polyatomic ion interferences on ^{93}Zr from ^{92}Mo^{1}H$^+$ and ^{92}Zr^{1}H$^+$.

The spiked steel samples (spiked with ^{93}Zr and ^{93}Nb) were initially run on the 8800 without dilution, using ^{101}Ru as an internal standard. However, even using the High Matrix Introduction (HMI) system with aerosol dilution on the 8800, the 5% steel matrix caused significant matrix deposition on the cones after running four to five samples. The nominal TDS limit for HMI is 3%. The matrix tolerance could potentially be improved with the UHMI available on the 8900 ICP-QQQ, which allows matrix levels up to 25% TDS to be analyzed.

Following a 1 in 10 dilution, the instrument sensitivity for the spiked steel was similar to the ^{93}Zr calibration standards. Figure 2 shows the calibration curve of ^{93}Zr in the dissolved stainless steel matrix, measured as $Zr(NH_3)_6^+$. The method detection limit (MDL) was 8.6 pg/g (0.8 mBq/g), which is significantly lower than the exemption limit of 10 Bq/g defined by IAEA/RS-G 1.7 (*4*).

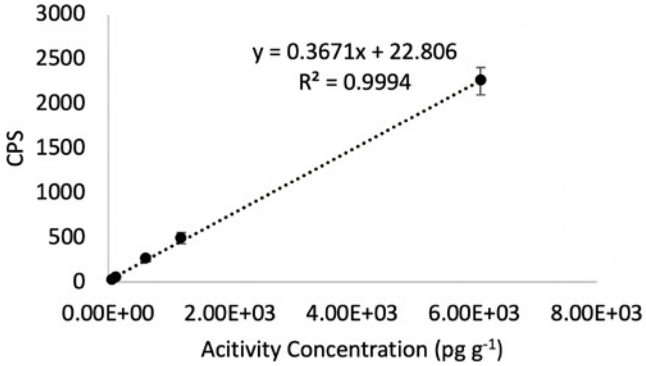

Figure 2. Dissolved stainless steel spiked with ^{93}Zr, measured as $Zr(NH_3)_6^+$ using ICP-QQQ.

Aqueous waste samples

Aqueous wastes containing a range of decommissioning radionuclides were measured without any sample treatment using the 8800 ICP-QQQ. General Purpose plasma conditions were used rather than HMI mode. The maximum Nb concentration was 1 × 10^4 pg/g, with a background of <20 cps at *m/z*=195, compared to ~40,000 cps when measured on mass at *m/z*=93 in He mode. The average ICP-MS/MS reaction cell interference removal factor (equivalent to the decontamination factor quoted for radiochemical separation experiments) was 3.5 × 10^3, with an MDL of 1.1 pg/g (0.1 mBq/g). This DL is significantly below the IAEA out-of-scope limit, and the World Health Organisation (WHO) drinking water regulation limit of 0.1 Bq/mL (*4, 7*). The results show that this ICP-QQQ method is suitable for the direct measurement of ^{93}Zr in drinking water samples.

Comparing the 8900 and 8800 ICP-QQQ

At NPL we also have access to a newer Agilent 8900 ICP-QQQ, but this instrument is in a laboratory that does not handle radioactive samples. To evaluate the relative performance of the 8800 and 8900, we used a stable, natural Zr standard to run a comparative test between the two instruments. For this comparison, the $^{90}Zr(NH_3)_6$ product ion was used as an analog of the target $^{93}Zr(NH_3)_6$ product ion. The 8900 was operated using the same General Purpose instrument operating conditions shown in Table 1.

The product ion scans obtained by the 8900 ICP-QQQ using the 10 ng/g mixed stable element standard agreed with the 8800 ICP-QQQ scan results. Both instruments identified $Zr(NH_3)_6^+$ at *m/z* 192 as the most intense ^{90}Zr product ion, using a mass shift of 102. As shown in Table 2, measuring Zr as $Zr(NH_3)_6^+$ offered the most efficient Nb interference removal method. The results also show that a maximum separation factor of >10,000 was achieved with the 8900 compared to 6,200 on the 8800. The 8900 also detected intense ^{90}Zr product ions not detected on the 8800, most notably at *m/z* 206 ($^{90}ZrN(NH_3)_6$) and 207 ($^{90}ZrNH(NH_3)_6$) (Table 2).

Table 2. Zr/Nb separation factors for 8800 and 8900 ICP-QQQ. Based on product ion scans of ^{90}Zr and ^{93}Nb in a 10 ng/g mixed stable element standard. Zr-90 counts were scaled to 100% abundance for this calculation.

Q1/Q2 (*m/z*)	90/155	90/159	90/175	90/176	90/177	90/192	90/206	90/207
Mass-shift	65	69	85	86	87	102	116	117
Zr/Nb Separation Factor (8800)	<1	<1	<1	1	4	6,200	<1	<1
Zr/Nb Separation Factor (8900)	2,300	470	715	155	400	10,200	2,800	4,300

The 8900 offers higher sensitivity and lower backgrounds compared to the 8800, as verified by the data presented in Table 3. The stable element calibration standards were measured by both instruments. The counts per second (cps) for the $^{90}Zr(NH_3)_6$ product ion at *m/z* 192 obtained by the 8900 were significantly higher than the 8800 (Table 3). The sensitivity improvement of the 8900 is due to more efficient ion transmission in the interface vacuum stage. Also, axial acceleration (0.5 V in this study) improves reaction product ion energy, overcoming collisional attenuation and space-charge effects.

Table 3. Difference in instrument sensitivity and instrument detection limit (IDL) for stable Zr standards.

Parameter	8800 ICP-QQQ		8900 ICP-QQQ	
Q1/Q2 (*m/z*)	90/90	90/192	90/90	90/192
^{90}Zr sensitivity (cps, 10 ng/g)	1,800	2,000	53,000	166,000
*IDL (pg/g)	6.5		0.1	
*IDL (mBq/g)	0.6		8.8×10^{-3}	

**IDLs were calculated from the 90/192 data.*

Conclusion

ICP-QQQ has been successfully used for the direct and accurate measurement of the long-lived radionuclide ^{93}Zr in decommissioning samples below IAEA out-of-scope limits. Since ICP-QQQ with MS/MS uses reaction chemistry in the CRC to separate analytes and interferences, there was no need for a separation-step before measurement, simplifying and speeding up the analysis.

Both active and stable element standards containing Nb and Zr were used during method development. The study shows the Agilent 8800 ICP-QQQ with MS/MS can eliminate isobaric overlaps from ^{93}Nb on ^{93}Zr using NH_3/H_2 as the reaction gas. Nb doesn't react with NH_3/H_2 in the CRC, so Nb remains at *m/z* 93, allowing ^{93}Zr to be measured as $^{93}Zr(NH_3)_6^+$ at *m/z* = 195, free from interference.

The integrated HMI aerosol dilution technology extends the matrix tolerance of Agilent ICP-QQQ for the analysis of high matrix samples. The 8800 was used to analyze ^{93}Zr in dissolved steel (using HMI) and aqueous waste samples.

An MDL of less than 1 mBq/g was achieved in both matrices, which is several orders of magnitude lower than regulatory limits for decommissioning wastes and drinking water. The study showed that the newer Agilent 8900 ICP-QQQ offers higher sensitivity and lower backgrounds compared to the 8800.

Compared to decay counting techniques, ICP-QQQ reduces the preparation time of samples dramatically, with sample-throughput further improved by the short measurement times of the technique. The ICP-QQQ method will be beneficial to analysts working in nuclear decommissioning and environmental monitoring labs.

References

1. Decay Data Evaluation Project, accessed September 2019, http://www.nucleide.org/DDEP_WG/Nuclides/Zr-93_tables.pdf
2. P. Cassette, F. Chartier, H. Isnard, C. Fréchou, I. Laszak, J. P. Degros, M. M. Bé, M. C. Lépy, I. Tartes, Determination of ^{93}Zr decay scheme and half-life. *Applied Radiation and Isotopes*, 2010, 68 (1), 122–130
3. F. Chartier, H. Isnard, J. P. Degros, A. L. Faure, C. Fréchou, Application of the isotope dilution technique for ^{93}Zr determination in an irradiated cladding material by multiple collector-inductively coupled plasma mass spectrometry. *Int. J. of Mass Spectrom*., 2008, 270 (3), 127–133
4. IAEA Safety Standards Series Safety Guide No. RS-G 1.7 Application of the concepts of exclusion, exemption and clearance, accessed September 2019, http://www-pub.iaea.org/MTCD/publications/PDF/Pub1202_web.pdf
5. Fourth Edition of Handbook of ICP-QQQ Applications using the Agilent 8800 and 8900, Agilent publication, 5991-2802EN
6. P. Petrov, B. Russell, D. N. Douglas, H. Goenaga-Infante, Interference-free determination of sub ng kg^{-1} levels of long-lived ^{93}Zr in the presence of high concentrations (µg kg^{-1}) of ^{93}Mo and ^{93}Nb using ICP-MS/MS. *Anal. Bioanal. Chem*, 2018, Volume 410 (3), 1029–1037
7. World Health Organisation Guidelines for Drinking Water Quality Fourth Edition, accessed September 2019, https://apps.who.int/iris/bitstream/handle/10665/254637/9789241549950-eng.pdf%3bjsessionid=92EE6E44405FC8DBD781EA0B1C957B18?sequence=1

> Return to table of contents
> Search entire document

Rapid Analysis of Radium-226 in Water Samples by ICP-QQQ

Authors

Ben Russell[1], Elsje May van Es[1,2],
Glenn Woods[3], David Read[1,2]

1. National Physical Laboratory, Teddington, UK

2. Chemistry Department, University of Surrey, Guildford, Surrey, UK

3. Agilent Technologies UK Limited, Lakeside, Stockport, UK

Introduction

Radium-226 is a radionuclide that occurs naturally as part of the uranium-238 decay series. ^{226}Ra decays with a half-life of 1,600 years to radon-222 with the emission of alpha and gamma radiation. The element is known for its historical use in the luminescent paint used in clocks, watches, and other instruments. These uses led to severe health problems for the so-called Radium Girls who painted the watch and clock dials. ^{226}Ra has a long half-life compared to the other Ra isotopes and is considered a significant contributor to occupational radiological dose with regards to industrial sources of naturally occurring radioactive materials (NORM).

^{226}Ra occurs naturally in waters through interaction with uranium-bearing minerals [1]. It is also present as a result of waste from the industrial exploitation of mineral resources (including uranium mining and processing sites, and produced waters following hydraulic fracturing). Radium waste producers are required to comply with stringent limits when discharging to watercourses. Analytical methods must therefore be capable of detecting ^{226}Ra at values ranging from 0.01 Bq/L to 1 Bq/L (equivalent to 0.3 – 30 pg/L (ppq) or 0.0003 – 0.03 ppt) [2,3,4].

^{226}Ra analysis is typically performed by alpha spectrometry, which requires time-consuming and labor-intensive separation before measurement, followed by count times of several days per sample to reach the target detection limits.

This study outlines a new method developed by the National Physical Laboratory (NPL) Nuclear Metrology Group for the rapid analysis of ^{226}Ra in water samples. The new method uses a preconcentration step prior to measurement of ^{226}Ra using triple quadrupole ICP-MS (ICP-QQQ)[5]. The procedural time is significantly reduced compared to decay counting techniques, and ^{226}Ra is measurable at concentrations required to meet the regulatory detection limits.

Experimental

Sample preparation

Radium-226 calibration standards were prepared from an in-house standard solution in a dedicated facility used for the preparation of aqueous radioactive sources for decay counting or mass spectrometry measurement. The calibration standards were diluted in 2% (v/v) HNO_3.

Groundwater samples were also investigated to assess the impact of a more complex sample matrix. Samples were evaporated to dryness and redissolved in 2% (v/v) HNO_3. The solutions were then spiked with ^{226}Ra over a concentration range of 0.03 – 30 ppt to represent the concentrations expected following preconcentration.

High volume water samples (1 L) were spiked over the same concentration range as the groundwater samples to represent samples close to, and higher than, the regulatory discharge limits. Samples were acidified to pH 2 and passed through a chromatographic column to trap ^{226}Ra [6]. The ^{226}Ra was then eluted, evaporated to incipient dryness and then made up in 5 mL 2% HNO_3, representing a concentration factor of ~200. Unspiked water samples were run through the same preconcentration procedure, and then measured to establish the elemental composition and confirm no contribution of polyatomic interferences to the background at $m/z = 226$. Matrix matched calibration standards were prepared by spiking water samples following preconcentration, which also enabled the recovery to be calculated (≥ 70% over the concentration range studied).

Instrumentation

An Agilent 8800 Triple Quadrupole ICP-MS (ICP-QQQ) was used throughout. The standard sample introduction system was used, comprising a quartz torch with 2.5 mm i.d. injector, a quartz spray chamber, glass concentric nebulizer, and nickel-tipped interface cones. The instrument operating conditions are summarized in Table 1.

Table 1. ICP-QQQ operating conditions; low matrix tuning is appropriate for samples where most of the matrix has been removed during analyte preconcentration.

Parameter	Setting	
Scan mode	Single Quad	
Plasma conditions	Low matrix (optimized for high sensitivity)	HMI
RF power (W)	1550	
Carrier gas (L/min)	1.07	0.60
Dilution gas (L/min)	0	0.35
Extract 1	0.0	
Extract 2	-200.0	
Omega Bias (V)	-100.0	
Omega lens (V)	13.6	
Octopole bias (V)	-8.0	
He cell gas (mL/min)	0 – 1.0	0.5 – 1.0

Results and discussion

Sensitivity of ICP-QQQ for ^{226}Ra

The half-life of ^{226}Ra is relatively short with regards to ICP-MS measurements (1 Bq/kg is equivalent to 27.3 ppq, compared to long-lived ^{238}U (half-life 4.5×109 years), where 1 Bq/kg is equivalent to 8.0×107 ppq). In practice, this means that calibration should be performed using standards prepared for the radioisotope of interest, rather than calibrating using a long-lived or stable isotope as an analog. The instrument detection limits (IDLs) for several operating conditions (Q1 modes and cell gas flows), were calculated from a calibration curve prepared by spiking 2% (v/v) HNO_3 with ^{226}Ra at concentrations of 0.01–30 ppt (Table 2).

Table 2. Limit of detection for different instrument conditions and cell gas flow rates.

Instrument mode	Single Quad			MS/MS		
He flow rate (mL/min)	0.0	0.5	1.0	0.0	0.5	1.0
Limit of detection (ppt)	0.08	0.10	0.02	0.04	0.04	0.07

The IDLs in Table 2 are close to the higher end of the regulatory limits quoted (0.03 ppt), and orders of magnitude higher than the lowest values (0.3 ppq). Measurement of ^{226}Ra at environmentally relevant levels therefore requires an effective preconcentration step prior to ICP-QQQ analysis, to rival the detection limits of traditional alpha spectrometry measurement.

Interference removal by ICP-QQQ

Multiple potential interferences from polyatomic ions including ^{88}Sr^{138}Ba$^+$, ^{87}Sr^{139}La$^+$, ^{86}Sr^{140}Ce$^+$, ^{208}Pb^{18}O$^+$, ^{186}W^{40}Ar$^+$, and ^{97}Mo^{129}Xe$^+$ can potentially affect ICP-MS measurement of ^{226}Ra. Multiple separation stages prior to sample introduction are often required to remove the interferences. As an alternative approach, helium (He) collision mode was investigated for the removal of polyatomic interferences, initially by introducing up to 100 ppm Sr + Ba, Sr + La, Ce, W, and Pb standards. The background at m/z = 226 was 0 cps in single quad mode when using 0.5–1.0 mL/min He cell gas, confirming the ability of He mode to attenuate all the polyatomic ions. Given that the on-mass polyatomic interferences are formed during sample introduction and not in the collision/reaction cell (CRC), MS/MS was not required, so the instrument was operated in single quad mode throughout.

Groundwater samples from different locations in North West England were then analyzed to determine the impact of a more complex sample matrix on instrument performance. The samples were spiked with ^{226}Ra and measured at varying He gas flow rates together with unspiked samples and blank solutions. Bismuth-209 was used as an internal standard. The impact of matrix suppression was overcome using robust plasma conditions and aerosol dilution with the High Matrix Introduction (HMI) system of the 8800. HMI allows higher matrix levels to be analyzed directly without requiring chemical separation prior to measurement, further reducing the total procedural time. The reduction in sensitivity when operating with 0.5 mL/min He cell gas was offset by the lower background, giving comparable or improved background equivalent concentrations (BECs) at m/z = 226 compared to no gas mode (Table 3). The sensitivity at 0.5 mL/min He cell gas is illustrated in the calibration plot shown in Figure 1.

Table 3. BECs of ^{226}Ra using no gas and He gas mode.

He flow rate (mL/min)	BEC (ppt)		
	Sample 1	Sample 2	Sample 3
0	0.015	0.017	0.0085
0.5	0.0083	0.0089	0.0092
1.0	0.011	0.0092	0.013

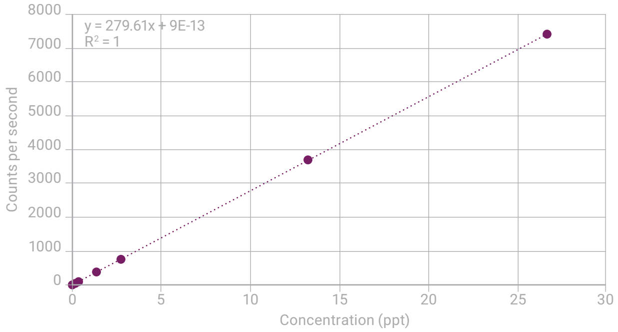

Figure 1. Calibration plot for ^{226}Ra standards in single quad mode with 0.5 mL/min He.

Measurement of high volume water samples

In water samples, ^{226}Ra was detected down to 0.03 ppt (1 Bq/L), which is equivalent to 5 mBq/L in the original sample, assuming a preconcentration factor of 200. The RSD was <10% at concentrations above 1.4 ppt (50 Bq/L), equivalent to 250 mBq/L in the original sample. The results demonstrate that ICP-QQQ combined with preconcentration from high volume water samples is capable of measuring ^{226}Ra at concentrations relevant to regulatory discharge limits. Improved accuracy at the lower limits is potentially achievable through higher preconcentration factors.

Conclusion

A method is presented that demonstrates the capabilities of ICP-QQQ for the measurement of the naturally occurring radionuclide ^{226}Ra. The use of He collision gas effectively removes potential polyatomic interferences, while operating with HMI reduces the impact of matrix suppression. When combined with preconcentration using chromatographic separation techniques, the detection limits achievable are applicable to the regulatory limits for water. The measurement time of several minutes per sample represents a significant improvement compared to several days using traditional alpha spectrometry. The increase in sample throughput is potentially beneficial for routine monitoring of water supplies, as well as routine environmental monitoring at nuclear and industrial sites.

References

1. P.L. Smedley, A survey of the inorganic chemistry of bottled mineral waters from the British Isles. *Applied Geochem.* **2010**, 25, 1872–1888
2. Environmental Permitting Guidance: Radioactive Substances Regulation, Environment Agency, London, 2010,
3. Guidelines for Drinking-water Quality (Fourth Edition), World Health Organisation, 2011, ISBN 978 92 4 154815 1
4. National Primary Drinking Water Regulations; Radionuclides; Final Rule (Part II), 40 CFR Parts 9, 141, and 142, Environment Protection Agency, 2011
5. E.M. van Es, B.C. Russell, P. Ivanov, D. Read, Development of a method for rapid analysis of Ra-226 in groundwater and discharge water samples by ICP-QQQ-MS. *App. Rad. & Isotopes*, 126, **2017**, 31-34
6. E.M. van Es, B.C. Russell, P. Ivanov, M. Garcia Miranda, D. Read, The behaviour of ^{226}Ra in high volume environmental water samples on TK100 resin. *J. Radioanal. Nucl. Chem.*, **2017**, 312: 10

> Return to table of contents
> Search entire document

Characterization of Rare Earth Elements used for Radiolabeling Applications by ICP-QQQ

Authors

B. Russell[1], P. Ivanov[1]
B. Webster[1,2], D. Read[1,2]

[1]Nuclear Metrology Group, National Physical Laboratory, Teddington, UK
[2]School of Chemistry and Chemical Engineering, University of Surrey, Guildford, UK

Analysis of radiogenic REE isotopes in bulk REE matrices

Introduction

Radiolabeling refers to a technique where a compound or substance is labeled (or tagged) with a radioactive isotope of an element. The labeled material can then be used for controlled delivery of the radiation emitted by the active isotope, or detected and traced from the radioactivity of the isotopic label.

The use of radiolabeled materials is growing steadily, with the market for radiolabeled pharmaceutical compounds expected to be worth over 5 billion US dollars by 2024 (*1*). Elements that can form useful radioisotopes include the lanthanides – also known as rare earth elements (REEs). Radio-lanthanide compounds are used in pharmaceutical and imaging applications.

To meet the rising demand for radio-lanthanides, there is a critical need for analytical techniques to support the production of traceable, high purity, labeled lanthanides (*2*). Production scale chemical purification and labeling of radio-lanthanides is challenging though, because all the lanthanides have similar chemical properties and tend to behave as a consistent group. To prepare a pure radio-lanthanide, it is necessary to accurately characterize the chemical composition of the non-radioactive natural or isotopically enriched starting material used. Before a candidate starting material can be used for routine radionuclide production, each batch must be tested and validated to ensure that radionuclide yields will be of the desired quantity and quality (*3*). To carry out this level of quality assurance (QA), accurate analytical procedures are needed, particularly to determine the level of trace lanthanide contaminants in the pure lanthanide starting material. Since any impurities need to be removed, the QA data is also useful to guide the design of robust, reproducible chemical separation methods (*4*). Determining the type and quantity of impurities present in the starting material also helps manufacturers predict whether unwanted radioactive side-products will be produced during irradiation.

Table 1 lists several radio-lanthanide product isotopes that have chemical and radioactive decay properties that make them suitable for applications in radiolabeling. In most of these examples, the starting material is a different element to the intended radio-lanthanide product isotope. This avoids the radio-lanthanide product isotope being affected by high concentrations of a stable isotope of the same element in the irradiated target, which cannot be removed by subsequent chemical separation. Typically, the radionuclides are produced by irradiating a lanthanide or lanthanide oxide starting material target at a nuclear reactor or cyclotron facility. For example, terbium-155 can be produced from gadolinium (III) oxide (Gd_2O_3) starting material in a cyclotron. The stable isotope ^{155}Gd is converted to the radioisotope ^{155}Tb via a (p, n) reaction, where a proton enters the nucleus and a neutron leaves the nucleus simultaneously.

Table 1. Starting materials and production route for radio-lanthanides used in labeling applications.

Radio-lanthanide	Starting Material*	Possible Nuclear Reaction Production Route**
^{153}Sm	^{152}Sm	$^{152}\text{Sm}(n, \gamma) \rightarrow {}^{153}\text{Sm}$
^{149}Tb	^{151}Eu	$^{151}\text{Eu}({}^{3}\text{He}, 5n) \rightarrow {}^{149}\text{Tb}$
^{155}Tb	^{155}Gd	$^{155}\text{Gd}(p, n) \rightarrow {}^{155}\text{Tb}$
^{161}Tb	^{160}Gd	$^{160}\text{Gd}(n, \gamma){}^{161}\text{Gd} \rightarrow {}^{161}\text{Tb} + \beta\text{-}$
^{166}Ho	^{164}Dy	$^{164}\text{Dy}(n, \gamma){}^{165}\text{Dy}(n, \gamma){}^{166}\text{Dy} \rightarrow {}^{166}\text{Ho} + \beta\text{-}$
^{169}Er	^{168}Er	$^{168}\text{Er}(n, \gamma) \rightarrow {}^{169}\text{Er}$
^{177}Lu	^{176}Yb	$^{176}\text{Yb}(n, \gamma){}^{177}\text{Yb} \rightarrow {}^{177}\text{Lu} + \beta\text{-}$

** Starting materials are often isotopically enriched targets.*
***n (neutron), p (proton), γ (gamma), ^{3}He (helium-3).*

The accurate characterization of REE materials is challenging for conventional single quadrupole ICP-MS. The REEs form hydride (MH^+), oxide (MO_x^+), and hydroxide (MOH^+) polyatomic ions in the plasma or during ion extraction, and these polyatomic ions can overlap the measured isotopes of other REEs. High intensity REE matrix element peaks can also cause peak tail overlaps on trace REE isotopes measured at adjacent masses. This peak tailing effect, known as the abundance sensitivity (AS), is different for different types of mass spectrometer. On commercial single quadrupole ICP-MS instruments, the AS is typically 10^{-7}, which means that every 10 million counts at a high intensity peak contributes one count to the adjacent masses. This AS performance means that an intense major element peak can cause peak tailing overlaps on trace analytes at adjacent masses when measured by single quadrupole ICP-MS.

Compared to single quadrupole ICP-MS, Agilent triple quadrupole ICP-MS (ICP-QQQ) instruments offer superior resolution of polyatomic interferences using reactive cell gases. This performance improves accuracy in complex sample types, including analysis of trace REEs in geological samples and materials applications (*5, 6*). Also, Agilent ICP-QQQ instruments use a tandem mass spectrometer configuration (MS/MS) with two full-sized quadrupole mass analyzers, Q1 and Q2, both housed in high vacuum regions. Two mass filtering steps reduce peak tail overlaps, as the overall AS in MS/MS is the product of the AS of the two quadrupoles, so $10^{-7} \times 10^{-7}$, or 10^{-14} *(7)*.

Previous studies suggest that ICP-QQQ methods can improve the accuracy of analysis of trace impurities in the lanthanide starting materials/targets used for radio-lanthanide production. Also, assessment of the concentration of impurities in the starting material recovered after chemical separation of the radioisotope could allow for re-use of the recovered material.

The chemical separation methods used to purify radio-lanthanide isotopes can be designed and optimized using stable isotopes of each lanthanide, rather than the radioactive material. ICP-QQQ can be used to measure the intended lanthanide product element at trace (ppt) levels in the presence of a high concentration (ppm level) of the bulk target material. This capability enables realistic testing of the separation scheme while using cheap, safe, and readily available natural REE materials.

In this study, several pairs of trace REE analytes and adjacent mass neighboring REE matrix elements relevant to radio-lanthanide production were measured by ICP-QQQ. The samples included materials that are typically used as irradiation targets for radio-lanthanide production. The use of ICP-QQQ for optimizing radiochemical separation of target lanthanides, and for measuring REE impurities in irradiated targets, was also demonstrated. The developed methods will enable end users to compile a REE impurity profile of materials of relevance to the production of radionuclides for labeling applications.

Experimental

Sample preparation

For the detection limit (DL) study, calibration standards from 1 ppt to 100 ppb were prepared for each trace REE in solutions containing 10 ppm of the neighboring REE matrix element. All solutions were stabilized with 2% HNO_3. These bulk-trace lanthanide pairs are summarized in Table 2. Similar solutions were prepared to test the extraction chromatography-based chemical separation procedures.

Table 2. Pairs of natural REE matrix elements and trace REE analytes used for preparation of calibration standard sets to test resolution of adjacent mass interferences.

Bulk REE Matrix (Isotopic abundance, %)	Trace REE Analyte (Isotopic abundance, %)
^{139}La (99.91)	^{140}Ce (88.45)
^{140}Ce (88.45)	^{141}Pr (100)
^{158}Gd (24.84)	^{159}Tb (100)
^{164}Dy (28.18)	^{165}Ho (100)
^{165}Ho (100)	^{166}Er (33.61)
^{168}Er (26.78)	^{169}Tm (100)
^{174}Yb (31.83)	^{175}Lu (97.41)

The performance of the ICP-QQQ MS/MS method with O_2 cell gas was investigated using analysis of Tb in the presence of a Gd matrix. Gadolinium (III) oxide powder (Gd_2O_3, 99.999 % purity) was gently dissolved in 8 M HNO_3, evaporated to dryness, and then redissolved in 2% HNO_3 to give a final concentration of 10 ppm Gd.

Irradiated Gd_2O_3 targets were dissolved in concentrated HNO_3. To determine the target radio-lanthanide activity levels and any other radionuclides produced, an aliquot was taken for measurement by gamma spectrometry. Following this analysis the sample was left for enough time to allow short-lived radionuclides to decay, after which the stable REE impurities were determined by ICP-QQQ.

Instrumentation

An Agilent 8800 ICP-QQQ was used in this study. The 8800 was equipped with a standard sample introduction system comprising a glass concentric nebulizer, a quartz spray chamber, a quartz torch with 2.5 mm i.d. injector, and nickel-tipped interface cones. The general instrument operating conditions are summarized in Table 3.

Table 3. ICP-QQQ operating parameters.

Parameter	Setting
Scan Mode	MS/MS
Plasma Conditions	Low matrix
RF Power (W)	1550
Extract 1 (V)	0
Extract 2 (V)	–175
Reaction Cell Gas	Oxygen
Oxygen Flow Rate (mL/min)	0.3 (30% of full-scale)
Octopole Bias (V)	–5.0
Energy Discrimination (V)	–7.0
Octopole RF (V)	200

Results and discussion

Instrument sensitivity and interference removal

To remove the matrix element hydride and peak tailing interferences for each of the trace REE analytes investigated, the 8800 ICP-QQQ was operated in MS/MS mode with O_2 cell gas. To compare the performance of single quadrupole ICP-MS, the measurements were also performed using the 8800 in single quad mode, where Q1 does not perform any mass selection.

Using the example of trace Tb analysis in a Gd matrix, Tb was measured as the product ion $^{159}Tb^{16}O^+$ at *m/z* 175 using mass shift. In single quad mode, the $^{158}Gd^1H$ and ^{158}Gd tailing interferences were not effectively avoided using O_2cell gas. A 10 ppm Gd standard gave a signal at *m/z* = 175 of approximately 1.3×10^6 counts per second (cps). This high background meant Tb could not be measured at concentrations below 100 ppt.

Using MS/MS mode with Q1 and Q2 set to *m/z* = 159 and 175, respectively, the *m/z* 175 background signal in the 10 ppm Gd matrix was reduced to ~4,400 cps, which enabled accurate low-level Tb measurement. Using MS/MS, a detection limit of 2.1 ppt was achieved for Tb in the 10 ppm Gd matrix with background subtraction (Figure 1).

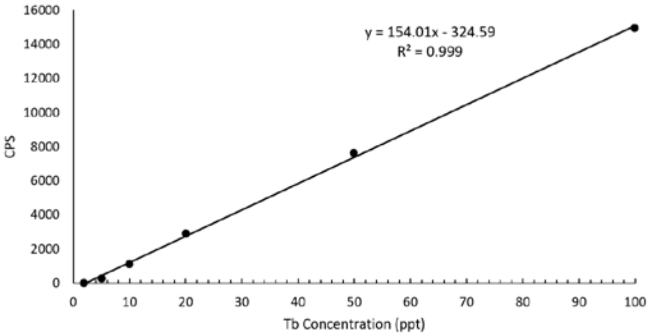

Figure 1. Calibration for Tb in the presence of 10 ppm ^{158}Gd. Tb measured as $^{159}Tb^{16}O^+$ by ICP-MS/MS in O_2 mass-shift mode.

A similar trend was seen for the other trace lanthanides listed in Table 4. Operating the 8800 in MS/MS with on-mass or mass-shift mode using O_2 cell gas, DLs in the low ppt range were achieved for most analytes. Only Ho (measured at *m/z* 165) in a Dy (164) matrix and Er (166) in a Ho (165) matrix showed higher DLs, up to 1.1 ppb in the case of Ho in Dy. The ppt level DLs are equivalent to purity levels of up to 2.1×10^{-7} relative to the 10 ppm concentration of each respective matrix element. This sensitivity is significantly better than the purity information currently provided by the manufacturers of lanthanide powders. The purity analysis also provides valuable information about possible radionuclides that may be formed from contaminants during irradiation of the lanthanide starting material powders.

The single O_2 cell gas mode used for this study gave acceptable data for all trace lanthanides studied. The DLs for some REEs, e.g., trace Ho in Dy, could be improved by further optimizing the cell conditions or using an alternative reaction gas such as N_2O or NH_3 (*6*).

Table 4. Detection limits achieved by 8800 ICP-QQQ for trace REEs in REE matrices. Analysis based on measurement of natural, stable isotope elemental standards.

Trace Element (Measured isotope)	Q1 / Q2	Matrix Element (10 ppm)	DL of Trace Element (ppt)
Ce (140)	140/156	^{139}La	12.2
Pr (141)	141/157	^{140}Ce	11.9
Tb (159)	159/175	^{158}Gd	2.1
Ho (165)	165/181	^{164}Dy	1100
Er (166)	166/182	^{165}Ho	186
Tm (169)	169/185	^{168}Er	2.3
Lu (175)	175/191	^{174}Yb	9.3

Measurement of lanthanide oxide samples

The concentrations of trace lanthanides in a solution containing 10 ppm Gd_2O_3 powder were determined using the 8800 ICP-QQQ with O_2 cell gas. As shown in Figure 2, most REEs were measured on-mass. Only ^{159}Tb, ^{172}Yb, and ^{175}Lu were measured as oxide product ions in mass-shift mode to avoid interferences from $^{158}Gd^{1}H$ at *m/z* 159, $^{156}Gd^{16}O$ at *m/z* 172, and $^{158}Gd^{16}O^{1}H$ at *m/z* 175 (Figure 2).

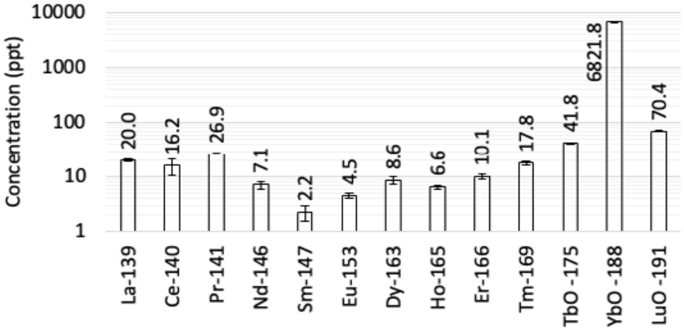

Figure 2. Impurity profile and ICP-MS measurement uncertainties (2σ) of Gd_2O_3 powder used for irradiation.

Elemental standard solutions are used to test chemical separation procedures, so the same ICP-QQQ method was used to measure impurities in a Gd single-element ICP standard. The results are shown in Figure 3. The relatively high measured concentration of YbO in the powder and ICP standard suggests that the interference from $^{156}Gd^{16}O$ and $^{156}Gd^{16}O_2$ on ^{172}Yb and $^{172}Yb^{16}O$, respectively, were not fully resolved. Yb is also not very reactive with oxygen cell gas, leading to low sensitivity for the YbO^+ product ion. The method could potentially be improved through further optimizing the cell conditions or using an alternative cell gas such as N_2O or NH_3 (*6, 7*).

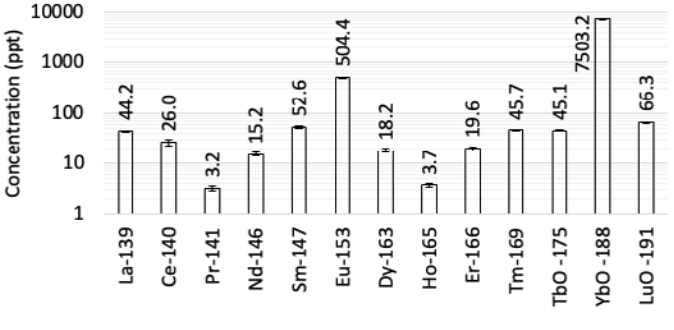

Figure 3. Impurity profile and ICP-MS measurement uncertainties (2σ) of a Gd ICP standard using 8800 ICP-QQQ in MS/MS mode with O_2 cell gas.

Chemical separation results

Operating the 8800 in MS/MS mode with O_2 cell gas and using stable element analogs in place of short-lived radioactive samples enables the optimization of separation procedures under realistic conditions. Realistic conditions refer to the separating of a trace level target lanthanide in the presence of high concentrations of a neighboring lanthanide. This approach enables the development of robust radiochemical procedures before testing with active samples. It also avoids the cost and safety issues of handling active materials during method development.

In this study, Tb was separated from Gd using an extraction chromatography column packed with a LN (lanthanide) resin (50–100 µm particle size, Triskem International). Figure 4 shows an elution profile for Gd and Tb at a 4.5×10^4 excess of Gd. Gd was expected to elute with 0.75 M HNO_3, while Tb was expected to be retained until conditions were switched to 1.0 M HNO_3 (*8*). To check if the separation scheme had been effective, each 1 mL fraction was collected and measured using ICP-MS/MS in O_2 mass-shift mode. The results showed that a small amount of ^{159}Tb was recovered in the ^{158}Gd fraction.

The effectiveness of the ICP-QQQ method to resolve Tb from Gd has been demonstrated using trace Tb standards in a Gd matrix. This performance gives confidence that the signal at *m/z* 159 seen in the Gd fraction was due to trace ^{159}Tb eluting together with the Gd, rather than an interference from ^{158}Gd^{1}H. Also, based on the starting concentration of Tb added to the column, the total Tb recovery was <100%, suggesting little or no contribution from Gd to the measured Tb signal.

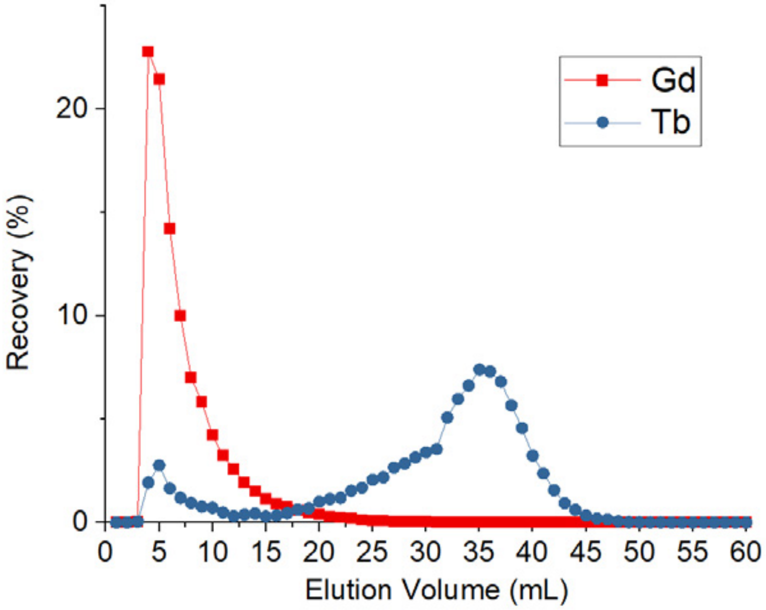

Figure 4. Elution profile for Tb and Gd.

Measurement of impurities in irradiated samples

A compacted Gd_2O_3 powder target was irradiated to produce ^{155}Tb (half-life of 5.32 days). The irradiated target was then dissolved in concentrated HNO_3 and an aliquot was used to measure the activity level of ^{155}Tb and other short-lived radionuclides by gamma spectrometry. After leaving the sample enough time for the radioisotopes to decay, the stable REE isotopes remaining in the Gd_2O_3 sample were measured using ICP-QQQ.

Lanthanum and Ce were the only REE contaminants detected in the final sample at concentrations of ~13.1 and 3.5 ppm, respectively. However, the concentration of both La and Ce was reduced to below background levels after chemical separation. The detection of La and Ce in the irradiated Gd_2O_3 powder shows the potential for stable and long-lived radionuclide impurities to be formed during irradiation. The findings illustrate the importance of chemical separation in the production of high purity radio-lanthanides.

The ICP-QQQ method can be used for post-separation analysis of the final radio-lanthanide product to assess the concentration of stable impurities still present, and to help assess the effectiveness of the chemical separation. Depending on the application, enriched or recycled target materials may be used that contain lanthanides at non-natural abundances, which will affect the level of impurities that can be measured. The measurement of such impurities is important as a QA measure, as high concentrations of impurities can lead to competition for the chelating agent used, which can reduce the radiolabeling efficiency.

Conclusion

The use of radio-lanthanides is of increasing interest in pharmaceutical and imaging applications. Preparation of high purity radio-lanthanides often requires separation of the low concentration target isotope from the high concentration stable REE matrix. To check the purity of the starting REE materials, the Agilent 8800 ICP-QQQ was operated in MS/MS mode with O_2 cell gas to measure all REE impurities in high-purity REE matrices. The ICP-QQQ method was much more effective at removing REE matrix-based polyatomic and peak tailing interferences compared to single quadrupole ICP-MS.

The measurement of trace levels of Tb in the presence of bulk Gd was used as an example. The results obtained from analyzing stable element standards showed that the method was useful for a range of radio-lanthanides.

Overall, the ICP-MS/MS method improved accuracy and confidence of the measurements needed for a complete REE impurity profile of materials used in the production of radionuclides for pharmaceutical and imaging applications. The study has shown that the method is suitable for:

- The measurement of REE impurities in the starting powders used for irradiation.
- Optimizing chemical separation conditions using stable element analogs.
- Assessing the REE impurities present in the irradiated target material post-irradiation.

References

1. Markets and Markets, Nuclear Medicine/Radiopharmaceuticals Market by Type (Diagnostic (SPECT - Technetium, PET- F-18), Therapeutic (Beta Emitters – I-131, Alpha Emitters, Brachytherapy – Y-90)), Application (Oncology, Cardiology) - Global Forecast to 2024, accessed online August 2020, https://www.marketsandmarkets.com/Market-Reports/radiopharmaceuticals-market-417.html
2. M. Van de Voorde *et al.* Radiochemical processing of nuclear-reactor-produced radio lanthanides for medical applications. *Coordination Chemistry Reviews* **2019**, 382 (1), 103–125
3. The International Pharmacopoeia, Ninth Edition. https://apps.who.int/phint/en/p/docf/
4. B. Webster *et al.* Chemical Purification of Terbium-155 from Pseudo-Isobaric Impurities in a Mass Separated Source Produced at CERN, *Nature Scientific Reports* **2019**, 9, 1–9
5. N. Sugiyama, Removal of hydride ion interferences (MH^+) on Rare Earth Elements using the Agilent 8800 Triple Quadrupole ICP-MS, Agilent publication, 5991-1481EN
6. N. Sugiyama and G. Woods, Direct measurement of trace rare earth elements (REEs) in high-purity REE oxide using the Agilent 8800 Triple Quadrupole ICP-MS with MS/MS mode. Agilent publication, 5991-0892EN
7. N. Sugiyama, Direct Analysis of Ultratrace Rare Earth Elements in Environmental Waters by ICP-QQQ, Agilent publication, 5994-1785EN
8. F. Monroy-Guzman and E. J. Salinas, Separation of Micro-Macrocomponent Systems: Ho-Dy and Lu-Yb by Extraction Chromatography, *J. Mex. Chem. Soc.*, **2015**, 59, 143–150

Learn more:
www.agilent.com/chem

https://www.agilent.com/chem/icpms

Buy online:
www.agilent.com/chem/store

U.S. and Canada
1-800-227-9770
agilent_inquiries@agilent.com

Europe
info_agilent@agilent.com

Asia Pacific
inquiry_lsca@agilent.com

DE44298.1812731481

Published in the USA, August 4, 2022
5994-3155EN

Agilent
Trusted Answers